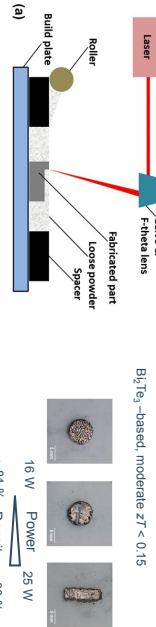


Thermoelectric (TE) technologies and devices

- Emerging fabrication techniques based on printing: laser printing

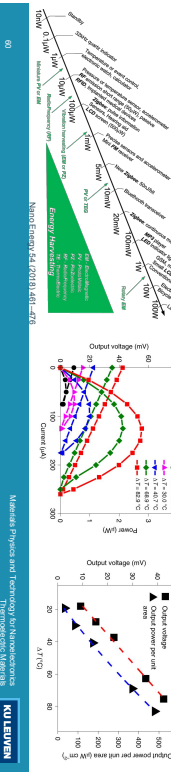
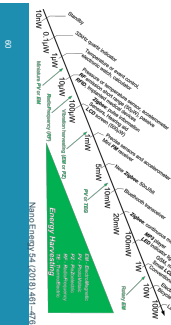
Laser active manufacturing of powdered bismuth telluride, *J Mater. Res.* 33(2018) 4033–4039



Thermoelectric (TE) technologies and devices

- Emerging fabrication techniques based on printing: microextrusion or direct ink writing (DIW)

Micro-devices based on Bi_2Te_3 can be printed offering few 100s of micro-watts per cm^2 for ΔT of 10s K.

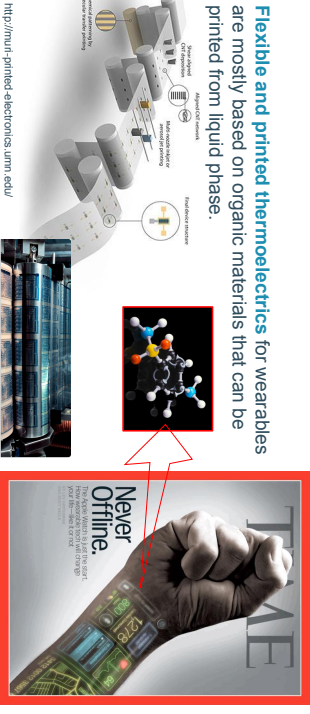


Nature Electronics, volume 4, pages 576–587 (2021)

KU LEUVEN

Thermoelectric (TE) technologies and devices

- Flexible and printed thermoelectrics for wearables are mostly based on organic materials that can be printed from liquid phase.

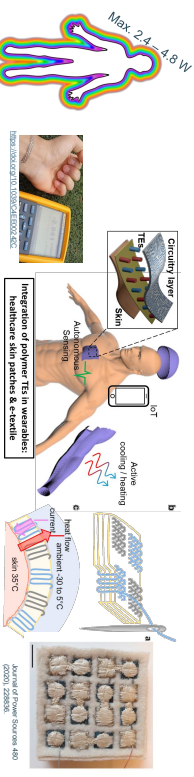


<http://multi-printed-electronics.unimelb.edu/>

Materials Physics and Technology for Nanoelectronics

Thermoelectric (TE) technologies and devices

- Flexible and printed thermoelectrics for wearables: energy harvesters



*1. Sauer J, A. Schubert, M. Gerspach, B. Brügel, Design, Fabrication, and Characterization of a Flexible Thermoelectric Device, *Bioelectron. Devices*, 2004, pp. 1–35.*

02

Nature Physics and Technology for Nanoelectronics
Materials Physics and Technology for Nanoelectronics
Thermoelectric Materials
KU LEUVEN

Thermoelectric (TE) technologies and devices

- Flexible and printed thermoelectrics for wearables: Flexible coolers for body thermal regulation



Hong et al., *Sci. Adv.* 2019; 5: eaaw0536, 17

Flexible thermoelectric device (TED) based on rigid Bi_2Te_3 rigid pillars, that can deliver more than 10°C cooling effect with a high coefficient of performance (COP > 1.5).

03

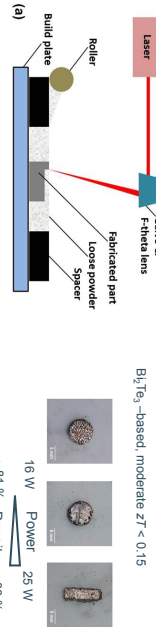
Nature Physics and Technology for Nanoelectronics
Materials Physics and Technology for Nanoelectronics
Thermoelectric Materials
KU LEUVEN

Thermoelectric (TE) technologies and devices

- Emerging fabrication techniques based on printing: laser printing

- Emerging fabrication techniques based on printing: energy harvesters

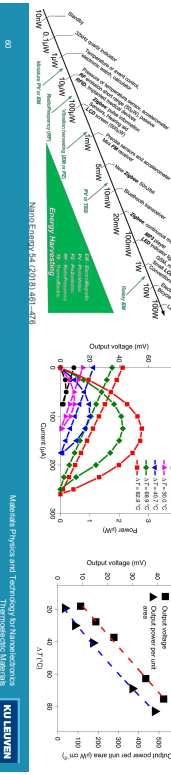
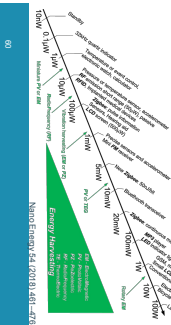
Laser active manufacturing of powdered bismuth telluride, *J Mater. Res.* 33(2018) 4033–4039



Thermoelectric (TE) technologies and devices

- Emerging fabrication techniques based on printing: microextrusion or direct ink writing (DIW)

Micro-devices based on Bi_2Te_3 can be printed offering few 100s of micro-watts per cm^2 for ΔT of 10s K.

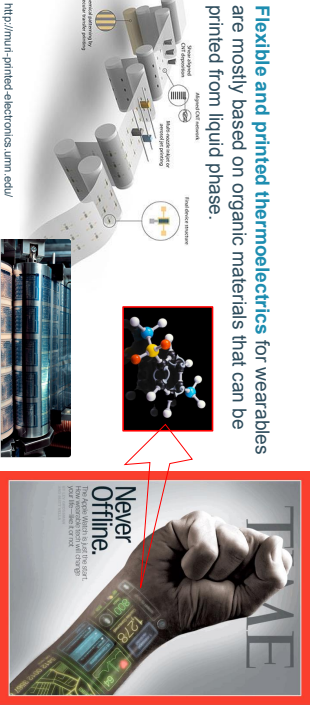


Nature Electronics, volume 4, pages 576–587 (2021)

KU LEUVEN

Thermoelectric (TE) technologies and devices

- Flexible and printed thermoelectrics for wearables are mostly based on organic materials that can be printed from liquid phase.



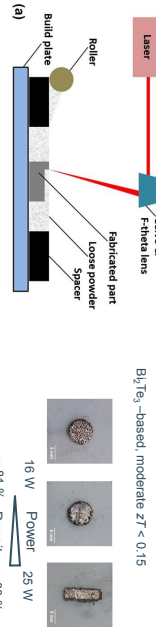
<http://multi-printed-electronics.unimelb.edu/>

Materials Physics and Technology for Nanoelectronics

Thermoelectric (TE) technologies and devices

- Emerging fabrication techniques based on printing: laser printing

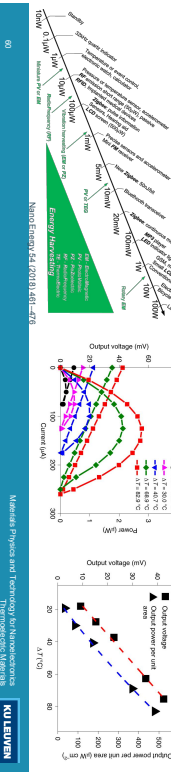
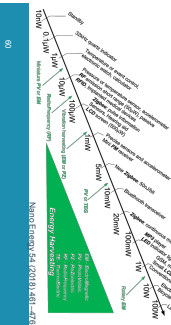
Laser active manufacturing of powdered bismuth telluride, *J Mater. Res.* 33(2018) 4033–4039



Thermoelectric (TE) technologies and devices

- Emerging fabrication techniques based on printing: microextrusion or direct ink writing (DIW)

Micro-devices based on Bi_2Te_3 can be printed offering few 100s of micro-watts per cm^2 for ΔT of 10s K.

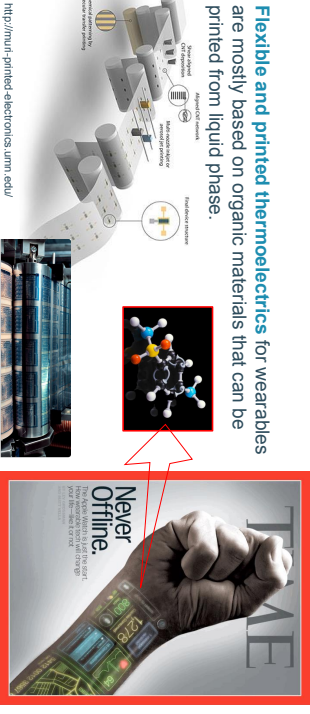


Nature Electronics, volume 4, pages 576–587 (2021)

KU LEUVEN

Thermoelectric (TE) technologies and devices

- Flexible and printed thermoelectrics for wearables are mostly based on organic materials that can be printed from liquid phase.



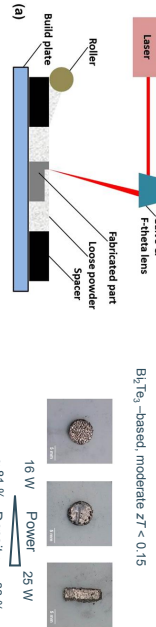
<http://multi-printed-electronics.unimelb.edu/>

Materials Physics and Technology for Nanoelectronics

Thermoelectric (TE) technologies and devices

- Emerging fabrication techniques based on printing: laser printing

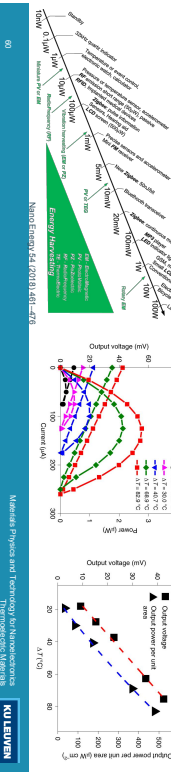
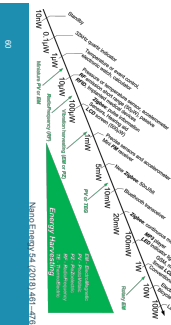
Laser active manufacturing of powdered bismuth telluride, *J Mater. Res.* 33(2018) 4033–4039



Thermoelectric (TE) technologies and devices

- Emerging fabrication techniques based on printing: microextrusion or direct ink writing (DIW)

Micro-devices based on Bi_2Te_3 can be printed offering few 100s of micro-watts per cm^2 for ΔT of 10s K.

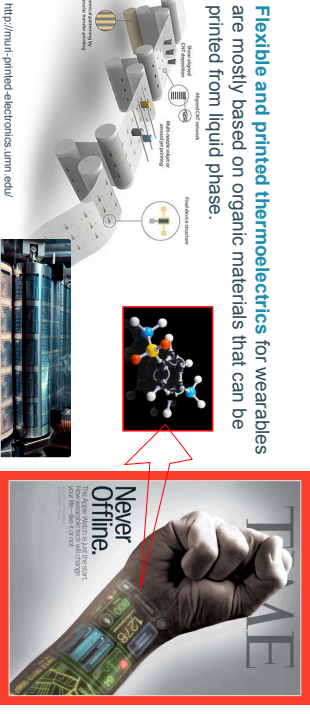


Nature Electronics, volume 4, pages 576–587 (2021)

KU LEUVEN

Thermoelectric (TE) technologies and devices

- Flexible and printed thermoelectrics for wearables are mostly based on organic materials that can be printed from liquid phase.



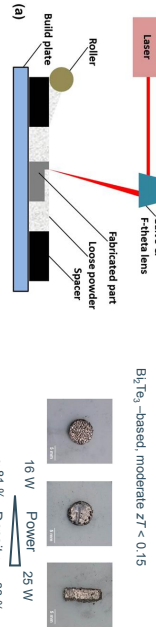
<http://multi-printed-electronics.unimelb.edu/>

Materials Physics and Technology for Nanoelectronics

Thermoelectric (TE) technologies and devices

- Emerging fabrication techniques based on printing: laser printing

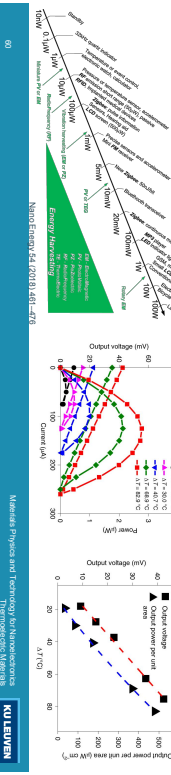
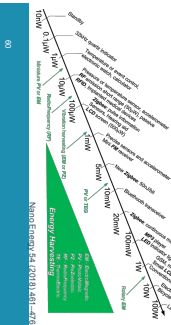
Laser active manufacturing of powdered bismuth telluride, *J Mater. Res.* 33(2018) 4033–4039



Thermoelectric (TE) technologies and devices

- Emerging fabrication techniques based on printing: microextrusion or direct ink writing (DIW)

Micro-devices based on Bi_2Te_3 can be printed offering few 100s of micro-watts per cm^2 for ΔT of 10s K.

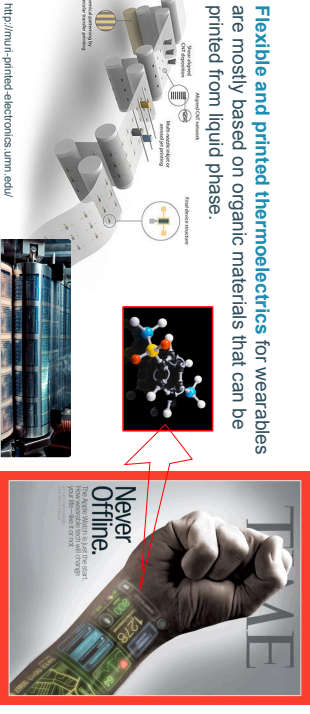


Nature Electronics, volume 4, pages 576–587 (2021)

KU LEUVEN

Thermoelectric (TE) technologies and devices

- Flexible and printed thermoelectrics for wearables are mostly based on organic materials that can be printed from liquid phase.

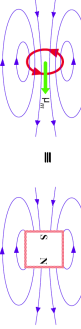


<http://multi-printed-electronics.unimelb.edu/>

Materials Physics and Technology for Nanoelectronics

Magnetic dipoles

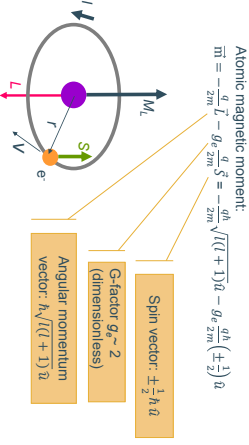
- Although electric and magnetic fields, as described by Maxwell's equations, are formally very similar, there is a striking asymmetry between electricity and magnetism in nature, associated with the apparent non-existence of elementary magnetic charges (*i.e.* magnetic monopoles) and magnetic current.
- There are, however, what appear to be magnetic dipoles, analogous to electric dipoles.
- A magnetic dipole is a system which when placed in an external magnetic field, experiences a torque that tries to rotate the system so as to align its axis parallel to the magnetic field.



Materials Physics and Technology for Nanoelectronics
Magnetic Materials

KU LEUVEN

- ## Magnetic dipoles
- The magnetic dipole is characterized by its **magnetic dipole moment**. Let's for example look into the magnetic dipole moment of a current carrying coil (magnetic dipole) of area A .
 - A magnetic moment is created defined by a vector $\mu = iA$, where i is the current through the coil and A is the area enclosed by the current coil.
 - The torque is given by: $\vec{\tau} = \vec{\mu} \times \vec{B}$. This torque tends to line up the magnetic moment with the magnetic field \vec{B} , so this represents its lowest energy configuration $E = -\vec{\mu} \cdot \vec{B}$.



Materials Physics and Technology for Nanoelectronics
Magnetic Materials

KU LEUVEN

- The magnetic effect in magnetic materials are due to atomic magnetic dipoles in the materials. The sources that contribute to atomic magnetic moments are:
 - The electrons "orbiting" around the nucleus in an atom behave like a current loop and have a magnetic dipole moment associated with it, called the **orbital magnetic moment**.
 - The magnetic moment due to spin of an electron, *i.e.* due to spin angular momentum, is called the **spin magnetic moment**.
 - In addition, there can be a small contribution from the nucleus, called **nuclear magnetic moment**. This effect is usually not significant.

- The most familiar example of a magnetic dipole is a bar magnet. The external magnetic field produced by a circular loop of current is identical to that produced by a point magnetic dipole, so the current loop is also a dipole.
- The magnitude of orbital angular momentum is $L = mvr = m\omega r^2$.
- Combining with previous equation yields:

- Electron in external magnetic field \vec{B} along the axis z , \vec{B} creates a torque that aligns $\vec{\mu}_S$ with \vec{B} . Quantum theory postulates that the projection of L on an axis (let's assume z) is $L_z = \hbar$. The minimum magnetic moment corresponds to $L_z = \hbar$, and:

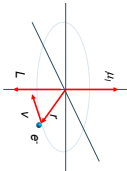
$$\mu_B = \frac{q}{2m} \hbar = 9.27 \times 10^{-24} \text{ Am}^2 \quad (\text{Bohr magneton})$$

$$i = -\frac{q}{T} = -\frac{q\omega}{2\pi}$$

where T is the orbital period of the electron.

- The current loop produces a magnetic field, with a moment μ_L :

$$\mu_L = iA = -\frac{q\omega}{2\pi} \pi r^2 = -\frac{1}{2} q\omega r^2$$



Materials Physics and Technology for Nanoelectronics
Magnetic Materials

KU LEUVEN

- ## Electron spin
- As well as mass and charge, an electron has another intrinsic property, *i.e.* spin angular momentum, or simply **spin**. In quantum mechanics, spin is a fundamental property of atomic nuclei and elementary particles and is an important **intrinsic degree of freedom**.
 - Although as the name indicates, spin was originally thought of particles spinning around their own axis, it had been shown by Dirac that electron spin arises naturally within relativistic quantum mechanics.
 - The component of **electron spin** measured along any direction can only take on the values: s_z with $s_z = \pm \frac{1}{2}$

- The atomic magnetic moment:

$$\vec{\mu} = -\frac{q}{2m} \vec{L} - g_e \frac{q}{2m} \vec{s} = -\frac{q\hbar}{2m} \sqrt{l(l+1)} \hat{u} - g_e \frac{\alpha h}{2m} (\pm \frac{1}{2}) \hat{u}$$
- G-factor $g_s \approx 2$ (dimensionless)
- Angular momentum vector: $\hbar \sqrt{l(l+1)} \hat{u}$

KU LEUVEN

11

- ## Magnetic materials
- The **Bohr magneton** is a physical constant and the natural unit for expressing the magnetic moment of an electron caused by its orbital or spin angular momentum.
 - Bohr magneton:

$$\mu_B = \frac{q\hbar}{2m} = 9.28 \times 10^{-24} [\text{Am}^2] \text{ or } [\text{J T}^{-1}]$$



Materials Physics and Technology for Nanoelectronics
Magnetic Materials

KU LEUVEN

Orbital magnetic dipole moments (extra)

- Consider an electron moving with velocity (v) in a circular Bohr orbit of radius r . It produces a current:

$$i = -\frac{q}{T} = -\frac{q\omega}{2\pi}$$

where T is the orbital period of the electron.

- The current loop produces a magnetic field, with a moment μ_L :

$$\mu_L = iA = -\frac{q\omega}{2\pi} \pi r^2 = -\frac{1}{2} q\omega r^2$$

- The magnitude of orbital angular momentum is $L = mvr = m\omega r^2$.

- Combining with previous equation yields:

$$\mu_B = \frac{q}{2m} \hbar = 9.27 \times 10^{-24} \text{ Am}^2 \quad (\text{Bohr magneton})$$

10

KU LEUVEN

Hund's rule

- In order to understand the magnetic properties of materials, we have to take a deeper look into the **electrons spin distribution**. Each electron state may be occupied by two electrons, one with spin up and one with spin down. The electron spin distribution is determined by **Hund's rule**.

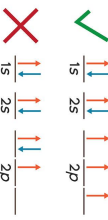


Illustration of Hund's rule in Nitrogen (7 electrons)

- The rule states that when there is orbital degeneracy, the electrons will be arranged to **maximize the total spin**. This means that each electron added to a set of degenerate levels will have the same **parallel spin** as the electron which preceded it. Hund's rule can cause a significant spin imbalance in some materials.
- The physical origin of this rule is Pauli's exclusion principle (two electrons with the same spin can never be found at precisely the same place), and the **repulsive Coulomb interaction energy** (if electrons are far from each other, the overall system energy is lower). The two effects above makes systems with the same spin energetically favorable.
- The difference in energy between the parallel and anti-parallel alignments is the **exchange energy**.

Magnetic Physics and Technology for Nanoelectronics
Magnetic Materials

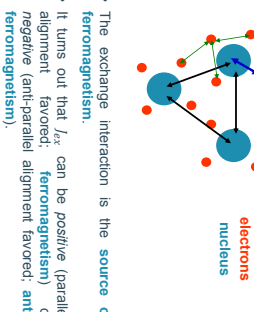
KU LEUVEN

- The periodic arrangement of the spins in these materials results from an electrostatic coupling between the electrons and nucleus of the neighboring atoms, called the **exchange coupling (or energy)**:

$$U_{ex} = -2J_e \vec{s}_i \cdot \vec{s}_j$$
- where \vec{s}_i and \vec{s}_j are the **spin vectors** on atoms i and j , and J_e is the **exchange integral**, which is related to the overlapping of the electronic orbitals i and j .
- The exchange integral J_e is related to the "electron – electron" and "electron – nucleus" interactions of neighboring atoms.

Magnetic Physics and Technology for Nanoelectronics
Magnetic Materials

electrons
nucleus



16

16

Magnetic Physics and Technology for Nanoelectronics
Magnetic Materials

KU LEUVEN

Magnetic materials

- In case of equal number of electrons with spin up and spin down, the material is **diamagnetic**, and the net spin magnetism is zero.
 - Many materials behave **paramagnetic**, i.e. the electron spins on each atom do not completely cancel; each atom has a net spin and a net magnetic dipole moment (χ_m slightly positive).
 - Paramagnetic materials remain typically very weakly magnetic because the **individual atomic magnets are uncoupled and point in random directions**. If an external magnetic field is applied, the individual magnets attempt to align with the magnetic field. The energy E of an atomic dipole of strength p_m in a field H is given by:
- $$E = -\mu_0 p_m H$$
- At room temperature and usual magnetic fields, the energy of an individual atomic dipole is small compared to $k_B T$, and this leads to only a tiny paramagnetic susceptibility.
 - The relative permeability μ_r of most paramagnetic materials is therefore approximately one, except at very high fields and very low temperatures.

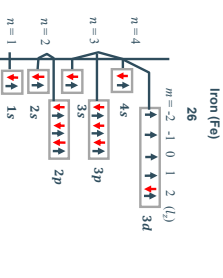
Magnetic Physics and Technology for Nanoelectronics
Magnetic Materials

KU LEUVEN

Magnetic materials

- The interesting applications of magnetic materials tend to come not from paramagnetism or diamagnetism, but from arrangements such as **ferromagnetism**, where the magnetic moments **remain aligned even in the absence of an external magnetic field**.
- Ferro is the Latin word for iron (this is the reason behind the atomic symbol of iron - Fe), which displays strong magnetic properties.
- In order to understand ferromagnetism we need to consider not just interactions between individual magnetic moments and the external field, but also **interactions between the magnetic moments**.

Illustration of Hund's rule for Fe. Notice the spin imbalance in the 3d orbital.

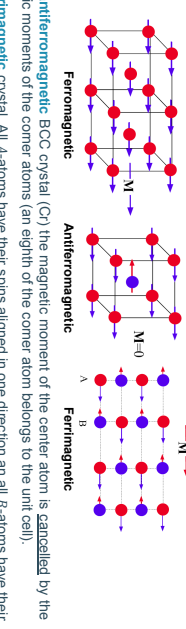


n = 1 1s
n = 2 2s
n = 3 3s 3p
n = 4 4s 4p

$m = -2, -1, 0, 1, 2$ (l₂)
 $m = -3, -2, -1, 0, 1, 2$ (l₃)
 $m = -4, -3, -2, -1, 0, 1, 2$ (l₄)

Magnetic materials

- In a magnetized region of a **ferromagnetic** material such as iron all the magnetic moments are spontaneously aligned in the same direction. There is a **strong magnetization vector M** even in the absence of an applied field.



17

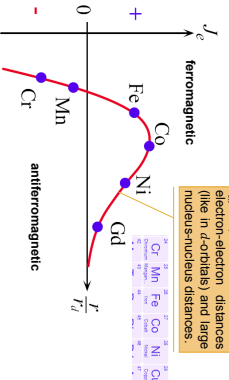
Magnetic Physics and Technology for Nanoelectronics
Magnetic Materials

KU LEUVEN

Magnetic materials

- If the exchange integral J_{ex} is positive, the exchange coupling is minimal (negative) for parallel spins i and j , and the material is **ferromagnetic**.
- If the exchange integral J_{ex} is negative, the exchange coupling is minimal for anti-parallel spins i and j , and the material is **antiferromagnetic**.

The exchange integral as a function of r/r_d , where r is the interatomic distance and r_d the radius of the d-orbit (or the average subshell radius). Cr to Nd are transition metals. For Gd, the x-axis is r/r_f , where r_f is the radius of the f-orbit.



17

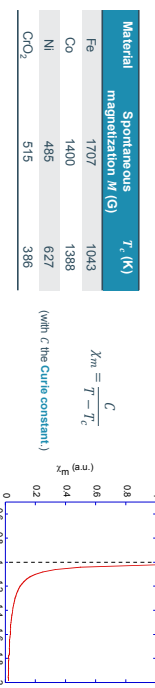
17

Magnetic Physics and Technology for Nanoelectronics
Magnetic Materials

KU LEUVEN

Ferromagnetic-paramagnetic phase transition

- Ferromagnetic materials exhibit a long-range ordering phenomenon at the atomic level which causes the unpaired electron spins to line up parallel with each other in a region called a **domain**.
- All ferromagnets have a **maximum temperature** where the ferromagnetic property disappears as a result of thermal agitation. This temperature is called the **Curie temperature** T_c . At T_c , thermal disorder induces a thermal transition from the ordered ferromagnetic phase to a disordered paramagnetic phase.
- The magnetic susceptibility χ_m presents a discontinuity at the Curie temperature.



19

Materials Physics and Technology: Nanoelectronics
Magnetic Materials

KU LEUVEN

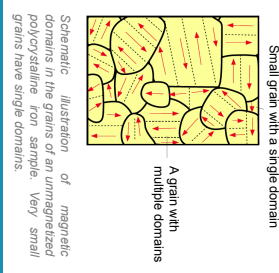
Magnetic domains

- At the **atomic scale**, spins of ferromagnetic materials are aligned and parallel. However, at the **macroscopic scale**, not all the spins are necessarily aligned, due to the formation of **magnetic domains**, which all have different orientations for the magnetization \vec{M} .
- Inside each domain, the magnetization is uniform. However, the relative orientation of \vec{M} varies from domain to domain.

- When an external magnetic field \vec{H} is applied to the material, all the domains tend to orient \vec{M} parallel to \vec{H} , to reduce the energy (per volume) of the system:

$$E_H = -\mu_0 M \vec{H} = -\mu_0 M H \cos(\theta) [\text{J/m}^3]$$

- However, the increase in exchange energy is balanced by a **net savings in stray field energy**.



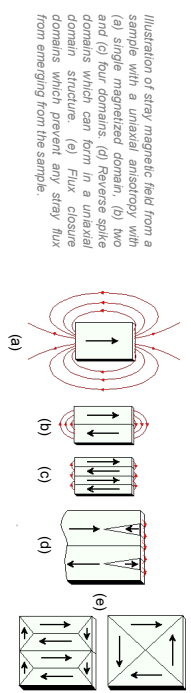
22

Materials Physics and Technology: Nanoelectronics
Magnetic Materials

KU LEUVEN

Magnetic domains

- The formation of domains does have some **energetic cost**. The exchange interaction in a ferromagnet aligns spins because that reduces the total energy of the system. At a **domain wall** (the boundary between two domains), where the perfect ferromagnetic alignment gets disrupted, the local energy should in principle be higher.
- However, the increase in exchange energy is balanced by a **net savings in stray field energy**.



23

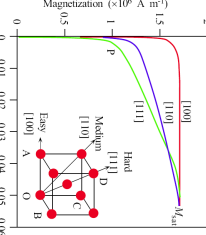
Materials Physics and Technology: Nanoelectronics
Magnetic Materials

KU LEUVEN

Magnetic anisotropy

- Most ferromagnetic materials present a **magnetic anisotropy**, i.e. they are preferentially magnetised in a particular direction, called their **easy axis**.
- If φ is the angle between the magnetization M and the direction of the easy axis, the **anisotropic energy** U_{an} (energy per volume) is given by:

$$U_{an} = K \sin^2 \varphi$$
- With K the anisotropy constant, which is dependent on material.



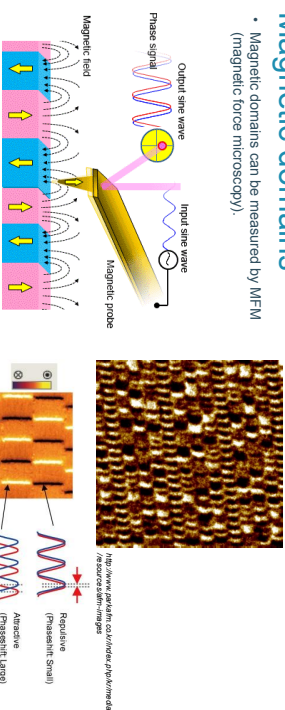
21

Materials Physics and Technology: Nanoelectronics
Magnetic Materials

KU LEUVEN

Magnetic domains

- Magnetic domains can be measured by MFM (magnetic force microscopy).

<https://www.ultrahighresolution.com/resource/photonics/>

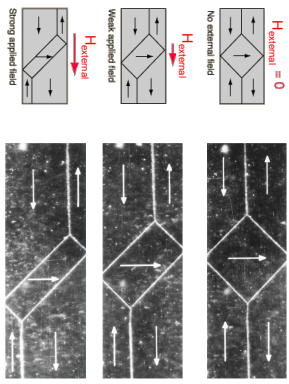
24

Materials Physics and Technology: Nanoelectronics
Magnetic Materials

KU LEUVEN

Magnetic domains

- These pictures illustrate the change of magnetic domains from unmagnetized (at zero field) state to magnetized (under field) state.

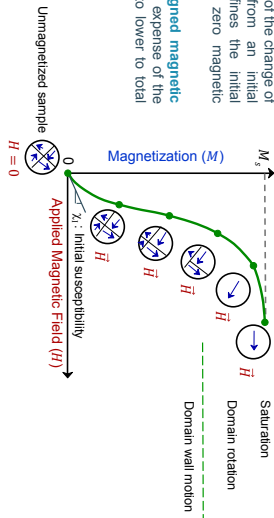


Materials Physics and Technology: Nanoelectronics
Magnetic Materials

KU LEUVEN

Magnetic domains

- Schematic illustration of the change of magnetic domains from an initial condition (which defines the initial susceptibility χ_i) at zero magnetic field to **saturation**.
- Domains with an **aligned magnetic moment** grow at the expense of the poorly aligned ones to lower to total energy.

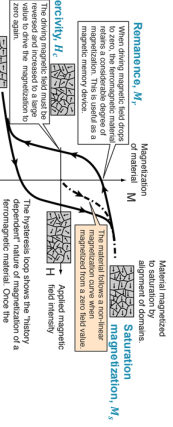


Materials Physics and Technology: Nanoelectronics
Magnetic Materials

KU LEUVEN

Magnetic hysteresis

- When a ferromagnetic material is magnetized in one direction, it will not relax back to zero magnetization when the imposed magnetizing field is removed.
- It must be driven back to zero by a field in the opposite direction. If an alternating magnetic field is applied to the material, its magnetization will trace out a loop called a **hysteresis loop**. This is related to the existence of magnetic domains in the material.
- Once the magnetic domains are reoriented, it takes some energy to turn them back again.



<http://hyperphysics.phy-astr.gsu.edu/hbase/SolidPhys.html>

27

Short note on S.I. versus c.g.s. units

Many people think there is one system called "The Metric System," but actually there are two systems:

- One is the "Système International" or S.I. system, which is the "Year" (upper-case) Metric System, which uses Metres, Kilograms and Seconds for length, mass and time. For this reason it is sometimes called the **MKS system**.
- The "other" (lower-case) metric system uses centimeters, grams and seconds. It is most often called the **c.g.s. system**, and sometimes is called the Gaussian system or the electrostatic system. There are other traditional differences in the two systems when measuring charge and electric and magnetic fields, for example:
 - The S.I. unit for magnetic field is the **Tesla, or T**. It comes from the cross-product equation for magnetic force on a moving particle: $F = qv \times B$. The magnetic field, B , must be in units of force per charge per velocity. So $1 \text{ T} = 1 \text{ Ns/(Cm)}$.
 - In c.g.s. units, the equation for magnetic force looks different. Instead of $qv \times B$, it is $(qv/c) \times B$. You have to divide by the speed of light, c . The unit for magnetic field, B , is called the **Gauss, G**, where $1 \text{ G} = 1 \text{ dyne/cesu}$ (cesu = statcoulomb). The Earth's magnetic field at the surface is about $1/2 \text{ G}$, which makes it a very popular unit.

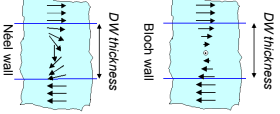
• Teslas are bigger than Gauss: $1 \text{ T} = 10^4 \text{ G}$.

<https://www.physicsclassroom.com/class/magnetic-fields/Lesson-1/Hysteresis>

28

Domain walls

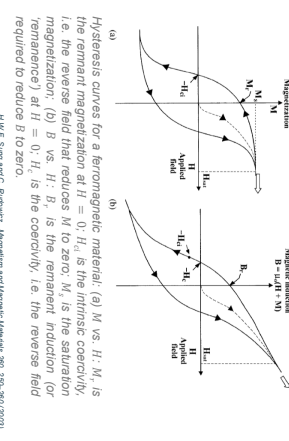
- Because of the strength of the exchange interaction, which wants to align neighboring spins, **abrupt changes in magnetization direction** (on the atomic scale) costs a lot of **extra energy**. As a result, the local magnetization spreads the change in direction out over **some distance**, i.e. the domain wall **thickness**.
- There are different kinds of domain walls that are possible:
 - In a **Block wall** the magnetization reverses direction by rotating out of plane, over some number of lattice sites. Energetically favored in thick materials.
 - In a **Neel wall** the magnetization rotates in its plane to reverse direction. Favored in thin materials.



29

Magnetic hysteresis

- It is customary to plot the magnetization M as a function of the magnetic field strength H , since H is a measure of the externally applied field which drives the magnetization.
- There is a distinction between the two notions of **coercivity** referred to the two $B(H)$ curve and the $M(H)$ curve, which turns out to be often confused in textbooks and scientific literature



Materials Physics and Technology: Nanoelectronics
Magnetic Materials

KU LEUVEN

Magnetic hysteresis

Many people think there is one system called "The Metric System," but actually there are two systems:

- One is the "Système International" or S.I. system, which is the "Year" (upper-case) Metric System, which uses Metres, Kilograms and Seconds for length, mass and time. For this reason it is sometimes called the **MKS system**.
- The "other" (lower-case) metric system uses centimeters, grams and seconds. It is most often called the **c.g.s. system**, and sometimes is called the Gaussian system or the electrostatic system. There are other traditional differences in the two systems when measuring charge and electric and magnetic fields, for example:
 - The S.I. unit for magnetic field is the **Tesla, or T**. It comes from the cross-product equation for magnetic force on a moving particle: $F = qv \times B$. The magnetic field, B , must be in units of force per charge per velocity. So $1 \text{ T} = 1 \text{ Ns/(Cm)}$.
 - In c.g.s. units, the equation for magnetic force looks different. Instead of $qv \times B$, it is $(qv/c) \times B$. You have to divide by the speed of light, c . The unit for magnetic field, B , is called the **Gauss, G**, where $1 \text{ G} = 1 \text{ dyne/cesu}$ (cesu = statcoulomb). The Earth's magnetic field at the surface is about $1/2 \text{ G}$, which makes it a very popular unit.

• Teslas are bigger than Gauss: $1 \text{ T} = 10^4 \text{ G}$.

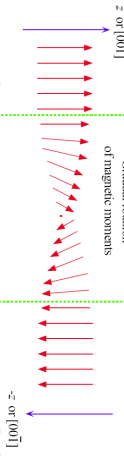
28

<https://www.physicsclassroom.com/class/magnetic-fields/Lesson-1/Hysteresis>

29

Ferromagnetic domains

- Let's take a closer look into the formation of a **Bloch wall** with a 180° change in the easy axis between two domains.



- The spins in the material will gradually rotate to the opposite magnetization direction. The domain wall will **adjust its thickness to minimize the total energy**.
- This total energy is the **sum of the exchange energy and the anisotropy energy**.

31

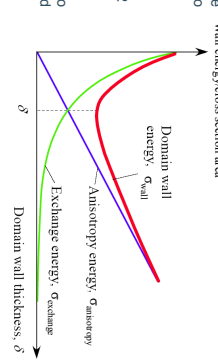
Materials Physics and Technology for Nanoelectronics Magnetic Materials

KU LEUVEN

- The exchange coupling tends to minimize the angle between two adjacent spins, in order to minimize the **exchange energy**:
- $$U_{ex} = -J_{ex} S_i^z S_j^z = -J_{ex} S^2 \cos\varphi$$
- As a result, the extension of the region between 2 domains (i.e. the domain wall width) would tend to be very large due to this contribution.

- The **anisotropy energy** (per volume) tends to reduce the angle between the magnetization and the easy axis:
- $$U_{an} = K \sin^2 \varphi$$

In the transition region, the spins are usually not parallel to the easy axis, such that this contribution tend to minimize the domain wall width.



Materials Physics and Technology for Nanoelectronics Magnetic Materials

KU LEUVEN

Ferromagnetic domains

- Consider a change of spin orientation by an angle of 180° between two domains.
- For an infinitesimal change in angle between two adjacent spins, the exchange energy between the two spins reads:

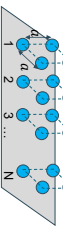
$$\Delta U_{ex} \approx J_{ex} S^2 \varphi^2 \quad (\text{see details in next slide})$$

If the total change in angle (180°) takes place over N atoms, then the smallest change is $\varphi = \pi/N$. The total exchange energy over these N atoms then reads:

$$N \Delta U_{ex} \approx J_{ex} S^2 \frac{\pi^2}{N} \quad (\text{see details in next slide})$$

- If the lattice constant of the material is a , then the energy per cross-sectional surface area of the domain wall, due to the exchange coupling is:

$$\sigma_{ex} \approx J_{ex} S^2 \frac{\pi^2}{Na^2}$$



32

33

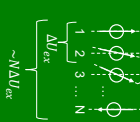
Materials Physics and Technology for Nanoelectronics Magnetic Materials

KU LEUVEN

Ferromagnetic domains (extra)

- $U_{ex} = -2J_{ex} S_i^z S_j^z = -2J_{ex} S^2 \cos\varphi \quad \left| \begin{array}{l} i, j \parallel \vec{S}_i \parallel \vec{S}_j \rightarrow U_{ex,0} = -2J_{ex} S^2 \cos 0^\circ \Rightarrow \vec{S}_i \uparrow \vec{S}_j \\ i, j \parallel [001] \rightarrow U_{ex,1} = -2J_{ex} S^2 \cos 90^\circ \Rightarrow \vec{S}_i \downarrow \vec{S}_j \end{array} \right. \right. \quad \vec{S}_i \uparrow \vec{S}_j \text{ is very small, } \lim_{\varphi \rightarrow 90^\circ} \cos\varphi \approx 1 - \frac{\varphi^2}{2} \quad (\text{Taylor series})$
- $\Delta U_{ex} = U_{ex,1} - U_{ex,0} = -2J_{ex} S^2 \left(1 - \frac{\varphi^2}{2} - 1 \right) = J_{ex} S^2 \varphi^2$
- The total spin flip ($\varphi_{\text{wall}} = \pi$) occurs over N atoms. Then $\varphi = \pi/N$ and $\Delta U_{ex} = J_{ex} S^2 \frac{\pi^2}{N^2}$
- The total energy to flip the spin is then:

$$N \Delta U_{ex} = J_{ex} S^2 \frac{\pi^2}{N}$$



34

Materials Physics and Technology for Nanoelectronics Magnetic Materials

KU LEUVEN

Ferromagnetic domains

- Over the domain wall, the maximum variation of the anisotropy surface energy (the energy per cross-sectional surface area of the domain wall) equals:

$$\sigma_{an} \approx K \pi a$$

where Na is the width of the domain (remember that U_{an} was energy per volume).

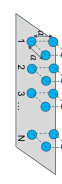
- The total surface energy is then:

$$\sigma \approx J_{ex} S^2 \frac{\pi^2}{Na^2} + K Na$$

- This energy is minimal when:

$$\frac{\partial \sigma}{\partial N} = 0 \Rightarrow \frac{\pi^2 J_{ex} S^2}{Na^2} + Ka = 0 \Rightarrow \delta = Na = \sqrt{\frac{\pi^2 J_{ex} S^2}{Ka}}$$

- This means that the domain wall width depends strongly on the **anisotropy constant K** of the material (it can change over few orders of magnitude). Materials with a **large anisotropy constant K** material typically have domain walls in the order of ~ 10 nm. Materials with a **small K value** have much wider domain walls that can range from ~ 1 to $10 \mu\text{m}$.



35

Soft and hard magnets

- Two type of ferromagnetic materials are distinguished, based on their response relative to an external magnetic field:
- For an infinitesimal change in angle between two adjacent spins, the exchange energy between the two spins reads:

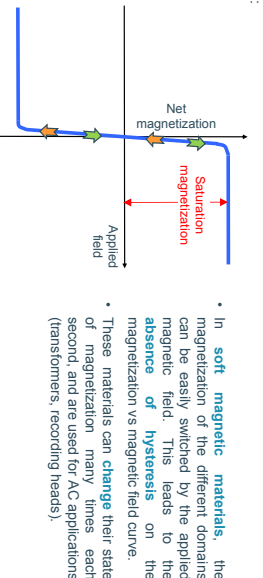
$$\Delta U_{ex} \approx J_{ex} S^2 \varphi^2 \quad (\text{see details in next slide})$$

If the total change in angle (180°) takes place over N atoms, then the smallest change is $\varphi = \pi/N$. The total exchange energy over these N atoms then reads:

$$N \Delta U_{ex} \approx J_{ex} S^2 \frac{\pi^2}{N} \quad (\text{see details in next slide})$$

- If the lattice constant of the material is a , then the energy per cross-sectional surface area of the domain wall, due to the exchange coupling is:

$$\sigma_{ex} \approx J_{ex} S^2 \frac{\pi^2}{Na^2}$$



36

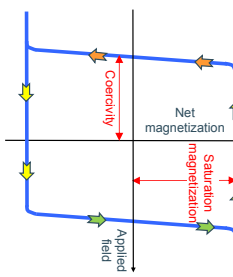
33

Materials Physics and Technology for Nanoelectronics Magnetic Materials

KU LEUVEN

Soft and hard magnets

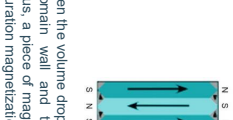
- Two type of ferromagnetic materials are distinguished, based on their response relative to an external magnetic field:



- In **hard magnetic materials**, the magnetization of the different domains cannot be switched easily, leading to a **hysteresis** on the field curve that shows the magnetization versus the magnetic field.
- These materials **maintain** their magnetization state over time and are used as permanent magnet and magnetic memory devices.

KU LEUVEN

40



- It is clear that when the volume drops below a certain critical value, it becomes energetically unfavorable to include a domain wall and the **uniformly magnetized state** becomes the **lowest energy** configuration. Thus, a piece of magnetic material below the **critical size** stays permanently magnetized at close to its saturation magnetization.

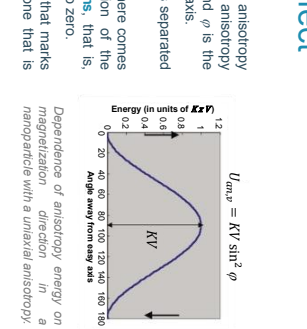
Soft and hard magnets

- A magnetic material is **soft** or **hard**, depending whether **domain-wall motion** (switching of magnetization between different domains) is **easy** or **difficult**. This depends much on the microstructure of the material.
- Inhomogeneous materials, with many grain boundaries (polycrystalline phases) present local variation of the surface energy γ of domain walls, which makes domain wall motion more difficult! Defects can act as 'pinning sites and **impede the domain wall motion**, especially if the domain walls are narrow, i.e. if K is high.
- Therefore, hard magnets are typically inhomogeneous high- K materials (the anisotropy constant).

41

Magnetic domains: size effect

- Consider a particle with a uniaxial anisotropy whose anisotropy energy is given by $U_{an,v} = KV \sin^2 \varphi$, where K is the anisotropy energy density (in J/m^3), V is the particle volume and φ is the angle between the magnetization vector and the easy axis.
- The system therefore has **two minimal energy** states separated by an **energy barrier** of height KV .
- As the volume decreases at a specific temperature, there comes another critical diameter, at which the magnetization of the nanoparticle is unstable against **thermal fluctuations**, that is, $KV \sim k_B T$ and the time averaged magnetization goes to zero.
- Thus for a given particle size, there is a temperature that marks the transition from a permanent static moment to one that is fluctuating in a nanoparticle.



42

Superparamagnetism

- The average **size** of the magnetic domains is a function of the system energy.
- As the volume of a piece of magnetic material is reduced the number of domains decreases.

- Homogeneous **low- K** materials, with only **few grain boundaries** and structural defects, have large domain motion of spins at the boundaries between different domains
- Soft magnets are usually homogeneous low- K materials.
- Magnetic materials with a broad range of coercivities are available.
- The **coercivity** is an extrinsic property and, therefore, is sensitive to the micro-structure of the material.

Range of coercivities (at 100 mT) available for various magnetic materials.

COERCIVITY
(log A/m)

Hard Magnetic Materials	Soft Magnetic Materials
Neodymium-Iron-Boron	Amorphous Iron Alloys
Alnico	Amorphous Cobalt Alloys
Tungsten Steel	
Carbon Steel	
Iron	
Soft Ferrites	
Temporary Magnetic Materials	
1	-1

(Temporary)

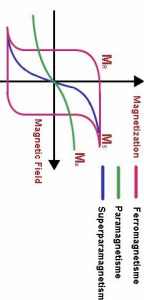
Materials

1

Amorphous Iron Alloys

Amorphous Cobalt Alloys

Range of coercivities (at 100 mT) available for various magnetic materials.



Superparamagnetism

- Due to the magnetic anisotropy of the nanoparticle, the magnetic moment has usually only **two stable orientations** antiparallel to each other, separated by an **energy barrier** KV . At finite temperature, there is a finite probability for the magnetization to flip and reverse its direction. The mean time between two flips is called the **Neel relaxation time** τ_N and is given by the Neel-Arrhenius equation:

$$\tau_N = \tau_0 \exp\left(\frac{KV}{k_B T}\right)$$

with τ_N the average time it takes for the nanoparticle's magnetization to randomly flip as a result of thermal fluctuations, τ_0 the attempt period (characteristic of the material), K is the nanoparticle's magnetic anisotropy energy density and V its volume. KV is therefore the energy barrier associated with the magnetization moving from its initial easy axis direction, through a 'hard plane', to the other easy axis direction. k_B is the Boltzmann constant and T is the temperature.

- The Neel relaxation time is an exponential function of the grain volume, which explains why the flipping probability becomes rapidly negligible for **bulk materials or large nanoparticles**.

Superparamagnetism

- Let us imagine that the magnetization of a single magnetic nanoparticle is measured and let us define τ_m as the measurement time.

- If $\tau_m \gg \tau_N$, the **nanoparticle magnetization** will flip several times during the measurement and the measured magnetization will **average to zero**.
- If $\tau_m \ll \tau_N$, the magnetization will not flip during the measurement and the measured magnetization will be what the instantaneous magnetization was at the beginning of the measurement. In the former case, the nanoparticle will appear to be in the **superparamagnetic state**, whereas in the latter case it will appear to be 'blocked' in its initial state.

The state of the nanoparticle (superparamagnetic or blocked) depends on the measurement time. A transition occurs when $\tau_m = \tau_N$. Typical in experiments, the measurement time is kept constant and the temperature is varied. Under these conditions the transition between the superparamagnetic and the blocked state is observed at a specific temperature for which $\tau_m = \tau_N(T)$ is satisfied. This temperature is called the **blocking temperature**, given by:

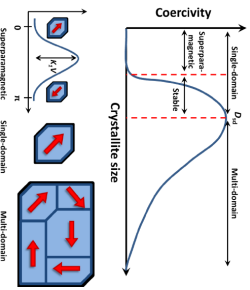
$$T_B = \frac{K V}{k_B \ln\left(\frac{\tau_m}{\tau_0}\right)}$$

Spin transport



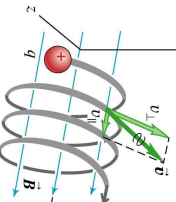
Size effect on coercivity

- Unlike saturation magnetization, which is, in principle, size-independent, the coercivity is very sensitive to the **size variation**. With decreasing particle size the coercivity of a particle gradually increases to a **maximum value** at a particular size and then rapidly decreases to zero as the particle size further decreases.



Magnetism and electrical resistivity

- The **magnetoresistance** phenomena is the tendency of a material to change the value of its electrical resistance in an externally-applied magnetic field.



Ordinary Magneto Resistance (OMR)

- The Lorentz force \vec{F} due to magnetic field $\vec{B} = -\vec{v} \times \vec{B}$ modifies the trajectory of electrons:

- The Ordinary Magneto Resistance (Lord Kelvin, 1856) results in small changes of the bulk resistivity, typically only $\Delta R/R < 5\%$.

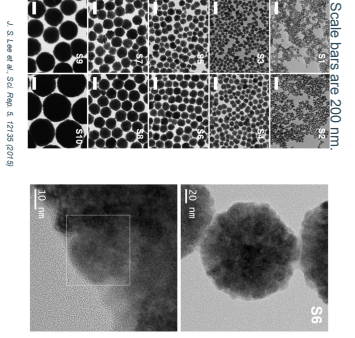
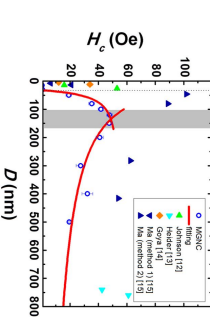
• The scalar resistivity is given by:

$$\rho_{xx} = \frac{1 + (\mu B)^2}{\sigma_0}$$

- where B is the magnetic field and μ the electron mobility.
- Since this effect is rather small, it is not very useful for practical applications.

- The size effect on coercivity was experimentally verified on the polyol syntheses of magnetite (Fe_3O_4) nanoparticles by adjusting the chemistry.

Estimated $D_{ad} \sim 105.4$ nm

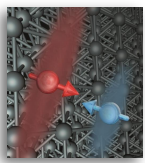


Spin polarized transport

Much more interesting applications can be obtained by using **spin-polarized currents**. Spin-polarized transport will occur naturally in any material for which there is an **imbalance of the spin populations** at the Fermi level. This imbalance commonly occurs in **ferromagnetic metals**.

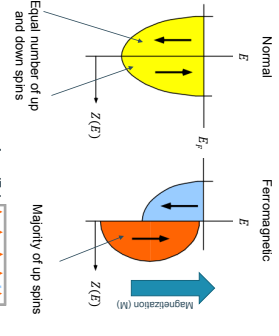
Mott model

- In the Mott model it is proposed that the electrical conductivity in metals can be described in terms of two largely **independent conducting channels**, corresponding to the **up-spin** and **down-spin** electrons, and electrical conduction occurs in parallel for the two channels.
- In non-magnetic conductors the scattering rate does not depend on the electron spin. However, in ferromagnetic metals the scattering rates of the up-spin and down-spin electrons are **different**. Mostly it is assumed that the scattering is strong for electrons with spin anti-parallel to the magnetization direction and weak for electrons with spin parallel to the magnetization direction (in a bulk material).



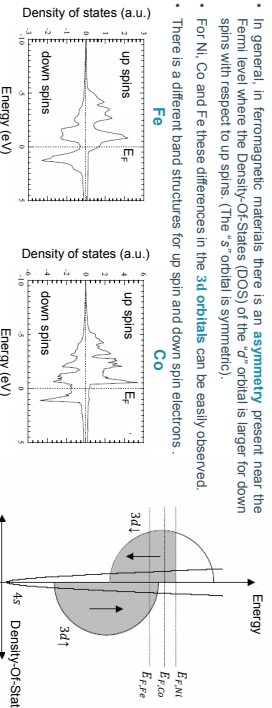
Band structure of magnetic materials

- The density of states $Z(E)$ as a function of energy E is then usually presented as in the right figure.
- Non-magnetic materials show an **equal number** of up and down spins in the DOS.
- Ferromagnetic materials have a **majority** of electrons in one spin state (up-state by convention).
- In this schematic diagram, it is seen that for the ferromagnetic material the available majority spin states (up-state) are **completely filled** at the Fermi level, while this is **not the case** for the minority spin states (down-state).
- This is a direct consequence of the **spin imbalance rule**.

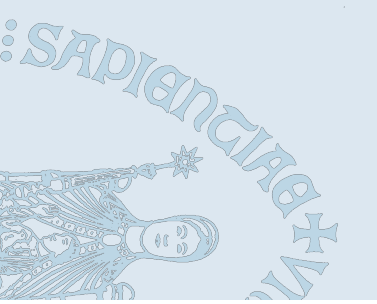


Band structure of magnetic materials

- In general, in ferromagnetic materials there is an **asymmetry** present near the Fermi level where the Density-Of-states (DOS) of the "d" orbital is larger for down spins with respect to up spins. (The "s" orbital is symmetric).
- For Ni, Co and Fe these differences in the 3d orbitals can be easily observed.
- There is a different band structures for up spin and down spin electrons.



Giant magnetoresistance



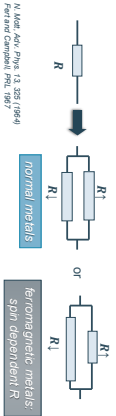
Spin dependent transport in the diffusion limit

- Fermi "golden rule": $\text{density of scattering probability} \propto \text{density of final states}$
- This rule states that the scattering probability relates to the density of final states to which the electron can scatter. As a result, in ferromagnetic materials the scattering probability depends on the spin of the electron.
- Ferromagnetic metals (e.g. Fe, Co, Ni and their alloys)
 - "s" and "d" electrons close to the Fermi energy contribute to the electrical conduction but "s" electrons have higher mobility. Therefore, they are the main responsible for the electrical transport.
 - The main scattering effect is the "sd" exchange interaction (i.e. a spin-up "s" electron scatters and occupies a spin-up "d" orbital).
 - The strong difference in density of 3d states at E_F for spin \uparrow and spin \downarrow results in strongly different spin dependent scattering rates. Many empty 3d states for spin \downarrow imply a large probability of scattering.
 - The change in mean free path λ_i implies changes in the resistivity, such as: mean free paths: $\lambda_{\downarrow} \ll \lambda_{\uparrow} \rightarrow$ conductivities: $\sigma_{\downarrow} \ll \sigma_{\uparrow}$

Spin polarized transport

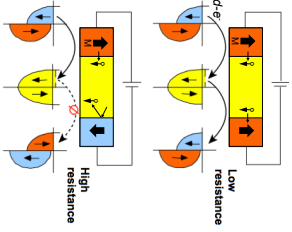
Mott model

- This translates into a **different bulk resistivity** for spin-up and spin-down electrons, dependent on the magnetization of the material.
- We assume that the probability of spin-flip scattering is very low.



Spin polarized devices

- The figure illustrates the basic action in a simple spin-polarized device, where it is assumed that the electrons are traveling from a ferromagnetic metal, through a normal metal, and into a second ferromagnetic metal.
- In the case where the magnetizations (or, equivalently, the magnetic moments) of the two ferromagnetic metals are in an aligned state, the electrons can freely move from one layer to the next and the resistance is low. When the layers are in the anti-aligned state the carrier movement is blocked at one interface and the measured resistance will be higher.
- In the geometry shown in the figure the current is perpendicular to the plane formed by the interface of the different materials (so-called **current-perpendicular-to-plane** or **CPP geometry**). Actual devices are generally not fabricated in this way, but in the **current-in-plane** (CIP) geometry

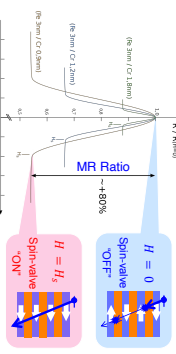


Materials Physics and Technology for Nanoelectronics Magnetic Materials

KU LEUVEN

Giant magnetoresistance (GMR)

- The CIP geometry makes use of the giant magnetoresistance (GMR) effect in thin magnetic multilayers.



Giant magnetoresistance in multi-layer structures.

Materials Physics and Technology for Nanoelectronics Magnetic Materials

KU LEUVEN

Giant magnetoresistance (GMR)

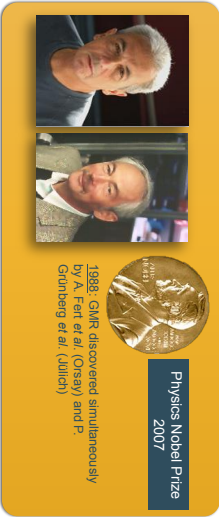
- A very simple resistor model is useful as a starting point for understanding the origin of the current-in-the-plane (CIP) GMR. In this model each metallic bilayer is treated as an independent resistor.
- If all the magnetic layers are aligned (spin-valve 'ON'), there is no strong interface scattering. Hence the whole stack acts as a bulk material (surface scattering is not important) and the resistance measured in the stack is the standard resistance, the GMR is zero.
- If the magnetic layers are antiparallel (spin-valve 'OFF'), thickness of each film is smaller than the mean free path of the electrons (λ), the electrons may scatter strongly at the interface and the resistance of each film is defined but such scattering:

$$R_{\text{film,fin.}} = 1 + \frac{2d}{D} (1 - P) \quad \text{which is valid for } \frac{\lambda}{D} > 0.3, P = 0 - 1 \quad (\text{Slides # 46, Chapter 3})$$

(then, if the magnetization of each fin is the same, the interface scattering is minimized. The material would be equivalent to have a thick conductive film with thickness $D \gg \lambda$, and the resistance measured for the stack is low. On the other hand, if the magnetization of each magnetic fin is opposite to the neighboring films, the material behaves as a stack of thin films with thickness $D < \lambda$, in which surface scattering is much higher. Therefore, GMR can be observed.)

Giant magnetoresistance (GMR)

- This spin polarization effect led to the discovery of the GMR.



58

KU LEUVEN

Spin polarized devices

Materials Physics and Technology for Nanoelectronics Magnetic Materials

KU LEUVEN

Hard Disk Drive (HDD) based on GMR

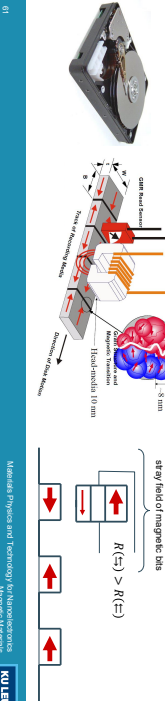
Materials Physics and Technology for Nanoelectronics Magnetic Materials

Spin polarized devices

- GMR: To make a technologically useful device, a "pinning" layer is added to make it harder to change the magnetization of one layer than the other.



- This structure can be used, e.g., to make GMR read heads which have found widespread application in hard disk drives (HDD).



61

Materials Physics and Technology/Nanoelectronics/Magnetic Materials

KU LEUVEN

Magnetic Tunnel Junction (MTJ) and Magnetic RAM (MRAM)



Magnetic Tunnel Junction (MTJ)

- A very important structure in spin electronics is the **magnetic tunnel junction** (MTJ).
- It is a magnetic storage and switching device in which two magnetic layers are separated by an insulating barrier (e.g. aluminum oxide, typically 1-2 nanometers thick) allowing an electronic current whose magnitude depends on the orientation of both magnetic layers to tunnel through the barrier when subject to an electric bias.

- The electron spin is not affected by the tunneling.
- The tunneling probability T depends on the barrier height and thickness of the layer:

$$\text{tunneling probability } T(E, V) f(E_F, \alpha) [1 - f(E_F, \alpha)]$$

(top figure),

spins states with down orientation can be injected from the cathode (M1), and occupy empty down spin states in the anode (M2), leading to a large tunneling current, since:

$$J_{\text{tunnel}} \propto T(E, V) f(E_F, \alpha) [1 - f(E_F, \alpha)]$$

spin dependent tunneling, $M/R = (R_{\parallel} - R_{\perp})/R_{\parallel} \gg 1$

Ferromagnetic metal 1

Tunnel barrier (Al_2O_3 , ...)

Ferromagnetic metal 2

Ferromagnetic metal 1

Tunnel barrier (Al_2O_3 , ...)

Ferromagnetic metal 2

- If the magnetic moments of the two ferromagnetic layers are parallel (top figure), spins states with down orientation can be injected from the cathode (M1), and occupy empty down spin states in the anode (M2), leading to a large tunneling current, since:



- The tunneling probability T depends on the barrier height and thickness of the layer:
- On the other hand, if the magnetic moments of the two ferromagnetic layers are anti-parallel (bottom figure), there are no empty states with down spins available at the anode (M2), and the tunneling current is much reduced.

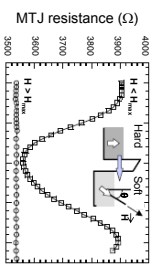
64

Materials Physics and Technology/Nanoelectronics/Magnetic Materials

KU LEUVEN

The Magnetic Tunnel Junction

- Since such $M1 / \text{Insulator} / M2$ structure allow the injection of electrons with a specific spin orientation, they are also called "spin valves".
- The resistance of the magnetic tunnel junction can be modulated by changing the orientation of the magnetization of one electrode with respect to the other, as illustrated in the figure for a CoFe/ Al_2O_3 /Co structure, where the resistance is shown as a function of the angle θ between the applied magnetic field and the direction along the magnetization of the CoFe magnetic layer.



Resistance of the magnetic Co-Fe/ Al_2O_3 /Co magnetic tunnel junction as a function of the angle of the applied field for fields below and above the critical value. The resistance varies ~10% between high and low values.

65

Materials Physics and Technology/Nanoelectronics/Magnetic Materials

KU LEUVEN

The Magnetic Tunnel Junction

- In the CoFe/ Al_2O_3 /Co structure, the CoFe (M1) layer is a hard-magnetic material, such that it keeps the orientation of its magnetization under the applied magnetic field, for $H < H_{\text{max}}$.
- The Co layer (M2) is a soft magnet, such that the orientation of its magnetization can be changed under the application of the magnetic field. When $\theta = 0$, the magnetizations in M1 and M2 are parallel, and the resistance is low. When $\theta \sim 180^\circ$, magnetizations in M1 and M2 are anti-parallel, and the resistance is large.
- When $H > H_{\text{max}}$, the magnetization of M1 and M2 follows the orientation of H , and they are always parallel, explaining the low resistance observed in this case.

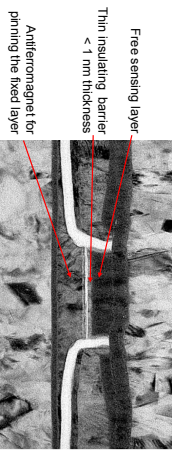
63

Materials Physics and Technology/Nanoelectronics/Magnetic Materials

KU LEUVEN

The Magnetic Tunnel Junction

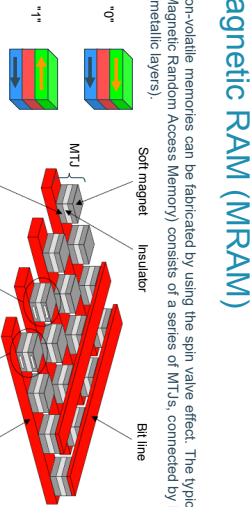
- MTJs are used in the write/read head of hard disk drives. As they are more sensitive than write/read heads based on GMR, they allow for a higher information density on the hard disk.



S. Mo 2001 (Seagate)

- For the tunnel layer typically amorphous oxides such Ti_2O_5 or Al_2O_3 were initially used. Later on, epitaxial tunnel oxides (MgO) were introduced, enhancing significantly the resistance contrast.

Materials Physics and Technology - Nanoelectronics
Magnetic Materials



- Magnetic non-volatile memories can be fabricated by using the spin valve effect. The typical structure of a MRAM (Magnetic Random Access Memory) consists of a series of MTJs, connected by bit lines and a word lines (metallic layers).

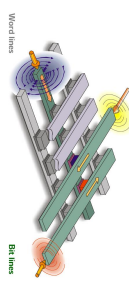
- Principle:
 - store binary information on arrays of magnetic tunnel junctions connected by conducting lines, that serve to address each cell individually for reading and writing
 - writing by sending current pulses in conducting lines

Materials Physics and Technology - Nanoelectronics
Magnetic Materials

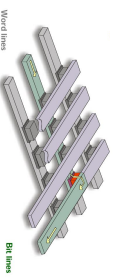


The Magnetic RAM (MRAM)

Writing



Reading



Word lines

Bit lines

From MRAM to 'spin transfer' STT-MRAM

- To write the bits of the MRAM, a high current is injected in the bit and word lines. These currents induce magnetic fields (Ampere's law) that add to each other, leading to a sufficiently high magnetic field to orient the magnetization of the soft magnetic layer in the magnetic tunnel junction.
- The magnetization of the soft magnet compared to the reference layer results in "low" or "high" values for the resistances of these junctions that can be associated with "1" and "0".

- In conventional field-induced MRAM the write operation is carried out by the current flowing through the wires. The currents generate magnetic fields around the wires. Switching occurs in the cell only if the magnetic fields from both currents are present at the magnetic pillar.



A. Manjavacas et al. *Semicond Sci Technol*, 21, 1205-1206

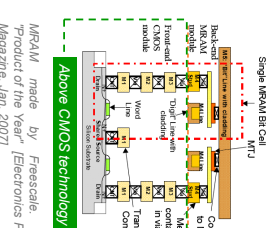
Spin Transfer Torque (STT) and STT-MRAM

71

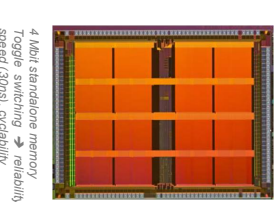


KU LEUVEN

• These memories initially received a lot of attention for specific applications as they are very robust and can be made on top of CMOS made circuits. However, due to various issues the technology never became a main-stream product.



MRAM made by Freescale. Named 'Product of the Year' [Electronics Products Magazine Jan 2007]

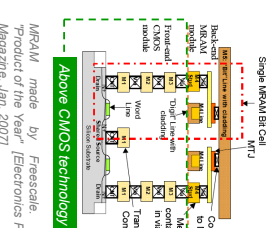


Materials Physics and Technology - Nanoelectronics
Magnetic Materials

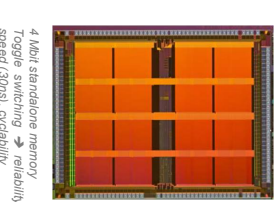


The Magnetic RAM (MRAM)

• These memories initially received a lot of attention for specific applications as they are very robust and can be made on top of CMOS made circuits. However, due to various issues the technology never became a main-stream product.



MRAM made by Freescale. Named 'Product of the Year' [Electronics Products Magazine Jan 2007]

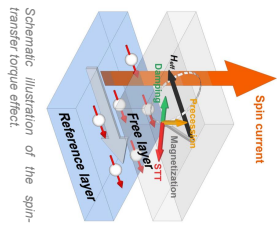


Materials Physics and Technology - Nanoelectronics
Magnetic Materials



From MRAM to 'spin transfer' STT-MRAM

- Spin Transfer Torque (STT) opened a new way of manipulating magnetic dynamics by using spin polarized currents instead of magnetic fields.
- In general, when electrons pass through the thick/hard fixed magnetic layer, the spins of the electrons become aligned with the magnetization of this layer.
- When these spin-polarized electrons enter the free layer (thinner/softer), their spin orientations are getting aligned with the magnetization of the free layer within a transition layer of a few Angstroms. But at the same time, those electrons exert a torque on the magnetization of the free layer by action-reaction, which can cause magnetization switching if the torque is large enough to overcome the damping.
- Smaller torque values result in magnetization precession around the effective magnetic field.



Schematic illustration of the spin-transfer torque effect.

A. Maniv et al. Secondary-Source Spin Technology, 3 (2016) 113–20

KU LEUVEN

- In 1935, Landau and Lifshitz have proposed an equation describing the damped motion of the magnetization in a ferromagnet known as the Landau-Lifshitz (LL) equation. This equation could be used only in case of small damping. In 1955, Gilbert proposed a modification to the equation which describes the strong damping in the thin films.
- A macro-spin model treats a nanomagnet with the assumption that its internal magnetic degrees of freedom are frozen, so the dynamics of macro-spins can be phenomenologically described by the Landau-Lifshitz-Gilbert (LLG) equation:

$$\frac{d\vec{M}}{dt} = -\gamma\mu_0(\vec{M} \times \vec{H}_{eff}) - \alpha\gamma\mu_0\vec{M} \times (\vec{M} \times \vec{H}_{eff})$$

where γ is the gyromagnetic ratio [rad s⁻¹T⁻¹], α the dimensionless damping coefficient, M_s is the saturation magnetization.

The LLG describes the MRAM switching by magnetic field. In order to be able to describe a switching STT-MRAM, an additional spin transfer torque (STT) term must be added. At the end yielding the Landau-Lifshitz-Gilbert-Slonczewski equation:

$$\frac{d\vec{M}}{dt} = -\gamma\mu_0(\vec{M} \times \vec{H}_{eff}) - \alpha\gamma\mu_0\vec{M} \times (\vec{M} \times \vec{H}_{eff}) - \beta\vec{M} \times (\vec{M} \times \vec{n}_j)$$

β the coefficient for the STT which depends on both the spin polarization and the geometric configuration between the incoming spin and the local moments in the free layer and j the current density. The spin transfer torque counteracts the damping.

Materials Physics and Technology: Nanoelectronics
Magnetic Materials

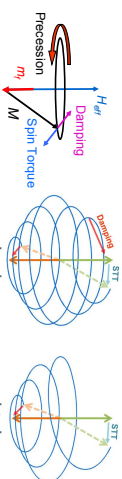
KU LEUVEN

Spin Transfer Torque (STT)

- Landau-Lifshitz-Gilbert-Slonczewski equation:

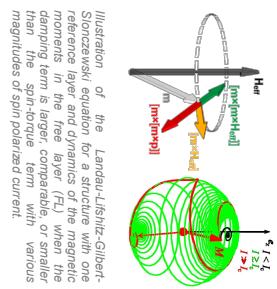
$$\frac{d\vec{M}}{dt} = -\gamma\mu_0(\vec{M} \times \vec{H}_{eff}) - \frac{\alpha\gamma\mu_0}{M_s}\vec{M} \times (\vec{M} \times \vec{H}_{eff}) - \beta\vec{M} \times (\vec{M} \times \vec{J}\vec{n}_j)$$

Spin evolution term: Excitation term: Intrinsic damping STT term



Precession of the spin in switching state for $J = J_c$ and $J > J_c$. The blue line shows the trajectory, and the bold arrows show the initial and final states of magnetization. The dotted arrows show an intermediate state of magnetization.

- For switching of the free layer to occur, a critical current is needed to make the spin torque larger than the damping force.
- When J is small and the spin torque term less than the damping term, the dynamics damp out into an equilibrium state.
 - When the spin torque is large enough that it overcomes the intrinsic damping (i.e. larger than the critical current), the effective damping coefficient becomes negative. In this case the deviation from the equilibrium state is amplified and the magnetic moments are switched, which can be detected by a resistance change in the magnetic sandwiched structure, e.g. MTJs or spin-valves.
 - When J and H satisfy certain conditions, persistent precession of the magnetization can be obtained at a frequency of several GHz. When the precession occurs, the angle between the magnetic moments in the free layer and the pinned layer changes rapidly. Due to the magnetoresistance effect, it gives rise to a resistance change at high frequency; therefore a DC current/voltage induced microwave emission can be observed in the device.



Materials Physics and Technology: Nanoelectronics
Magnetic Materials

KU LEUVEN

Spin Transfer Torque (STT)

- In this way the spin transfer torque can be used to write a 0 or a 1 into the magnetic memory just by changing the direction of the current flow.

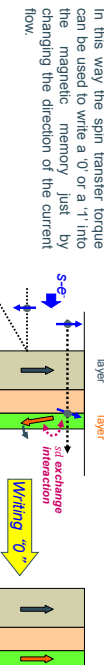


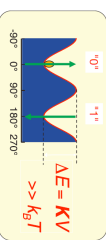
Figure illustrating the writing of a 0 or 1 by a bipolar current density J_+ and J_- .
J. C. Slonczewski, Jmmm 19, 1 (1989)

Materials Physics and Technology: Nanoelectronics
Magnetic Materials

KU LEUVEN

Magnetic energies for storage

- In order to be useful for non-volatile memory applications, a high thermal (bit) stability is required.
- The stability of the magnetic memory is determined by the magnetic anisotropy energy of the system.
- The volume must be large enough to keep magnetic energy larger than thermal energy. There is a limit in the scaling!!



Magnetic anisotropy energy
Total energy changes with the orientation of \vec{M}
magnetic storage of information

77

78

Materials Physics and Technology for Nanoelectronics

Organic electronics

KU Leuven
Clement Merckling
mec
KU Leuven
Francisco Medina-Lopez
merckling.clement@mech.kuleuven.be
medina-lopez.francois@mech.kuleuven.be
MATERIALS AND
KU Leuven
KU Leuven
KU Leuven

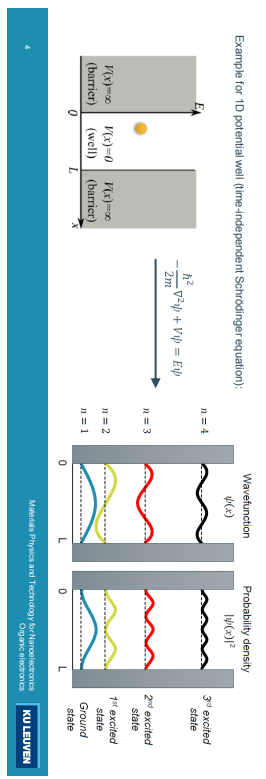
Outline

- Hybridization
- Electronic structure of conjugated molecules
- Transport in organic electronic materials
- Applications of organic electronic materials



Hybridization

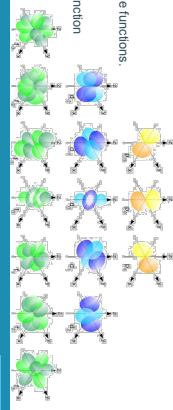
- Atomic orbitals (review from Chapter 2: Solids)
 - The Schrödinger equation provided the **wavefunction**, $\Psi(\vec{r}, t)$, of an electron in an atom, the probability of finding it at certain place, $|\Psi|^2$, and its quantized **energy**, E .



Hybridization

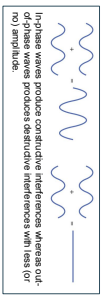
- Atomic orbitals (review from Chapter 2: Solids)
 - The probability density function $|\Psi|^2$ in 3D led to the definition of the **atomic orbitals (AOs)** (or zones in the atom where the chances to find electrons are high)

Overview of atomic orbitals shapes of s, p, d and f wave functions.
The color of orbitals represent the phase of the wavefunction (positive or negative amplitude).



Hybridization

- Molecular orbitals (review from Chapter 2: Solids)
 - The solution of the Schrödinger eq. to define molecular orbitals (MO) come from the **linear combination of AOs (LCAO)**:



Example H₂:

(a), (b) Wavefunctions ψ of two H 1s AO and formation of a bonding σ_{g} MO. The probability density $|\psi|^2$ of finding the electron in between the two nuclei is high. The node corresponding to zero electron probability density between the nuclei.

(c), (d) Formation of an antibonding σ^{*} MO and probably density $|\psi|^2$ illustrating the nodes corresponding to zero electron probability density between the nuclei.

(e), (f) Wavefunctions combined for σ_{g} . In-phase waves produce constructive interference whereas out-of-phase waves produce destructive interference which less (or no) amplitude.

5 Materials Physics and Technology for Nanoelectronics
Organic electronics
KU LEUVEN

Hybridization

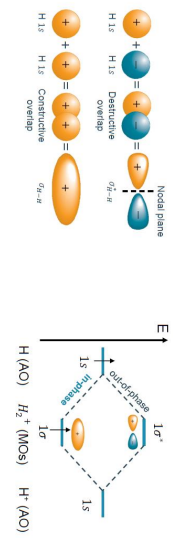


Hybridization

- Molecular orbitals (review from Chapter 2: Solids)

- The MO's present different **energy** states that depends on whether the **wavefunction of the electrons from the bonding atoms are in-phase or out-of-phase**

Example of H_2 :



$\text{H}(\text{AO}) \quad \text{H}_2 \text{ (MOs)} \quad \text{H}^+(\text{AO})$

KU LEUVEN

10

- Hybridization: Issue of LCAO
- Consider borane (boron trihydride, BH_3):

Greater accuracy can be obtained by using trial wave functions incorporating two or more AOs from individual atoms (forming **hybrid AOs**) as this can lead to MOs of lower energy through increased overlap.

“**Hybridization**” is a mathematical process which is useful in modifying electron densities to allow bonding geometries and electron densities in more complex molecules to be described. The driving force is looking the lowest net potential energy.

Hybridization

- Hybridization: Issue of LCAO

- In the LCAO approach, MO's were built **only from one AO** from each atom.



Schematic drawing of bonding and antibonding MO's formed by p-p overlap

Does this approach correspond to reality?

Materials Physics and Technology for Nanoelectronics
Organic electronics

KU LEUVEN

11

Hybridization

- Hybridization: Explains structure of molecules

- Consider borane (boron trihydride, BH_3):
Using hybridization we can construct three equivalent hybrid AOs for B that explains the regular structure of BH_3 :



These hybrid AOs extend far from the B nucleus in directions at 120° to each other. The energy cost of creating the hybrid AOs is more than offset by the increased overlap and more negative bond integrals, thereby producing a more stable BH_3 molecule. Such hybrids are called **sp2** or **trigonal hybrids**.



KU LEUVEN

- Hybridization: Issue of LCAO
- Consider borane (boron trihydride, BH_3):



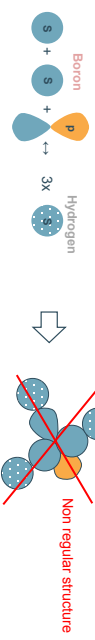
Hybridization

- Hybridization: Issue of LCAO

- Consider borane (boron trihydride, BH_3):

The electronic ground state of B is $1s^2 2s^2 2p^1$:

If we assume the MO's being formed from the 3 orbital above, the symmetry of BH_3 can not be explained!



Hybridization

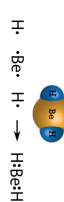
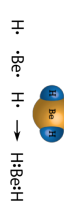
- Hybridization: Energy implications

- Consider, for example, beryllium dihydride (BeH_2):

This is known to be a linear molecule ($\text{H}-\text{Be}-\text{H}$) with an angle of 180° between the two Be-H bonds. MOs to describe the Be-H bonds must be built from the 1s AOs of hydrogen.

The ground state of Be atoms is: $1s^2 2s^2$

... but constructing MOs for the two Be-H bonds using only 2s AOs of Be yields results for the bond strength and bond length that disagree strongly with experiment.



Hybridization

- Hybridization: Energy implications

- Consider, for example, beryllium dihydride (BeH_2): Suppose we instead construct our MOs for BeH_2 with the following hybrid AOs that also contain $2p$ AOs (which have energies only slightly higher than our $2s\text{-AOs}$):

$$\phi_1 = \frac{\phi_{2s} + \phi_{2p_x}}{\sqrt{2}}$$

Because the $2p$ orbitals have a slightly higher energy than the $2s$ -AOs, but these hybrids extend much farther from the nucleus, they produce more overlap with the $1s$ orbitals, resulting in a bond integral H_{12} that is more negative, resulting in a lower total energy (stronger bond).

$$\langle \rho \rangle = \int \psi^* \psi d\tau$$

$$H_{12} = \int \phi_1 H_{12} \phi_1 d\tau = \int \phi_2^* H_{12} \phi_2 d\tau = H_{12}$$

$H_{12} = H_{12}$ is called the Bond (or resonance) integral and $H_{11} = H_{22}$ the Coulomb Integral.

(We have chosen p_z because we define the molecular axis as the x -axis).
The $\sqrt{2}$ normalizes the functions).

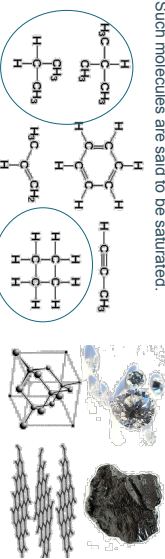


Hybridization

- Hybridization: Energy implications

- The four valence electrons of carbon ($Z = 6$), combined with various degrees of hybridization, give carbon a great versatility in bonding. This versatility is responsible for the richness of organic chemistry.

In many molecules, carbon uses sp^3 hybridization to form bonds with four other atoms. Such molecules are said to be saturated.



16

KU LEUVEN

Molecular Physics and Technology: Organic electronics

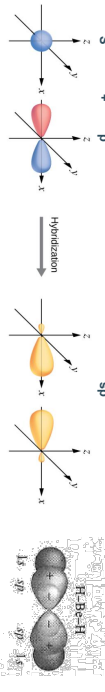
Chapter 2: solids

KU LEUVEN

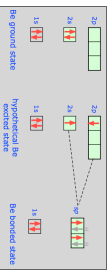
Hybridization

- Hybridization: Energy implications

- Consider, for example, beryllium dihydride (BeH_2): $\phi_1 = \frac{\phi_{2s} + \phi_{2p_x}}{\sqrt{2}}$ and $\phi_2 = \frac{\phi_{2s} - \phi_{2p_x}}{\sqrt{2}}$



Such hybrids are called sp or linear hybrids



Molecular Physics and Technology: Organic electronics

KU LEUVEN

17

KU LEUVEN

KU LEUVEN

KU LEUVEN

Hybridization

- Hybridization: summary

Number of hybrid orbitals	Arrangement	Hybridization
2	linear	sp
3	triangular	sp^2
4	tetrahedral	sp^3
5	pentagonal bipyramidal	sp^{3d}
6	octahedral	sp^3d^2

sp or linear hybrids

sp² or trigonal hybrids

sp³ or tetrahedral hybrids

sp^{3d} or pentagonal bipyramidal hybrids

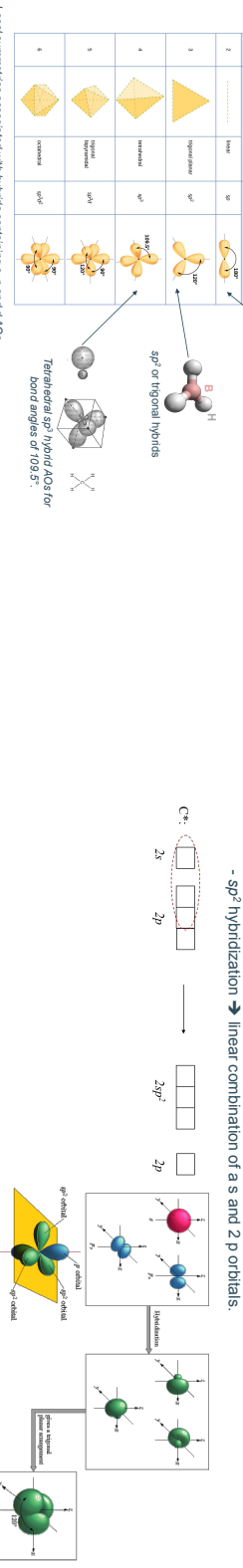
sp^{3d}² or octahedral hybrids

Tetrahedral sp^3 hybrid 4AOs for bond angles of 109.5°

Hybridization

- Carbon hybridization:

- sp^2 hybridization \rightarrow linear combination of a s and $2p$ orbitals.



18

KU LEUVEN

KU LEUVEN

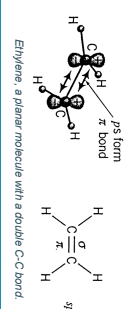
KU LEUVEN

Hybridization

- Carbon hybridization:

- sp^2 hybridization \Rightarrow Example for ethylene.

This molecule is planar, and each carbon has only three neighbors, with two C-H bonds and one C-C bond. The one $2p\text{AO}$ on each carbon, extending out of the molecular plane, forms a π bond with the corresponding $2p\text{AO}$ on the other carbon. The C-C bond is therefore a **double bond** consisting of one σ bond (sp^2-sp^2) and one π bond ($p-p$).



19

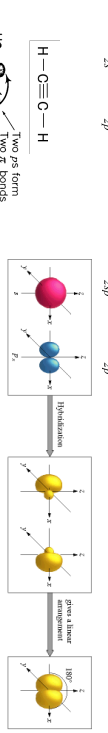
Molecular Physics and Technology: Nanoelectronics
Organic electronics



Hybridization

- Carbon hybridization:

- sp hybridization \Rightarrow linear combination of a s and a p orbital.



Acetylene, a linear molecule with a triple C-C bond.

20

Molecular Physics and Technology: Nanoelectronics
Organic electronics



Electronic structure of conjugated molecules



21

Molecular Physics and Technology: Nanoelectronics
Organic electronics



Electronic structure of conjugated molecules

- Conjugated molecules:

- Those with connected p orbitals with delocalized electrons, which in general lowers the overall energy of the molecule and increases stability \rightarrow **alternating multiple single bond**.

- In most polyatomic molecules, bonding can be described in terms of MOs that are essentially localized on individual bonds (built from AOs of two neighboring atoms). This approach breaks down for conjugated compounds.

22

Molecular Physics and Technology: Nanoelectronics
Organic electronics



Electronic structure of conjugated molecules

- Conjugated molecules: delocalization

- π -bonding between sp^2 C atoms results in delocalized MOs.



Two resonance structures
(polyacetylene).



23

Molecular Physics and Technology: Nanoelectronics
Organic electronics

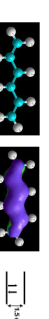


Electronic structure of conjugated molecules

- Conjugated molecules: delocalization
 - Orbitals extend to the whole molecule



Polystyrene: insulator



Polyacetylene: semiconductor

Nobel Prize in Chemistry 2000 "for the discovery and development of conductive polymers"



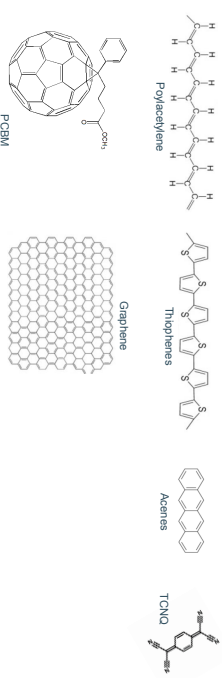
24

Molecular Physics and Technology: Nanoelectronics
Organic electronics



Electronic structure of conjugated molecules

- Conjugated molecules: examples

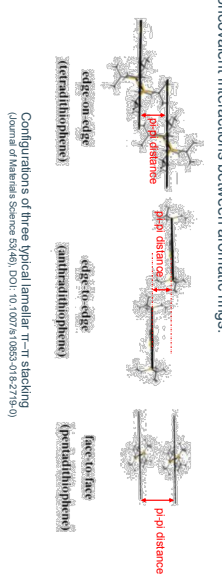


25

Materials Physics and Technology for Nanoelectronics
Organic electronics

Electronic structure of conjugated molecules

- Conjugated molecules: π - π stacking
- Noncovalent interactions between aromatic rings.



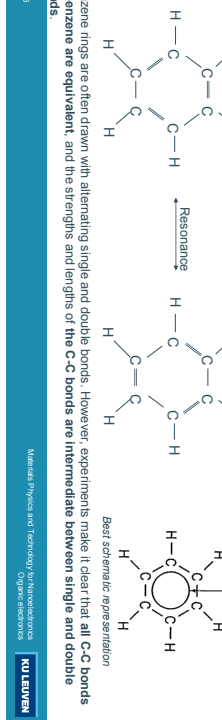
26

Materials Physics and Technology for Nanoelectronics
Organic electronics
(Journal of Materials Science 2017, 50, 10:26-41; DOI: 10.1007/s10853-016-0178-0)

Electronic structure of conjugated molecules

- Conjugated molecules: Benzene

- Each of the C atoms is in a sp^2 hybridized state, forming a σ bond with H, a single σ bond with one neighbor-C atom, and a double (σ and π) bond with its other C neighbor. The π bonds results from the overlap between two adjacent $2p_z$ orbitals, considering the molecule lies in the (x, y) plane (planar molecule).



26

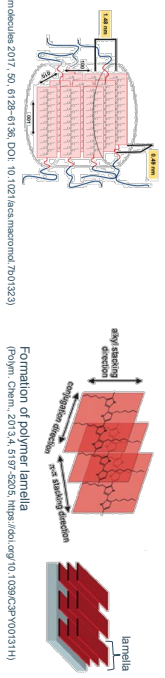
Materials Physics and Technology for Nanoelectronics
Organic electronics

Electronic structure of conjugated molecules

- Conjugated molecules: π - π stacking

- Responsible of the lamella formation in electronic polymers.
- Leads to the crystallinity of electronic polymers. Electronic polymers are semicrystalline (amorphous and crystalline domains coexist).

- Conduction is best intramolecular (along conjugation direction) and along π - π stacking direction.



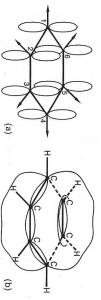
26

Materials Physics and Technology for Nanoelectronics
Organic electronics

Electronic structure of conjugated molecules

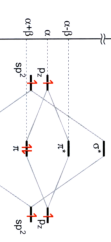
- Conjugated molecules: Benzene

- The π bonds results from the overlap between two adjacent $2p_z$ orbitals, considering the molecule lies in the (x, y) plane.



- Conjugated molecules: Energy structure
- The delocalization of the π electrons gives rises to a stable and strong bonding between the C atoms.

- When considering the electronic properties of conjugated systems, one need only to consider the delocalized π electrons (treated as valence electrons), usually lying at a higher energy level rather than the σ electrons (treated as core electrons).



27

Materials Physics and Technology for Nanoelectronics
Organic electronics

Electronic structure of conjugated molecules

- Conjugated molecules: Energy structure: The Hückel method.

• Applying the LCAO method to conjugated planar systems (called Hückel method when applied to π LCAs) allows to understand their electronic properties. We can illustrate this with benzene. With LCMO-MO theory, we can understand the benzene molecule by constructing delocalized π MOs that extend around the entire molecule: $\psi = c_1\phi_1 + c_2\phi_2 + c_3\phi_3 + c_4\phi_4 + c_5\phi_5 + c_6\phi_6$

- Each of the ϕ are $2p$ AOs, centered on each of the six carbon atoms and directed out of the molecular plane. The ring nature of benzene requires that ϕ_i bonds with ϕ_{i+1} as well as with ϕ_{i-1} .
- In the Hückel approximation the following simplifying assumptions are made:
 - The Coulomb integrals I_{ij} for each ϕ_j from adjacent carbon atoms are all the same (call them $\beta < 0$)
 - The bond integrals J_{ij} for each ϕ_j from adjacent carbon atoms are all zero. This assumption is also called the transfer integral.
- The overlap integrals $S_{ij} = \int \phi_i \phi_j dV$ are all zero. This assumption can be made legitimate with modest adjustments in the AOs. It is a severe approximation that makes the physics less realistic, but the maths easier.

- 31
- Molecular Physics and Technology: Nanoelectronics
Organic electronics
- KU LEUVEN
- Conjugated molecules: Energy structure: The Hückel method.
- Applying the Hückel method when applied to π electrons allows to understand their electronic properties. We can illustrate this with benzene. With LCMO-MO theory, we can understand the benzene molecule by constructing delocalized π MOs that extend around the entire molecule: $\psi = c_1\phi_1 + c_2\phi_2 + c_3\phi_3 + c_4\phi_4 + c_5\phi_5 + c_6\phi_6$
1. The Coulomb integrals I_{ij} for each ϕ_j from adjacent carbon atoms are all the same (call them $\beta < 0$)
2. The bond integrals J_{ij} for each ϕ_j from adjacent carbon atoms are all zero. This assumption is also called the transfer integral.
3. The overlap integrals $S_{ij} = \int \phi_i \phi_j dV$ are all zero. This assumption can be made legitimate with modest adjustments in the AOs. It is a severe approximation that makes the physics less realistic, but the maths easier.

Notice that the amplitude of the molecular MO is modulated by a sinusoid with wavelength (λ)
 \rightarrow Higher energy bands have more nodes which means larger values of the wavenumber $k=2\pi/\lambda$

32

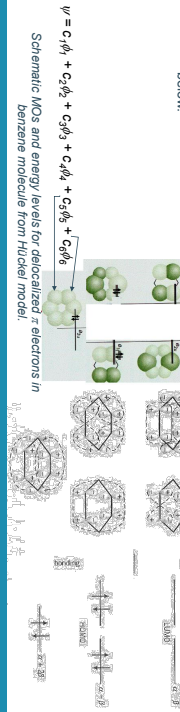
Molecular Physics and Technology: Nanoelectronics
Organic electronics

KU LEUVEN

Electronic structure of conjugated molecules

- Conjugated molecules: Energy structure: The Hückel method.

• Applying the Hückel method to benzene results schematically illustrated below.



33

KU LEUVEN

Electronic structure of conjugated molecules

- Conjugated molecules: Energy structure: The Hückel method.

• Applying the Hückel method to benzene...

1. Yields 6 MOs (three bonding and three antibonding). The lowest energy MO corresponds to all c_i being equal. The highest energy MO corresponds to c_i with alternating signs, with nodal planes between each atom pair.

2. Also shown are the corresponding energy levels, which include two pairs of degenerate levels. The energy of the bottom level is found to be $\alpha + 2\beta$ (the bond integral β is negative).

3. There are two degenerate bonding MOs with $E = \alpha + \beta$ (these are the Highest Occupied MOs, the HOMO level(s), two degenerate antibonding MOs with $E = \alpha - \beta$ (these are the Lowest Unoccupied MOs, the LUMO levels), and the highest antibonding MO level with $E = \alpha - 2\beta$.

4. The Coulomb energy α represents the reference state for 12 p_z electrons, and the difference in energy between the highest and lowest level is four times the bond integral β .

5. In the ground state of the benzene molecule, the three bonding levels are occupied, and the three antibonding levels are unoccupied.

Electronic structure of conjugated molecules

- Conjugated molecules: Energy structure: The Hückel method.

• Applying the Hückel method to butadiene...

1. Each of the carbon atoms in butadiene (C_4H_6) has three neighbors and sp^2 hybrids form σ bonds. The remaining 2p AOs, directed out of the molecular plane, form delocalized π MOs that extend along the carbon chain, and can be treated in the Hückel approximation.

2. The figure shows the relative orientation of the p AOs in each of the four MOs (two bonding, two antibonding), with dashed lines suggesting the outline of the various MOs. The four energy levels are $\alpha + 1.62\beta$, $\alpha + 0.62\beta$, $\alpha - 0.62\beta$, and $\alpha - 1.62\beta$.

35

Molecular Physics and Technology: Nanoelectronics
Organic electronics

KU LEUVEN

Electronic structure of conjugated molecules

- Conjugated molecules: Energy structure: HOMO and LUMO shifting.

• The highest occupied orbital (HOMO) corresponds to the valence band edge of a semiconductor, while the lowest unoccupied orbital (LUMO) corresponds to the conduction band edge. The band-gap thus corresponds to the difference between HOMO and LUMO energy levels.

All the levels are confined in between an energy interval of 4β .

Energy levels and electron occupation for conjugated hydrocarbon with unbranched chain structures of one to 16 C atoms as calculated by the Hückel theory. The system with one C atom represents a spin-polarized CH_3^+ radical.

36

Molecular Physics and Technology: Nanoelectronics
Organic electronics

KU LEUVEN

Electronic structure of conjugated molecules

- Conjugated molecules: Energy structure: The Hückel method.

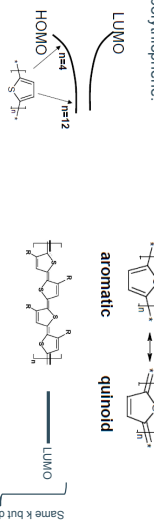
• Applying the Hückel method to butadiene...



- 34
- Molecular Physics and Technology: Nanoelectronics
Organic electronics
- KU LEUVEN

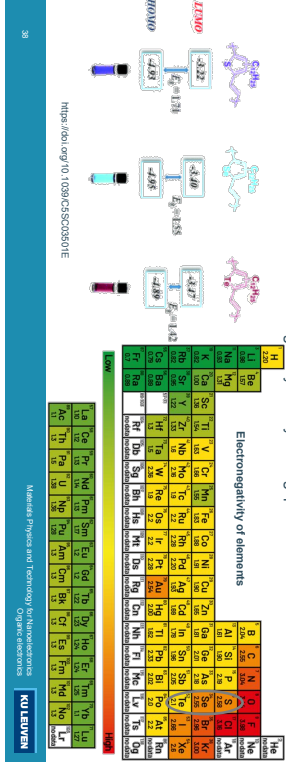
Electronic structure of conjugated molecules

- Conjugated molecules: Energy structure. HOMO and LUMO shifting.
- Example for polythiophene.



Electronic structure of conjugated molecules

- Conjugated molecules: Energy structure. HOMO and LUMO shifting.
- Heteroatoms with different electronegativity modify band gap



https://doi.org/10.1399/CSCC0301E

Materials Physics and Technology for Nanoelectronics

KU LEUVEN

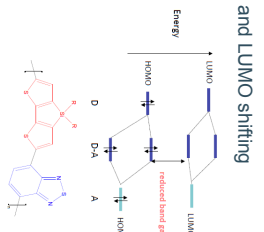
Electronic structure of conjugated molecules

- Conjugated molecules: Energy structure. HOMO and LUMO shifting
- Backbone twist



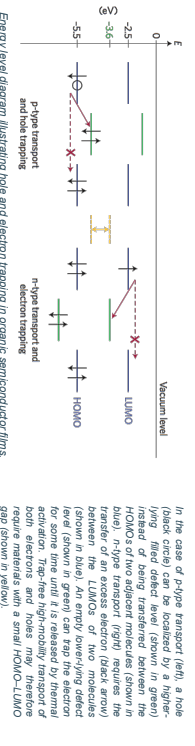
Twist reduces pi-orbital overlap -> bandgap increases

- Conjugated molecules: Energy structure. HOMO and LUMO shifting
- Donor-acceptor polymers. The push-pull approach.
- Molecular orbital hybridization reduces the bandgap
- Why is small bandgap convenient...?



Electronic structure of conjugated molecules

- Conjugated molecules: Energy structure. HOMO and LUMO. Why it matters?
 - Charge trapping: Electrons and holes differ strongly in their sensitivity to trapping at defects or impurities. The different susceptibility of electrons and holes to trapping results from the dissimilar energies of the HOMO and LUMO. For most organic semiconductors, the HOMO is located around -5 to -6 eV versus vacuum, whereas the LUMO ranges from about -2 to -3 eV.



41

Electronic structure of conjugated molecules

- Conjugated molecules: Energy structure. HOMO and LUMO. Why it matters?
 - Charge trapping: Defects or impurities frequently have empty orbitals between -3 eV and -5 eV that can take up an electron. Filled orbitals above -5 eV (suitable for accepting holes) are more elusive.



42

Electronic structure of conjugated molecules

- Conjugated molecules: Energy structure. HOMO and LUMO. Why it matters?
- Ambient stability: Polymers with ionization potential < 4.9 eV get oxidized by wet oxygen. Hence they are unstable in air.
- In most n-type materials, oxidation traps electrons from the LUMO reducing electron mobility \rightarrow Lack of n-type material!
- In some p-type materials, oxidation can act as a dopant. P-type materials with low HOMO are more stable. The HOMO can be lowered by making electron poor materials \rightarrow Electron withdrawing groups, backbone twist, configuration weak, etc.

Polymer with $E_{\text{ion}} < 4.9$ eV tend to be unstable with respect to oxidation (oxidizing) by wet oxygen.

44

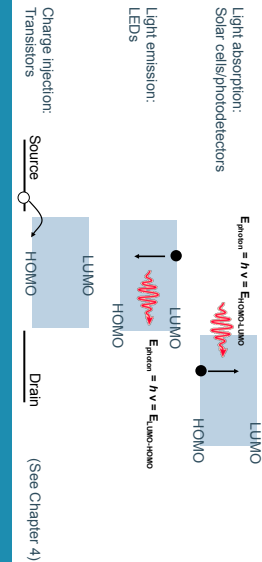


Polymer with $E_{\text{ion}} < 4.9$ eV tend to be unstable with respect to oxidation (oxidizing) by wet oxygen.

44

Electronic structure of conjugated molecules

- Conjugated molecules: Energy structure: HOMO and LUMO. Why it matters?
- Tuning performance of devices



45

Materials Physics and Technology: Organic electronics

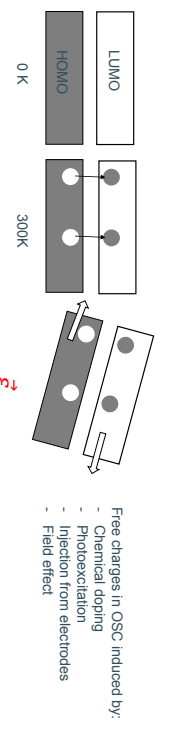
KU LEUVEN

Transport in organic electronic materials

- Conductivity and mobility: Charge carrier mean charge density
- Current density: $J = \sigma \epsilon = [n q] \mu \epsilon$

$$\mu = \frac{\nu}{\eta} \frac{\epsilon}{\epsilon}$$

Conductivity Electric field



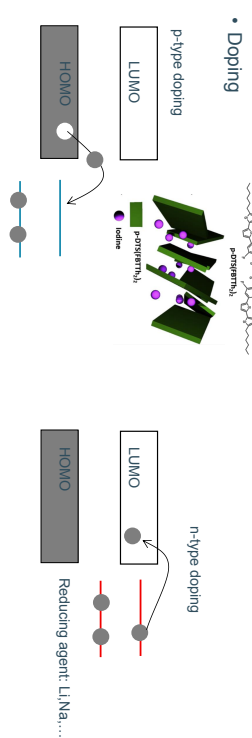
47

Materials Physics and Technology: Organic electronics

KU LEUVEN

Transport in organic electronic materials

- Doping



48

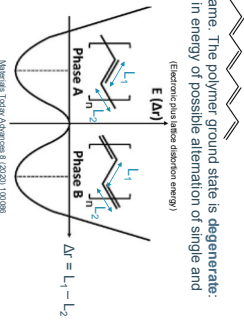
Organic Electronics, Volume 24, 2016, Pages 19-32

Materials Physics and Technology: Organic electronics

KU LEUVEN

Transport in organic electronic materials

- Degenerated vs non-degenerated conjugated molecules
 - In a polymer such as polyacetylene, the energy of phase A and phase B configurations are energetically equivalent with no change in energy of single and double bonds.
- The charge carriers created by doping in degenerated conjugated polymers are called solitons.



49

Materials Physics and Technology: Organic electronics

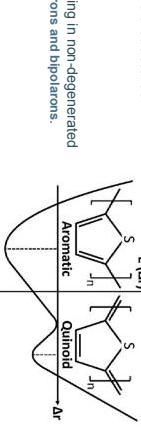
KU LEUVEN

Transport in organic electronic materials

- Degenerated vs non-degenerated conjugated molecules
 - In a polymer such as PEDOT, 

a non-degenerate ground-state is present due to the differences in energy between the aromatic (or benzenoid) and quinoid structures.

- The charge carriers created by doping in non-degenerated conjugated polymers are called polarons and bipolarons.



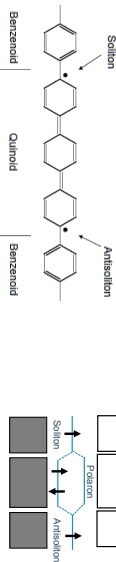
Materials Today Advances 3 (2020) 100366

KU LEUVEN

Transport in organic electronic materials

- Charges moving in organic semiconductors create changes in the bond-length alternation pattern.
- Quasi particles: Polarons

- Polaron: a bound soliton – antisoliton. The neutral polaron is not stable since soliton and antisoliton will annihilate.



53

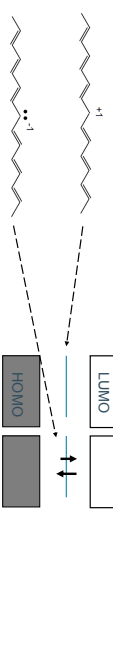
KU LEUVEN

Transport in organic electronic materials

- Charges moving in organic semiconductors create changes in the bond-length alternation pattern. Charge transport comes along chain distortion forming quasiparticles.
- Quasi particles: Solitons
 - Solitons: domain boundary between the A and B phases.



- A soliton can be ionized and transport charge



54

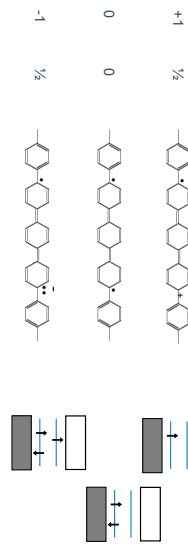
KU LEUVEN

Transport in organic electronic materials

- Quasi particles :

- Charged polarons: The charge and associated deformation act like a quasi-particle that transport charge across the molecule.

Charge Spin

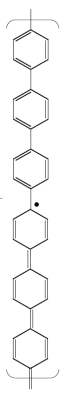


55

KU LEUVEN

Transport in organic electronic materials

- Charges moving in organic semiconductors create changes in the bond-length alternation pattern.
- Quasi particles: Solitons
 - Solitons: A soliton in a non-degenerate ground-state conjugated polymer costs energy because the quinoid part has more energy than the benzenoid part. Therefore, solitons are not stable in this kind of structures.



Benzene

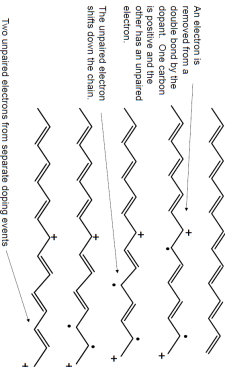
Quinone

- Solitons: A soliton in a non-degenerate ground-state conjugated polymer costs energy because the quinoid part has more energy than the benzenoid part. Therefore, solitons are not stable in this kind of structures.

Transport in organic electronic materials

- Quasi particles:

- Bipolarons: Are introduced via doping.



An electron is removed from the HOMO level and paired with a hole on the same chain. One electron is positive and the other has an unpaired electron.

The unpaired electron

shifts down the chain.

To two unpaired electrons from separate doping events reform a single bond. This is known as a recombination.

56

KU LEUVEN

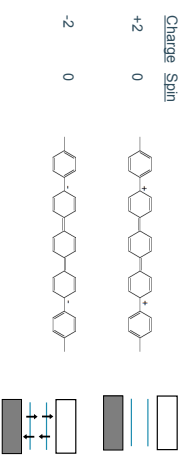
52

Materials Physics and Technology: Organic electronics

KU LEUVEN

Transport in organic electronic materials

- Quasi-particles:
 - Positive- and negatively-charged bipolarons: they also act as a quasi-particle that transport charge and lattice deformation throughout the molecule.

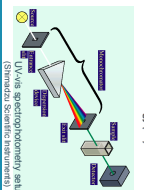
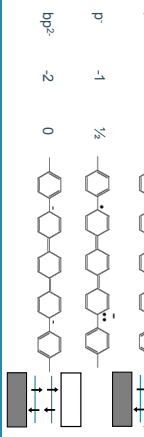
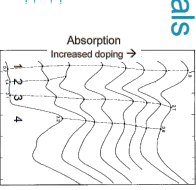
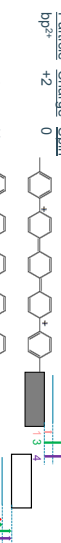


Materials Physics and Technology for Nanoelectronics
Organic electronics



Transport in organic electronic materials

- Quasi particles :



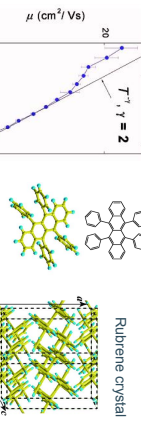
Materials Physics and Technology for Nanoelectronics
Organic electronics



Transport in organic electronic materials

- Mobility vs temperature: Band-like transport

Reviews of Modern Physics, Volume 78, 2006



DOI: 10.1103/PhysRevB.88.115458

TEMPERATURE (K)



DOI: 10.1103/PhysRevB.88.115458

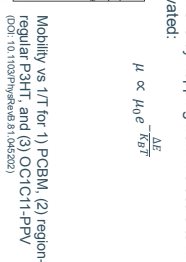
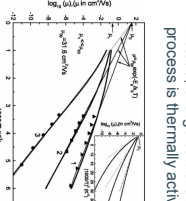
Band transport-like behavior observed in highly purified and crystalline organic semiconductors (OSC)

Materials Physics and Technology for Nanoelectronics
Organic electronics



Transport in organic electronic materials

- Mobility vs temperature: Variable Range Hopping (VRH) Transport
 - But most of the times OSC are too disordered to exhibit band transport behavior.
 - Instead charge carriers move by hopping from molecule to molecule. The hopping process is thermally activated:



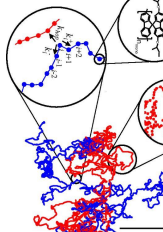
Materials Physics and Technology for Nanoelectronics
Organic electronics



Transport in organic electronic materials

- Mobility: connectivity

Crystalline aggregates
Amorphous phase



<https://doi.org/10.1021/bm000021q000020>

DOI: 10.1021/bm000021q000020

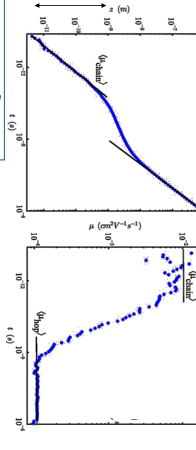
Which molecule would have larger L_p ?
Thiophenes
Acenes because tie rings are rigid

$\Delta L_{agg} \gg L_{percolation}$

$\Delta L_{agg} \ll L_{percolation}$

If the distance between aggregates $\Delta L_{agg} \leq L_p \rightarrow$

Tie-chain can bridge efficiently → High mobility

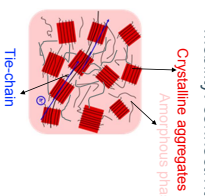


Materials Physics and Technology for Nanoelectronics
Organic electronics



Transport in organic electronic materials

- Mobility: time and length scales



Which molecule would have larger L_p ?
Thiophenes
Acenes because tie rings are rigid

$\Delta L_{agg} \sim L_{percolation}$

$\Delta L_{agg} \gg L_{percolation}$

$\Delta L_{agg} \ll L_{percolation}$

$\mu \propto \mu_0 e^{-\frac{\Delta E}{k_B T}}$

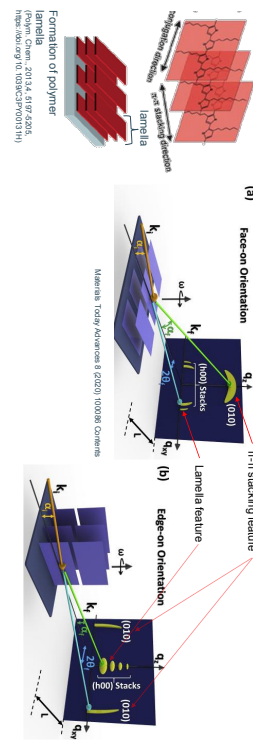
Materials Physics and Technology for Nanoelectronics
Organic electronics



61

Transport in organic electronic materials

- How to measure crystallinity: Grazing incidence wide angle X-ray diffraction (GWAXD patterns).



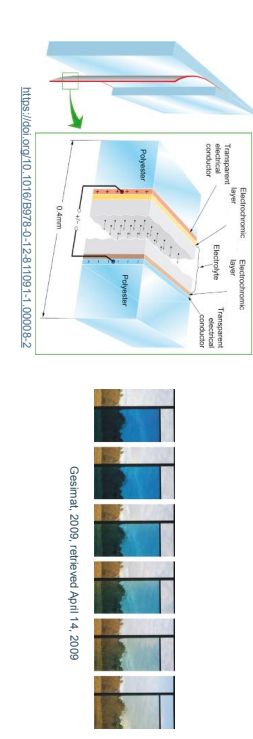
63

Materials Physics and Technology for Nanoelectronics
Light, Air and Space Electronics: Organic electronics

KU LEUVEN

Transport in organic electronic materials

- Electrochromic devices (ECDs): More visible light absorption by polarons -> "darker glasses" activated electrically



Materials Physics and Technology for Nanoelectronics
Organic electronics

KU LEUVEN

Applications of organic electronic materials

- Organic field effect transistors (OFETs)

• Historical evolution

Active-matrix displays are possible with OFETs
Frequency $\propto \mu$

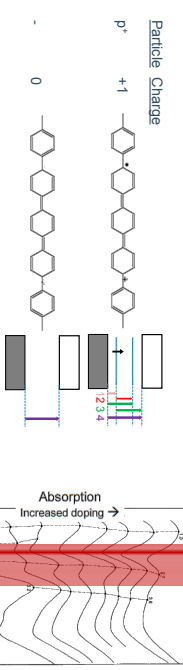


Applications of organic electronic materials

• Electrochromic devices (ECDs): Controlled doping of the material introduce visible light absorption by polarons

Transport in organic electronic materials

- Electrochromic devices (ECDs): Controlled doping of the material introduce visible light absorption by polarons



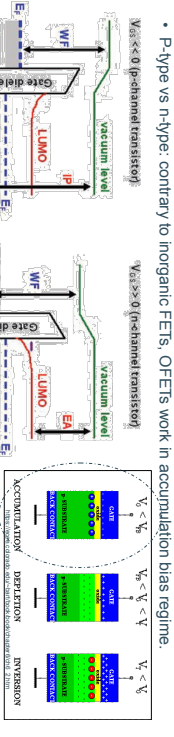
64

Materials Physics and Technology for Nanoelectronics
Organic electronics

KU LEUVEN

Applications of organic electronic materials

- Organic field effect transistors (OFETs)
 - P-type vs n-type: contrary to inorganic FETs, OFETs work in accumulation bias regime.

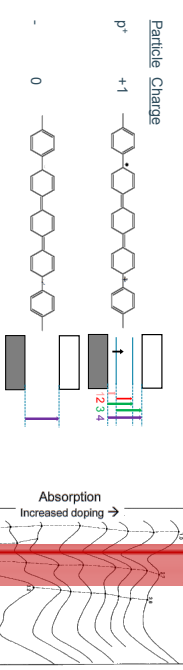


Applications of organic electronic materials

• Electrochromic devices (ECDs): Controlled doping of the material introduce visible light absorption by polarons

Transport in organic electronic materials

- Electrochromic devices (ECDs): Controlled doping of the material introduce visible light absorption by polarons



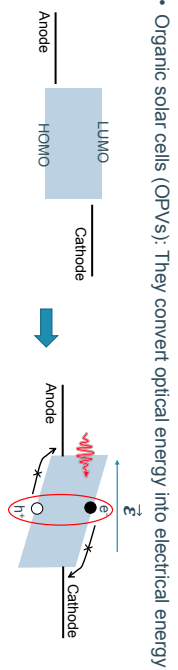
64

Materials Physics and Technology for Nanoelectronics
Organic electronics

KU LEUVEN

Applications of organic electronic materials

- Organic solar cells (OPVs): They convert optical energy into electrical energy



Exciton: quasi particle composed of a bound electron-hole pair.

Materials Physics and Technology: Nanoelectronics
Organic electronics

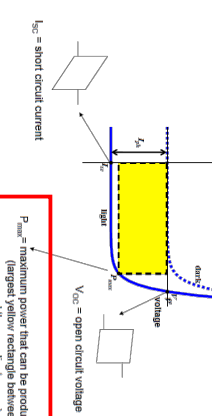


74

Applications of organic electronic materials

- Organic solar cells (OPVs): Performance

$$\text{Fill factor} = \frac{P_{\text{max}}}{I_{\text{SC}} V_{\text{OC}}} I_{\text{current}}$$

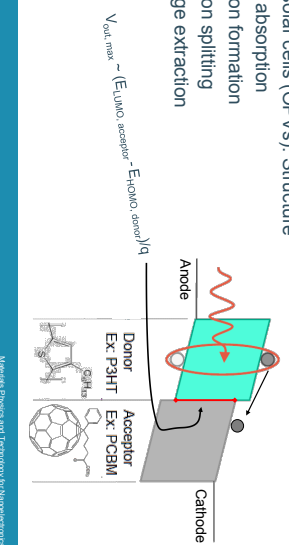


75

Applications of organic electronic materials

- Organic solar cells (OPVs): Structure

1. Light absorption
2. Exciton formation
3. Exciton splitting
4. Charge extraction



Materials Physics and Technology: Nanoelectronics
Organic electronics



76

Applications of organic electronic materials

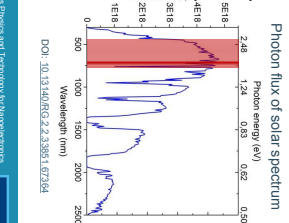
- Organic solar cells (OPVs): Efficiency

- Internal quantum efficiency (IQE)
(Photons ABSORBED / electrons out)
- External quantum efficiency (EQE)
(Rate of photons arriving to the device / rate of electrons out)
- Or incident photon to converted electron (IPCE)

$$I_{\text{sc}} = q \int E \Omega E(\lambda) / \text{PhotonFlux}(\lambda) d\lambda$$

- IQE & EQI < 1, IQE>EQI
- Power conversion efficiency (PCE)

$$\text{PCE} = \frac{\text{Electrical power generated}}{\text{incident optical power}} = \frac{P_{\text{max}}}{P_{\text{in}}}$$



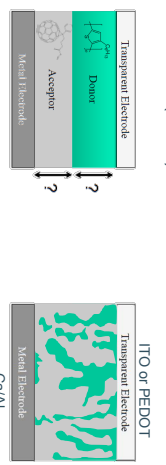
KU LEUVEN



77

Applications of organic electronic materials

- Organic solar cells (OPVs): Structure



- The thickness of the material should be at least 100 nm to absorb most of the light

- However, the exciton mean free path (before recombination) is only 10 nm

- It is necessary to split the exciton (reach a D/A interface) before it recombines!

→ Bulk heterojunction morphology: allow thick layers with many interfaces everywhere

78

Materials Physics and Technology: Nanoelectronics
Organic electronics



79

Applications of organic electronic materials

- Organic light emitting diodes (OLEDs)
- The most successful case of organic electronics



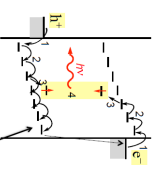
Materials Physics and Technology: Nanoelectronics
Organic electronics



80

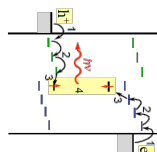
Applications of organic electronic materials

- Organic light emitting diodes (OLEDs)
- Structure: Multilayer



One layer makes it difficult to have balanced charge transport needed for high efficiency, specially considering the different mobility of h^+ and e^- (hole mobility is larger than electron mobility in organics).

Multilayer allows tuning charge transport balance



• An OLED (active matrix organic LED) makes up 15% of mobile device displays in 2016 (LG, Samsung, etc.)

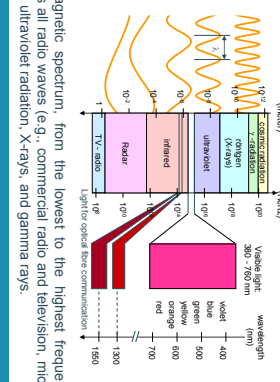
Applications of organic electronic materials

- Organic light emitting diodes (OLEDs)
- Structure: Multilayer



Electromagnetic spectrum

The theoretical description of light as electromagnetic waves has had an enormous impact on physics in the past two centuries.



The entire electromagnetic spectrum, from the lowest to the highest frequency (longest to shortest wavelength), includes all radio waves (e.g., commercial radio and television, microwaves, radar), infrared radiation, visible light, ultraviolet radiation, X-rays, and gamma rays.

2

Materials Physics and Technology for Nanoelectronics
Photonics

KU LEUVEN

The refractive index of a material n is a dimensionless number that describes how light propagates through that medium. It is defined as: $n = c/v$ where c is the speed of light in vacuum and v is the phase velocity of light in the medium.



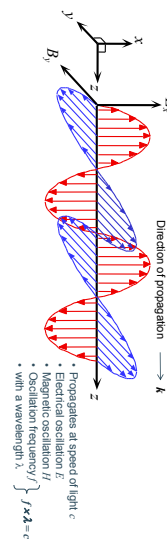
5

Materials Physics and Technology for Nanoelectronics
Photonics

KU LEUVEN

Refractive index

An electromagnetic wave is a travelling wave which has time varying electric and magnetic fields which are perpendicular to each other and the direction of propagation, z .



Materials Physics and Technology for Nanoelectronics
Photonics

KU LEUVEN

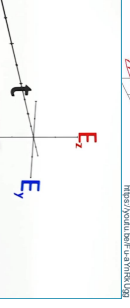
Light polarization



The electric field (note that we will ignore magnetic field now) of **linearly polarized light** is confined to a single plane along the direction of propagation.

The electric field of **circularly polarized light** consists of two perpendicular, equal in amplitude, linear components that have a phase of difference of $\pi/2$. The resulting electric field describes a circle.

The electric field of **elliptically polarized light** consists of two perpendicular linear components with any amplitude and any phase difference. The resulting electric field describes an ellipse.



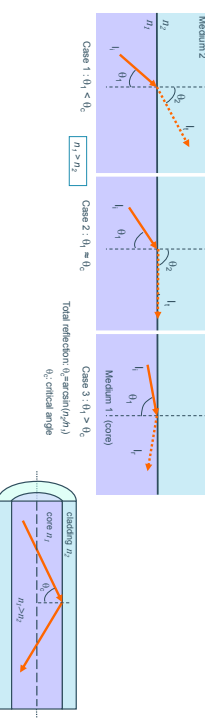
Light is called unpolarized if the direction of this electric field fluctuates randomly in time. Many common light sources such as sunlight, halogen lighting, LED spotlights, and incandescent bulbs produce unpolarized light. If the direction of the electric field of light is well defined, it is called polarized light. The most common source of polarized light is a laser.

Materials Physics and Technology for Nanoelectronics
Photonics

KU LEUVEN

Light propagation in optical fibers

According to the ray theory of light propagation, a light beam incident at the interface between two transparent materials with refractive indexes $n_1 > n_2$ behaves as follows (Snell's Law): $n_1 \sin(\theta_1) = n_2 \sin(\theta_2)$



Above a critical angle, $\theta_c = \arcsin(n_2/n_1)$, total reflection occurs. This property can be used to confine light into an optical fiber.

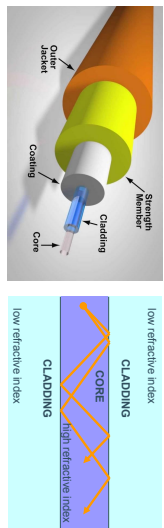
4

Materials Physics and Technology for Nanoelectronics
Photonics

KU LEUVEN

Optical fibers

Optical fibers are made from a ‘sandwich’ of material with a high refractive index between material with a low refractive index. Light is guided by total internal reflection in a core of high refractive index surrounded by a cladding of low refractive index. The total internal reflection takes place at the cladding – core interface.

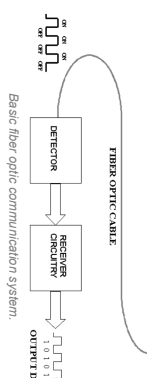


Optical fibers use total internal reflection to keep a light ray trapped within the denser glass of the center of a composite cylindrical glass fiber, the core. It is as if light rays are guided down the core of the fiber in a zigzag path by a succession of total internal reflections at the boundary between the core glass and the less dense glass surrounding it – the cladding.

8

Fiber optics

Fiber optics is a major building block in the telecommunication infrastructure. Its high bandwidth capabilities and low attenuation characteristics make it ideal for gigabit transmission and beyond.



Basic fiber optic communication system.

A basic fiber optic system consists of a transmitting device that converts an electrical signal into a light signal, an optical fiber cable that carries the light, and a receiver that accepts the light signal and converts it back into an electrical signal.

9

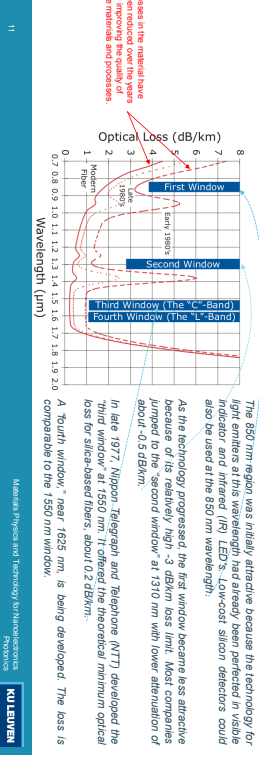
Light attenuation

Attenuation is loss of power. Light travelling through an optical fiber loses its power over distance. This phenomenon is mainly dependent on the wavelength of the light and the properties of the propagating medium.



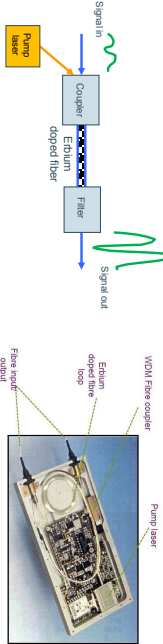
The output intensity decreases with increasing z : $I(z) = I_0 e^{-az}$. The attenuation is expressed in decibels per kilometer (dB/km): $dB = -10 \log_{10}(I_0/I(z))$. There are several reasons for this including absorption by the core and cladding (caused by the presence of impurities) and the leaking of light from the cladding. When light reflects off the cladding /core it actually travels for a short distance within the cladding before being reflected back. Today fibers have typical attenuation rates of -0.2 to -1 dB/km (5 to 20% attenuation) -> Example of 5% attenuation: $-10 \log_{10}(0.95) \sim -0.2 \text{ dB/km}$

The basic material used in optical fibers is vitreous silica dioxide (SiO_2). Various dopants are also used. The 850 nm region was initially attractive because the technology for light emitters at this wavelength had already been perfected in visible light sources such as LEDs. Later, erbium-doped fibers were developed. In late 1977, Nippon Telegraph and Telephone (NTT) developed the third window at 1550 nm. It offered the theoretical minimum optical loss for silica-based fibers, about 0.2 dB/nm. As the technology progressed, the first window became less attractive because of its relatively high -3 dB/km loss limit. Most companies jumped to the “second window” at 1310 nm with lower attenuation of about 0.5 dB/km. In late 1983, NTT developed the fourth window at 1625 nm. It is being developed. The loss is comparable to the 1550 nm window.



Fiber amplifiers

For some applications, the attenuation of light in an optical fiber must be compensated. This is realized with a fiber amplifier. Modern fiber amplifiers are based on the emission of stimulated light (laser effect – light amplification by stimulated emission of radiation) in the fiber.



In a fiber amplifier, a portion of the fiber is doped with some active impurities. The most common impurity used in SiO_2 is Erbium (Er); so called Erbium-doped fiber amplifiers. The laser effect is used in this portion of the fiber to amplify the signal. The inversion population is obtained with the help of a pump laser at another wavelength.

10

Fiber amplifiers

Erbium

From Wikipedia, the free encyclopedia
Erbium is a chemical element with the symbol **Er** and atomic number 68. A silver-white solid metal when artificially isolated, natural erbium is always found in chemical combination with other elements. It is a lanthanide, a rare-earth element, originally found in the gadolinium mine in Ytterby, Sweden, which is the source of the element's name.

Erbium-praseo lasers, for which have optical fluorescent properties particularly useful in certain laser applications. Erbium-doped glasses or crystals can be used as optical amplification media, where Er³⁺ ions are optically pumped at around 980 or 1480 nm and then emit light at 1550 nm in stimulated emission. This process results in an unusually mechanistic single laser optical amplifier for signal transmission by fiber optics. The 1550 nm wavelength is especially important for optical communications because standard single mode optical fibers have minimal loss at this particular wavelength.

In addition to optical fiber amplifiers, there is a large variety of medical applications, e.g. dermatology, dentistry, etc. on the erbium only standard single mode lasers. A large variety of medical applications are available, making its effects very superficial. So, erbium lasers are often used in dentistry and for the aesthetic production of soft tissue.

Erbium, $\alpha\text{-Er}$



Properties
- 3.03 m (at 20 °C)
Appearance: silvery white
Standard atomic weight: 167.26(3)
Erbium in the periodic table

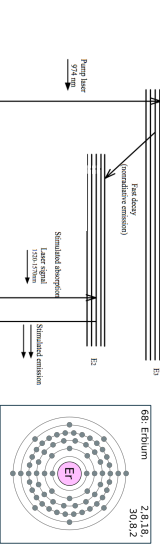
Contents (1)
1 Characteristics
1.1 Physical properties
1.2 Chemical properties
2 History

11

10

Er-based optical amplifier

An erbium-doped fiber is an optical fiber, of which the core is doped with rare-earth element erbium ions Er^{3+} . A simplified energy level diagram of the Er^{3+} ion is shown below.



Materials Physics and Technology for Nanoelectronics
Photonics



Er-based optical amplifier

If a laser signal with a wavelength between 1520 and 1570 nm, and a 974 nm pump laser are fed into an erbium-doped fiber simultaneously, there are three possible outcomes for the signal photon:

- The signal photon can propagate unaffected through the fiber.
- Absorption: the signal photon excites an erbium ion from the state E_1 to a higher level E_2 and become annihilated in the process.
- Stimulated emission:** the signal photon stimulates an Erbium ion at state E_2 to decay to E_1 , producing another identical photon. This process amplifies the incoming signal. In order to achieve this we need to obtain population inversion between the energy level E_2 and E_1 of the Erbium-doped fiber. For this to occur the pump laser power must be sufficiently high.



Schematic illustration of the stimulated emission process. The stimulated photons are in phase with the incident photon, have the same wavelength and travel in the same direction. In this way the incoming light signal can be amplified.

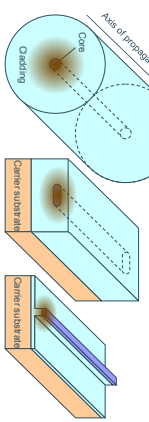
14

Materials Physics and Technology for Nanoelectronics
Photonics



From optical fibers to waveguides

Optical fibers are rather large and usually have a relatively small refractive index contrast between the core and the cladding. When the refractive index contrast $\frac{n_{\text{in}}}{n_{\text{cl}}} \approx \frac{\lambda}{D}$ is increased in all directions, the light can be confined in a smaller core according the expression $D \sqrt{\frac{n_{\text{in}}}{n_{\text{cl}}}} \approx \lambda$ (with D being a typical dimension of confinement). This allows to fabricate photonic wires, the first step towards integrated optics.

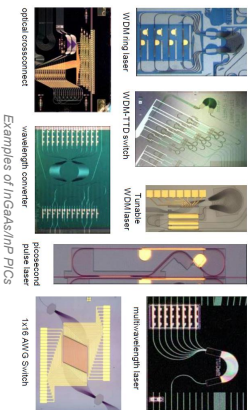


- Optical fibers (low refractive index contrast, typically ~1.46-to-1.44); core diameter ~10µm
- Waveguides in semiconductor and air (high index contrast, 3.45-to-1); core ~0.2 x 0.5µm → photonic wires

Materials for photonic integrated circuits

InGaAsP / InP

- allows monolithic integration (integration of active and passive components)
- relatively high index contrast allows to make compact waveguides ($\sim 1 \mu\text{m}$)
- coupling to fiber is difficult



Examples of InGaAsP/InP PICs

15

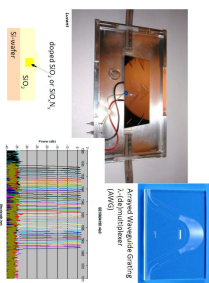
Materials Physics and Technology for Nanoelectronics
Photonics



Materials for photonic integrated circuits

Glass-like materials (SiO_x , SiO_xN_y)

- very low losses
- optimized for fiber coupling
- most common implementation consist of Silica on Silicon (SiO_2 on Si)
- low index contrast, hence large waveguide (as in optical fiber)



Examples of silica on silicon waveguides

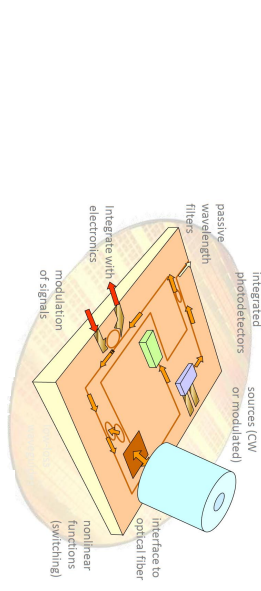
16

Materials Physics and Technology for Nanoelectronics
Photonics



Photonic Integrated Circuits (PICs)

Photonic circuits requires often interconnections with waveguides to communicate with the outer world.



17

Materials Physics and Technology for Nanoelectronics
Photonics



16

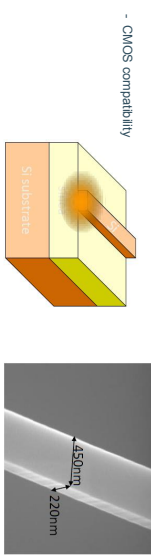
Materials Physics and Technology for Nanoelectronics
Photonics



Materials for photonic integrated circuits

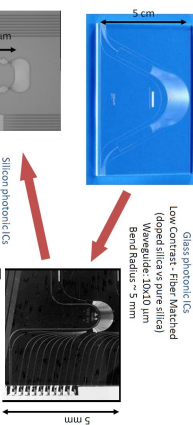
soi (Silicon-on-Insulator)

- Silicon layer bonded onto Silica (SiO_2)
- Silicon is transparent at telecom wavelengths (1550nm and 1300nm)
- High index contrast
- 3.45 (Silicon) to 1.0 (air) / 1.45 (silica)
- C-MOS compatibility



Silicon nanophotonics

Silicon nanophotonic waveguides (or photonic wires) can strongly confine light in a submicron waveguide core, allowing sharp bends and compact components.



21

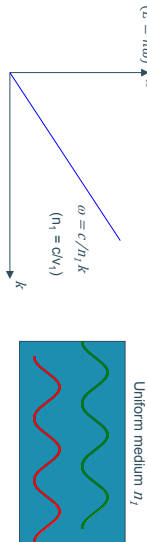
Materials Physics and Technology for Nanoelectronics Photonics

KU LEUVEN

Photonic crystals

Photonic wires are like ‘conductors’ for light. The next step is to make structures that are the equivalent of ‘semiconductors’, i.e. photonic crystals.

The dispersion relation defines the relationship between angular frequency ω of the photon and its wavevector $k = 2\pi/\lambda$. This dispersion relation describes the optical properties of a material, and a plot of ω against k will indicate the allowed energies (bands) or states at given k -vectors.

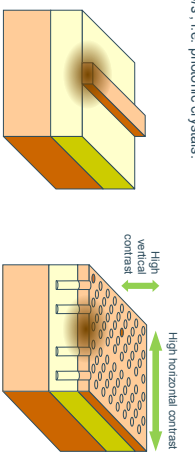


For a one-dimensional, homogeneous material with a uniform dielectric function, the band structure or dispersion relation is simply: $\omega = ck/\rho$ where n is the refractive index of the material.

23

Materials Physics and Technology for Nanoelectronics Photonics

W. Broers, IMEC



Formation of an optical bandgap

However for a periodic material, the periodic function causes moving waves to be partially reflected at every interface. For frequencies that fulfill the Bragg condition ($\lambda/2=d/4$), there will be total reflection conditions in the material and the interference of the forward and backward waves creates a standing wave at the edge of the Brillouin zone (π/a).

$\alpha(k)$ flattens out, i.e. the group velocity of the propagating waves $d\omega/dk$ vanishes.

Light with frequencies within the photonic band gap cannot propagate in the photonic crystal.

Note that the reflected waves have a phase shift of $\pi/2$ compared to the wave incident on the periodic medium. The reflected wave has a phase shift of $\pi/2$ compared to the wave incident on the periodic medium.

A schematic of a standing wave $\eta(x)$ is shown. The wave is periodic with a period a and has a phase difference of $\pi/2$ between two consecutive half-wavelengths. The wave is zero at $x=0$ and reaches a maximum at $x=a$.

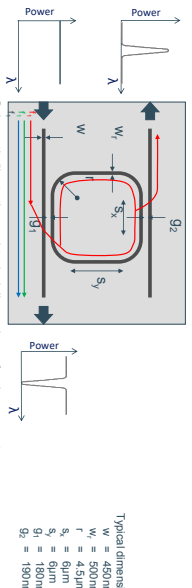
24

Materials Physics and Technology for Nanoelectronics Photonics

KU LEUVEN

Ring and racetrack resonators

An interesting application of waveguides are ring resonators. They allow to separate a well-defined wavelength band from a broadband spectrum.



In a ring resonator, light resonates if the wavelength fits a whole or multiple times in the circumference of the ring. Incoming light from the bus waveguide is coupled to the ring via a directional coupler.

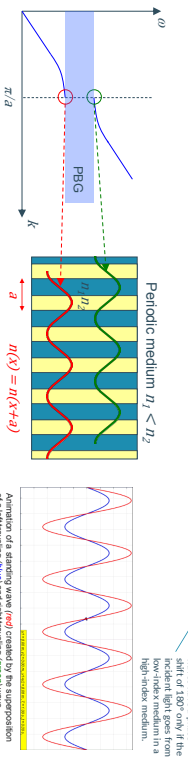
On resonance: light is transferred by the ring to the drop waveguide.
Off-resonance: light stays in the bus waveguide.

Formation of an optical bandgap

However for a periodic material, the periodic function causes moving waves to be partially reflected at every interface. For frequencies that fulfill the Bragg condition ($\lambda/2=d/4$), there will be total reflection conditions in the material and the interference of the forward and backward waves creates a standing wave at the edge of the Brillouin zone (π/a).

$\alpha(k)$ flattens out, i.e. the group velocity of the propagating waves $d\omega/dk$ vanishes.

Light with frequencies within the photonic band gap cannot propagate in the photonic crystal.



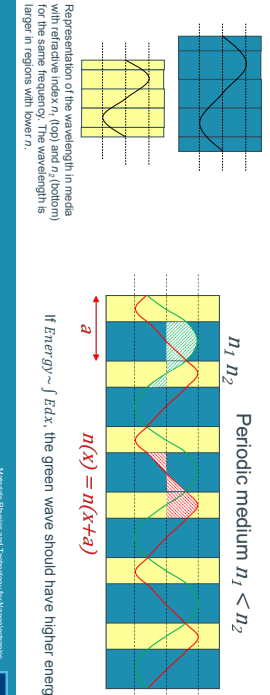
25

Materials Physics and Technology for Nanoelectronics Photonics

KU LEUVEN

Photonic crystals

- 1-d photonic crystal: distributed Bragg reflector. A visual description
The condition $a=2\pi/\lambda$ imposes a different "a"-distance for each n because λ depends on n (for a fixed frequency).

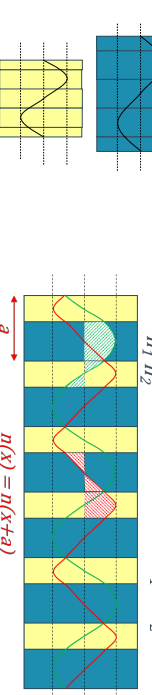


26

Materials Physics and Technology for Nanoelectronics
Photonics

KU LEUVEN

- In a homogeneous medium, $n(z)$ is constant and the solution of the wave equation is a plane wave.
- $E(z,t) = E_0 e^{i(kz-\omega t)}$, where $k = 2\pi/\lambda$ and $\omega = (c/n)k$
- Now consider a 1D crystal with a periodic refractive index $n(z)=n(z+a)$. According to the Floquet-Bloch theorem, the solution of the wave equation then becomes:



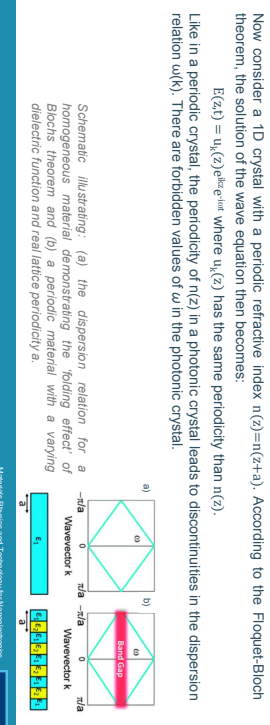
27

Materials Physics and Technology for Nanoelectronics
Photonics

KU LEUVEN

Photonic crystals

- In a homogeneous medium, $n(z)$ is constant and the solution of the wave equation is a plane wave.
- $E(z,t) = E_0 e^{i(kz-\omega t)}$, where $k = 2\pi/\lambda$ and $\omega = (c/n)k$
- Now consider a 1D crystal with a periodic refractive index $n(z)=n(z+a)$. According to the Floquet-Bloch theorem, the solution of the wave equation then becomes:



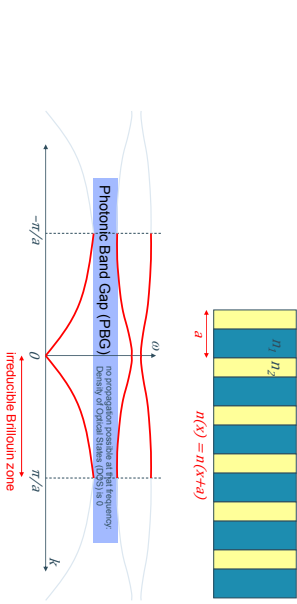
28

Materials Physics and Technology for Nanoelectronics
Photonics

KU LEUVEN

Photonic crystals

1-d photonic crystal: distributed Bragg reflector. A visual description



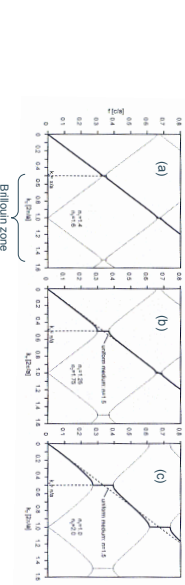
29

Materials Physics and Technology for Nanoelectronics
Photonics

KU LEUVEN

Photonic crystals

Like in a periodic crystal, the periodicity of $n(z)$ in a photonic crystal leads to discontinuities in the dispersion relation $\omega(k)$. There are forbidden values of ω . The bigger the diffraction index contrast, the larger the bandgap.



The dispersion relation for a 1-D periodic medium with a) $n_1 = 1.4$ and $n_2 = 1.6$, b) $n_1 = 1.25$ and $n_2 = 1.5$, or c) $n_1 = 1$ and $n_2 = 2$ with $n_1 a_1 = n_2 a_2$. The linear dispersion relation of a uniform medium with $n = 1.5$ is also plotted.

30

Materials Physics and Technology for Nanoelectronics
Photonics

KU LEUVEN

Photonic crystals

A photonic crystal is a material whose dielectric function varies periodically. This periodicity requires the solution of the wave equations to satisfy the Floquet-Bloch theorem, which states that the solutions to the equations for periodic media are plane waves modulated by a periodic function with lattice periodicity.

Let's consider a 1D homogeneous medium. The wave equation (Maxwell equations, see slide #48 chapter 3, but without damping term):

$$\nabla^2 E - \mu \epsilon \frac{\partial^2 E}{\partial z^2} = 0, \text{ for the electric field } E(z,t) \text{ of an electromagnetic wave is given by :}$$

$$\frac{c^2}{n'(z)} \frac{\partial^2 E(z,t)}{\partial z^2} - \frac{\partial^2 E(z,t)}{\partial t^2} = 0 \quad (c^2 = \frac{1}{\mu \epsilon_0}, n = \sqrt{\mu \epsilon})$$

Photonic crystals versus electronic crystals

Photonic crystal can be seen as equivalent to a periodic solid for electrons. Both have a periodic structure and therefore, in both cases Bloch's theorem can be used resulting in a band structure.

Periodic crystal

- Particles = electrons

Photonic crystal

- Electromagnetic waves

Photonic crystal

- Maxwell equations

Photonic crystal

- Periodic potential

Photonic crystal

- Band structure

Photonic crystal

- Allowed energy states

Photonic crystal

- Forbidden energy states

Photonic crystal

- (Band Gaps)

- Photonic Band Gap

28

Materials Physics and Technology for Nanoelectronics
Photonics

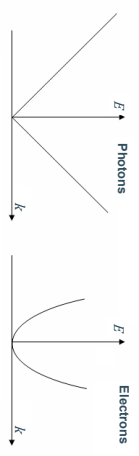
KU LEUVEN

Photons and electrons

The free space propagation of both electrons and photons can be described by plane waves.
The momentum for both electrons and photons: $\mathbf{p} = \hbar \mathbf{k}$

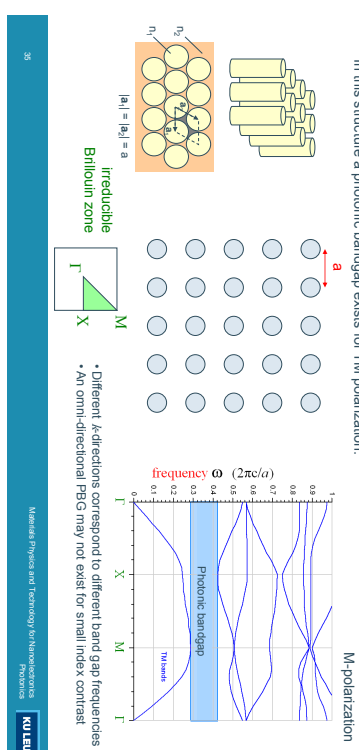
- For photons \mathbf{k} is given by $\mathbf{k} = (2\pi/\lambda)$ and the energy $E = \hbar c(n)\mathbf{k}$ and the energy $E = \mathbf{p}^2/2m = \hbar^2 k^2/2m$
- For electrons $\mathbf{k} = mv/\hbar$ and the energy $E = p^2/2m = \hbar^2 k^2/2m$
- Light waves are described by a vector field while the electron wavefunction is scalar.
- Photons sail s/F Bose-Einstein statistics while electrons are Fermions.

Other important differences between electrons and photons are:



Molecular Physics and Technology for Nanoelectronics
Photonics

KU LEUVEN



In this structure a photonic bandgap exists for TM polarization.
 a
M-polarization

No photonic bandgap is observed for the TE bands.

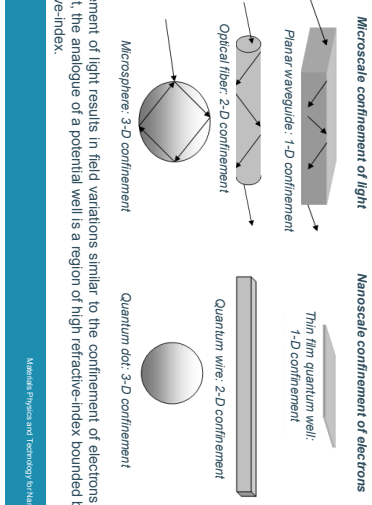
Different k -directions correspond to different band gap frequencies

An omni-directional PBG may not exist for small index contrast

Molecular Physics and Technology for Nanoelectronics
Photonics

KU LEUVEN

Confinement of light and electrons

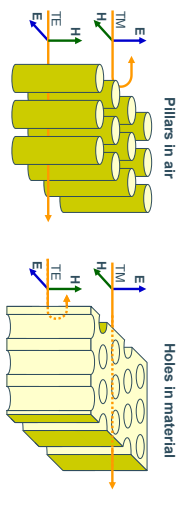


Molecular Physics and Technology for Nanoelectronics
Photonics

KU LEUVEN

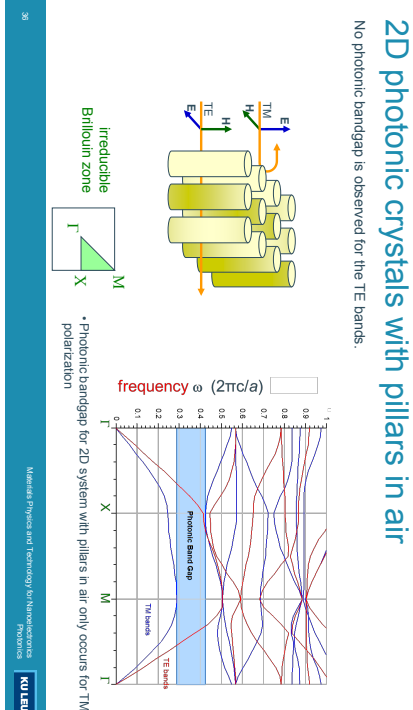
Polarization in 2D photonic crystals

2D photonic crystals can be realized making two-dimensional periodic structures. The dispersion and the bandgap depends on the light polarization.



Only photonic bandgap for light with the electric field parallel to the pillar axis (= TM-polarisation)
Only photonic bandgap for light with the electric field perpendicular to the pillar axis (= TE-polarisation)

TM polarization (transverse magnetic field) E in the plane of the structure
TE polarization (transverse electric field) E perpendicular to the structure
Note: a high refractive index contrast is needed in both cases



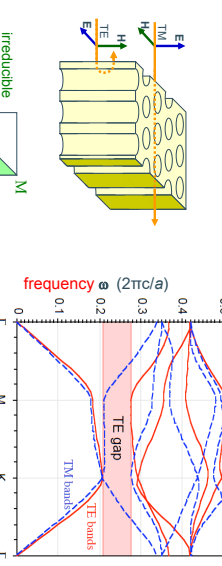
In this structure no photonic bandgap is observed for TM bands, only for TE bands.

Photonic bandgap for 2D system with pillars in air only occurs for TM polarization

KU LEUVEN

2D photonic crystals with holes in material

In this structure no photonic bandgap is observed for TM bands, only for TE bands.



Only photonic bandgap for light with the electric field parallel to the pillar axis (= TM-polarisation)
Only photonic bandgap for light with the electric field perpendicular to the pillar axis (= TE-polarisation)

TM polarization (transverse magnetic field) E in the plane of the structure
TE polarization (transverse electric field) E perpendicular to the structure
Note: a high refractive index contrast is needed in both cases

33

34

35

36

Slow light in photonic crystals

At certain parts of the diagram some special observations are made.



In a photonic crystal the phenomenon of slow light is created by the resonant interaction of the guided mode with the periodic lattice, resulting in the formation of a slow moving interference pattern (the 'slow mode'). Slow light might be interesting for sensing, to enhance the interaction between light and the sample under test.

Adapted from T. Tan, "Slow light in photonic crystals," *Nature Photonics*, 4, 24-27 (2009).

Materials Physics and Technology for Nanoelectronics
Photonics



Slow light leads to enhanced optical linear and nonlinear effects: spatial compression of light energy



Interferometer with reduced arm length using slow light in photonic crystal waveguide

Permittivity and permeability of conventional materials derive from the response of constituent atoms to applied fields and ϵ_0, μ_0 represent an average response of the system. On a length scale much greater than the separation between atoms we need to know about the system is given by ϵ_r, μ_r . Metamaterials carry this idea one step further: the constituent material is structured into sub-units, and on a length scale much greater than that of the sub-units, properties are again determined by an effective permeability and permittivity valid on a length scale greater than the size of the constituent units. In the case of electromagnetic radiation this usually means that the sub-units must be much smaller than the wavelength of radiation (this is why nanotechnology could enable them). In our way the properties of a complex structure can be summarized by $\epsilon_{eff}, \mu_{eff}$ which is a great simplification in our thinking. So the concept is a familiar one but with the difference that the sub-units can take very many different forms. This flexibility in design enables metamaterials to have values for $\epsilon_{eff}, \mu_{eff}$ which are not encountered in nature and in the present context that will mean one or both of these parameters being negative. Furthermore these materials can give magnetic activity at frequencies where previously materials have been thought of as magnetically inert.

J.G. Purdy, *Comments Phys.*, 35, 191 (2004)

Materials Physics and Technology for Nanoelectronics
Photonics



Negative refraction in photonic crystals

Another interesting effect is the occurrence of a negative refractive index. This results in some remarkable optical properties and allows to make *superlenses*.



Illustration of the optical effect of negative refractive index. (a) Calculated ray-tracing image of a metal rod in an empty drinking glass. (b) Same scenario, but the glass is filled with normal water, $n=1.3$, leading to ordinary refraction. (c) The water is replaced by water with a fictitious refractive index of $n=-1.3$.

C. Luo et al., "Negative refraction in three dimensions in photonic crystals," *Appl. Phys. Lett.* 81, 2232 (2002).



Materials Physics and Technology for Nanoelectronics
Photonics



Metamaterials

Even though natural materials provide substantial means to control electromagnetic waves, they exhibit important shortcomings.

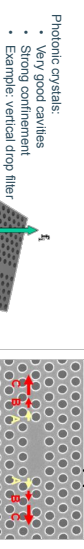


(left) A traditional material is composed of atoms and it derives its optical properties from the interaction of electromagnetic waves with its atoms. A metamaterial is composed of electric circuits that take over the role of atoms as basic constituents for the interaction with electromagnetic waves. (middle) One of the first microwave metamaterials (right) Metamaterials are an optical material with negative index of refraction.

We can devise artificial materials (*metamaterials*), in which atoms are replaced by small electric or plasmonic resonators as the basic constituents for the interaction with electromagnetic waves. The large freedom in their design allows for materials with electromagnetic and optical properties that are not achievable or much weaker in conventional materials, e.g. negative refractive index.

Photonic crystal cavities

High quality optical filters can be produced using photonic crystals. Small changes in the local structure create a nano-cavity corresponding to a well-defined defect. These defects allow specific wavelengths to escape from the waveguide.



Light trapped in a missing hole.
Waveguides made by removing a row of holes.
Sharp bend in an optical waveguide.

In this way waveguides can be made that confine the light in a narrow region. The waveguides can make sharp bends so the light can not get out of the waveguide into the photonic crystal, i.e. the light can not miss the bend. Light can be much more confined and follow much sharper bends than in optical fibres.



S. Noda, *Nature*, 407, p. 68 (2000)

Materials Physics and Technology for Nanoelectronics
Photonics



Metamaterials

Permittivity and permeability of conventional materials derive from the response of constituent atoms to applied fields and ϵ_0, μ_0 represent an average response of the system. On a length scale much greater than the separation between atoms we need to know about the system is given by ϵ_r, μ_r . Metamaterials carry this idea one step further: the constituent material is structured into sub-units, and on a length scale much greater than that of the sub-units, properties are again determined by an effective permeability and permittivity valid on a length scale greater than the size of the constituent units. In the case of electromagnetic radiation this usually means that the sub-units must be much smaller than the wavelength of radiation (this is why nanotechnology could enable them).

In our way the properties of a complex structure can be summarized by $\epsilon_{eff}, \mu_{eff}$ which is a great simplification in our thinking. So the concept is a familiar one but with the difference that the sub-units can take very many different forms. This flexibility in design enables metamaterials to have values for $\epsilon_{eff}, \mu_{eff}$ which are not encountered in nature and in the present context that will mean one or both of these parameters being negative. Furthermore these materials can give magnetic activity at frequencies where previously materials have been thought of as magnetically inert.

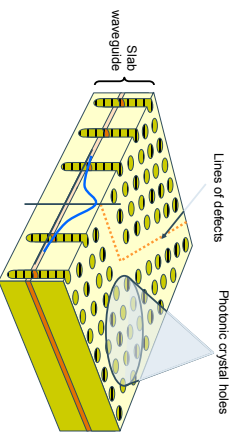
J.G. Purdy, *Comments Phys.*, 35, 191 (2004)

Materials Physics and Technology for Nanoelectronics
Photonics



Photonic crystal slab

In real applications 2D crystals are usually combined with slab waveguides to confine the light vertically as well.



The vertical confinement is obtained by a layered waveguide. The horizontal confinement is formed by the photonic crystal (with a high index contrast).

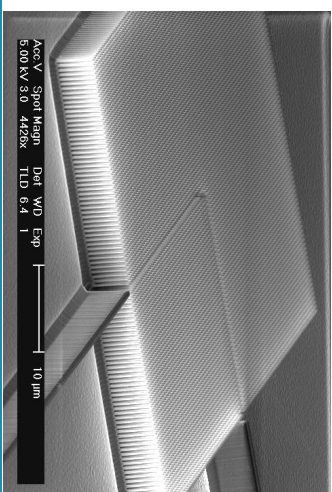
W. Bourennane, RPEC

KU LEUVEN

Materials Physics and Technology for Nanoelectronics
Photonics

44

Photonic crystals



Silicon-based photonic crystal with a line of defects

Materials Physics and Technology for Nanoelectronics
Photonics

KU LEUVEN

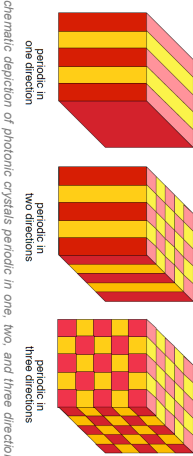
3D photonic crystals

In order to make a 3D photonic crystal a three-dimensional periodic structure is needed.

1-D

2-D

3-D



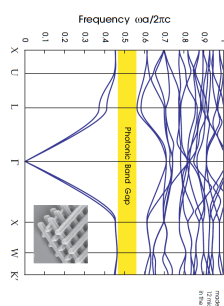
Schematic depiction of photonic crystals periodic in one, two, and three directions, where the periodicity is in the material structure of the crystal.

Only a 3D periodicity, with a more complex topology than is shown here, can support an omnidirectional photonic bandgap.

45

3D photonic crystals

3D "Woodpile" photonic crystal.



On the colour of wing scales in butterflies: iridescence and preferred orientation of single gyroid photonic crystals

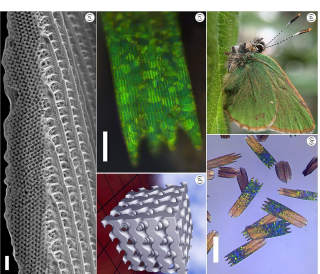
Published at 15 June 2017 https://doi.org/10.1093/rstb/2016.0154

Babu M, Cooke and E.S.C. Izquierdo

KU LEUVEN

Materials Physics and Technology for Nanoelectronics
Photonics

46



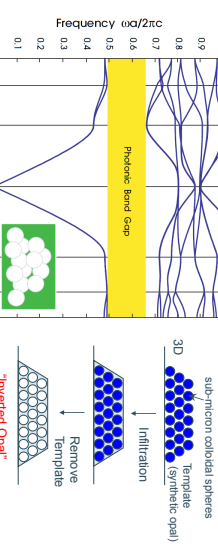
(a) Gyroidal slab (40 nm scale, ~17.5μ) also known as the green hairstreak; (b) optical micrograph of large NAs (high magnification, 100x) of a common green hairstreak showing that the characteristic greenish color arises from many individual photonic crystal domains. Note that the longitudinal ribs are also visible; (c) computer-generated single gyroid model, 4 × 4.4 μm unit cell; (d) a coloured wing scale showing the ribbed upper surface in a perspective view; (e) SEM image of a woodpile slab showing the ribbed upper surface in a perspective view; note the continuous network spanning crystal grain boundaries in different orientations. Note the planes, yet with some lattice defects such as dislocation planes and holes. Scale bars: (b, c and e) 100, 20 and 1 μm, respectively.

47

Photonic crystals in nature

3D photonic crystals

3D photonic bandgap in diamond lattice of air spheres in a dielectric material.



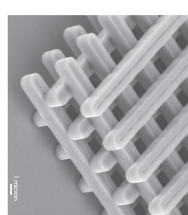
The photonic band structure for the lowest bands of a diamond lattice of air spheres in a high dielectric material ($\epsilon=13$). A complete photonic band gap is shown. The wave vector values across the irreducible Brillouin zone between the labeled high-symmetry points.

W. Bourennane, RPEC

KU LEUVEN

Materials Physics and Technology for Nanoelectronics
Photonics

48



KU LEUVEN

Materials Physics and Technology for Nanoelectronics
Photonics

49

46

Materials Physics and Technology for Nanoelectronics
Photonics

KU LEUVEN

The versatile bonding of Carbon

The best-known carbon crystal is diamond, whose hardness and high dispersion of light make it useful for industrial applications and jewelry.

Under ambient pressures and at room temperature, however, the most stable form of carbon is **graphite**, which is used as an industrial lubricant and as the 'lead' in pencils. Graphite is a layered material in which each layer consists of a sheet of carbon atoms forming hexagonal structures (similar to benzene rings).

A monolayer of graphite is called **graphene** and a carbon nanotube is a cylinder made of graphene.



Materials Physics and Technology for Nanoelectronics



Carbon nanotubes were discovered by Sumio Iijima during the synthesis of fullerene C₆₀ in 1991. A nanotube exhibits **extraordinary mechanical properties** that make it ideal for **reinforced composites**; it has a huge Young modulus, is as stiff as diamond and the estimated tensile strength is more than ten times that of steel wire with the same weight.



Materials Physics and Technology for Nanoelectronics



KU LEUVEN

Materials Physics and Technology for Nanoelectronics

Carbon Materials

Diamond
Carbon atoms in diamond have tetrahedral bonds (i.e. in four spatial directions) and do not have any free electrons to each other. sp^3 configuration

Graphite
Natural graphite consists of layers of carbon atoms lying on top of each other arranged in the form of a hexagonal honeycomb structure. sp^2 configuration

Nanotubes (CNTs)
Carbon nanotubes have similar properties to graphite, but can be pictured as a graphite layer rolled into a cylinder

Graphene
Single Isotropic graphite monolayer is referred to as graphene. Carbon atoms are in sp^2 configuration. Zero bandgap semiconductor with high carrier mobility

Fullerenes
Prismane (fullerene C₆₀) resembles to a football ('Buckyball'). sp^2 configuration

Lonsdaleite
Very rare mineral form of Carbon occurs during the transformation of graphite into diamond where the original hexagonal crystal lattice is preserved. Also named mineral diamond. sp^3 configuration

HOPG (graphene)
SWNT
MWNT

Carbon Materials

Copper Metallurgy
Copper Metallurgy can be divided into two main categories:
1. Copper Smelting (smelting of copper minerals)
2. Copper Refining (refining of copper minerals)

mtec
mtec is a KU Leuven spin-off company.
Responsible for the development of the first industrial scale plant for the production of MWNTs.

François Molina Lopez
francisco.molina.lopez@kuleuven.be
KuLeuven University, Belgium

KU LEUVEN

Carbon allotropes

Bonds config.	0D	1D	2D	3D
sp^2	Fullerene	Nanotubes	Graphene	Graphite
sp^3	Diamondoids	Nanoribbons	Graphene	Diamond

Various fields of all-carbon device applications:

- Electronics
- Opto-electronics / Photonic
- Energy
- Biosensors
- Mechanics
- Radiation detectors

Energy

- Li-ion batteries
- Transistors
- CNT/C₆₀

Electronics

- Graphene
- Graphene/diamond
- CNT/C₆₀

Opto-electronics

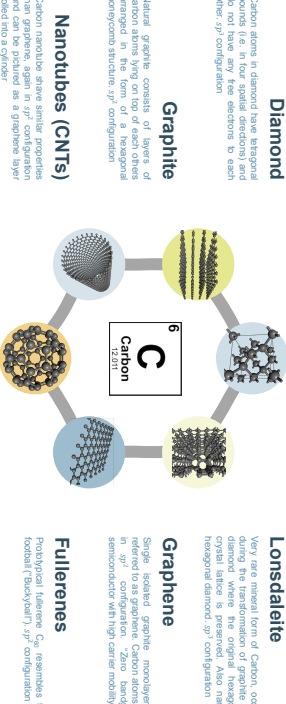
- Graphene
- CNT/C₆₀
- Solar cells
- CMOS graphene

Mechanics

- Radiation detectors
- CNT/Graepne
- Strain Sensors

Biosensors

The Carbon cosmos



Materials Physics and Technology for Nanoelectronics



5



Materials Physics and Technology for Nanoelectronics



2

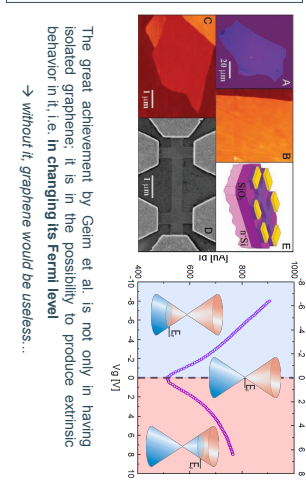
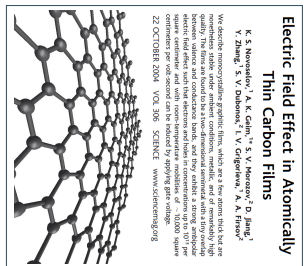


Outline

- Carbon based materials
- Graphene
 - Fundamentals & properties
 - Synthesis
 - Devices & applications
- CNTs
 - Fundamentals & properties
 - Synthesis
 - Devices & applications



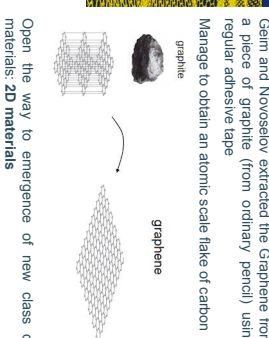
Graphene 'discovery'



Nobel Prize in Physics 2010



The Nobel Prize in Physics 2010 was awarded jointly to Andre Geim and Konstantin Novoselov "for groundbreaking experiments regarding the two-dimensional material graphene".



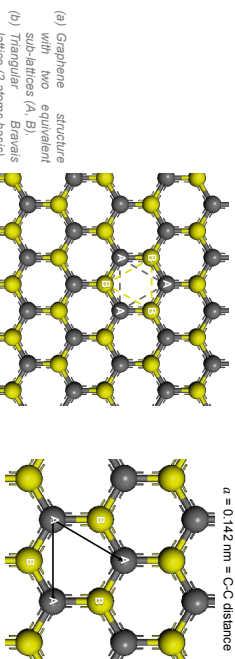
Open the way to emergence of new class of materials: 2D materials

10

Graphene lattice structure

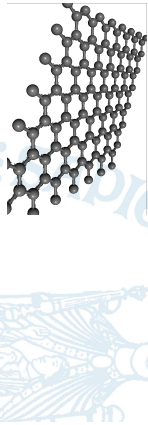
The hexagonal lattice of graphene can be regarded as two interleaving triangular lattices. This perspective was successfully used as far back as 1947 when Wallace calculated the band structure for a single graphite layer using a tight-binding approximation.

$$a = 0.142 \text{ nm} = \text{C-C distance}$$



Graphene

Fundamentals & properties



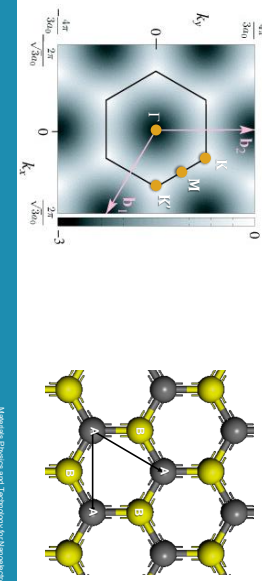
Graphene

Fundamentals & properties

Graphene

Graphene reciprocal lattice

Correlation of the hexagonal graphene lattice between real and reciprocal space.



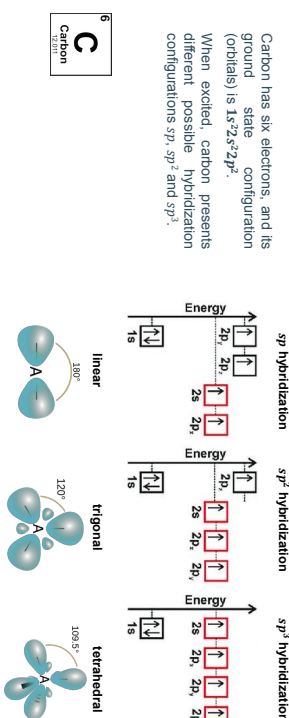
13

Materials Physics and Technology for Nanoelectronics
Carbon Materials



Electronic structure of carbon

Carbon has six electrons, and its ground state configuration is $1s^2, 2s^2, 2p^2$. When excited, carbon presents different possible hybridization configurations sp, sp^2 , and sp^3 .



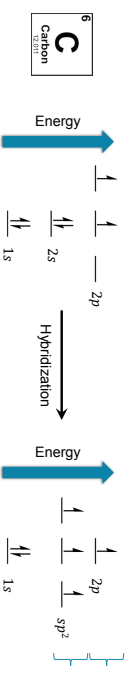
14

Materials Physics and Technology for Nanoelectronics
Carbon Materials



Electronic structure of graphene

When arranged in the honeycomb crystal (i.e. graphene), two electrons remain in the core 1s orbital, while the other orbitals hybridize, forming three sp^2 -bonds and leaving one p_z orbital. The sp^2 orbitals form the σ -band, which contains three localized electrons. The bonding configuration among the p_z orbitals of different lattice sites generates a valence band, or π -band, containing one electron, whereas the antibonding configuration generates the conduction band (π'), which is empty.



15

Materials Physics and Technology for Nanoelectronics
Carbon Materials

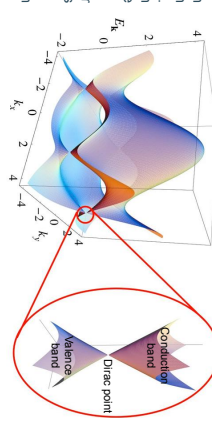


Graphene electronic structure

Graphene has two atoms per unit cell, which results in two 'conical' points per Brillouin zone where band crossing occurs, K and K' . Near these crossing points, the electron energy is linearly dependent on the wave vector.

Graphene is a zero-gap semiconductor because the conduction and valence bands meet at the Dirac points.

The Dirac points are locations in momentum space on the edge of the Brillouin zone.



16

Materials Physics and Technology for Nanoelectronics
Carbon Materials



Dirac matter

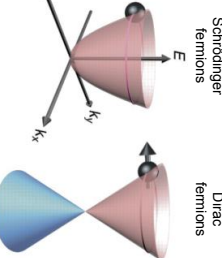
Conventionally, in condensed matter physics nearly free charge carriers are effectively described using the Schrödinger Hamiltonian with quadratic dispersion (where m^* is the carrier effective mass (being different from the free electron mass) and \vec{p} being the momentum operator).

Contrary to that, Dirac matter is any material where relativistic particles in the zero-mass limit can be described in the low-energy excitation spectrum by the Dirac Hamiltonian, where v_F is the Fermi velocity and $\hat{\sigma}$ is the Pauli matrix:

$$\hat{H} = \hat{p}^2/2m^*$$

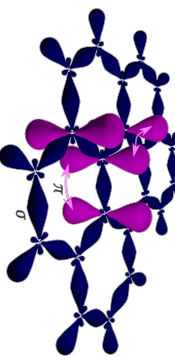
$$\hat{H} = v_F \vec{\sigma} \cdot \hat{\vec{p}}$$

Comparison between Schrödinger and Dirac fermions in condensed matter physics.



Each carbon atom is about $a = 1.42 \text{ \AA}$ from its three neighbors, with each of which it shares one σ -bond. The fourth bond is a π -bond, which is oriented in the z -direction (out of the plane). Due to the sp^2 bonding, the carbon atoms in graphene form a hexagonal lattice on a two-dimensional plane with ultra-thin atomic thickness ($t_{\text{lat}} = 3.45 \text{ \AA}$).

One can visualize the π -orbital as a pair of symmetric lobes oriented along the z axis and centered on the nucleus. Each atom has one of these π -bonds, which are then hybridized together to form what are referred to as the π -band and π' -bands. These bands are responsible for most of the peculiar electronic properties of graphene.



Graphene electronic structure

Each carbon atom is about $a = 1.42 \text{ \AA}$ from its three neighbors, with each of which it shares one σ -bond.

The fourth bond is a π -bond, which is oriented in the z -direction (out of the plane).

Due to the sp^2 bonding, the carbon atoms in graphene form a hexagonal lattice on a two-dimensional plane with ultra-thin atomic thickness ($t_{\text{lat}} = 3.45 \text{ \AA}$).

One can visualize the π -orbital as a pair of symmetric lobes oriented along the z axis and centered on the nucleus. Each atom has one of these π -bonds, which are then hybridized together to form what are referred to as the π -band and π' -bands. These bands are responsible for most of the peculiar electronic properties of graphene.

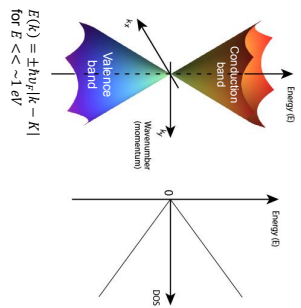
Electronic structure of graphene

Because of the linear spectrum, one can expect that quasi-particles in graphene behave differently from those in conventional metals and semiconductors, where the energy spectrum can be approximated by a parabolic (free electron-like) dispersion relation.

Quasi-particles in graphene exhibit a linear dispersion relation $E(k) = \pm v_F |k - K|$, as if they were massless relativistic particles (for example, photons), but the role of the speed of light (c) is played here by the Fermi velocity:

$$v_F \approx c = 10^6 \text{ m/s}$$

Due to the zero density of states at the Dirac points, electronic conductivity is quite low.



$E(k) = \pm \hbar v_F |k - K|$

$$\text{for } E < \sim 1 \text{ eV}$$

KU LEUVEN

Materials Physics and Technology for Nanoelectronics Carbon Materials

19

Graphene electronic conductivity

It is said that graphene electrons act very much like photons in their mobility due to their lack of mass. These charge carriers are able to travel sub-micrometer distances without scattering, a phenomenon known as ballistic transport. The electronic mobility of graphene is very high, with theoretical potential limits of $200\,000 \text{ cm}^2 \text{ V}^{-1} \text{s}^{-1}$ (limited by the scattering of graphene's acoustic phonons). However, the quality of the graphene and the substrate that is used will be the limiting factors. With silicon dioxide as the substrate, for example, mobility is potentially limited to $40\,000 \text{ cm}^2 \text{ V}^{-1} \text{s}^{-1}$.

Given as appropriate doping enables an in-plane conductivity of 100 MSM for the graphene flakes with a flake size in the tens of micrometers, the macroscopic graphene can reach an electrical conductivity of up to 80 MSM. Graphene semimetal is potentially better at conducting electricity than, for example, copper at room temperature (58 MSM).

A graphene-based conductor with 80 MSM in electrical conductivity allows enormous efficiency gains, weight as well as volume savings and enables new designs for the powertrain in e-mobility.



20

Materials Physics and Technology for Nanoelectronics Carbon Materials

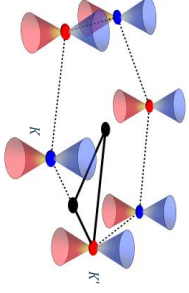
KU LEUVEN

Electronic structure of graphene

The hexagonal lattice of graphene can be regarded as two interleaving triangular sub-lattices A and B. From a kinetic energy point of view, the electronic single particle dispersion in graphene is essentially defined by the hopping of the electrons between nearest neighbor carbon sites in the honeycomb lattice.

Unlike square or triangular lattices, the honeycomb lattice is spanned by two different sets of Bravais lattice generators, forming a two-component basis with one set for each triangular sublattice.

There are two sets of three Dirac points. Each set is not equivalent with the other set of three.



Graphene vibrational properties

In order to obtain the phonon dispersion, it is necessary to consider the **vibrational modes** of the crystal in thermal equilibrium. This is done by considering the displacement of each atom from its equilibrium position. Each atom is effectively coupled to its neighbors by some **torsional** and **longitudinal force** constants, which only depend on the relative positions of the atoms.

In graphene the two sublattices A and B have to be considered explicitly to solve the eigenspectrum of the **dynamical matrix**. However, the atoms can vibrate in all three dimensions, hence the dynamical matrix has to be written in terms of both the sublattices A and B as well as the 3 spatial dimensions.

Ultimately this leads to **6 eigenvalues**. Two of the eigenvalues correspond to the **out-of-plane vibrations**, oTA (acoustic) and oTO (optical), and the remaining 4 correspond to the **in-plane vibrations**: ITA (transverse acoustic), iTO (transverse optical), LA (longitudinal acoustic), and LO (longitudinal optical).

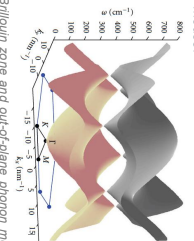
21

Materials Physics and Technology for Nanoelectronics Carbon Materials

KU LEUVEN

Graphene phonon dispersion

At the K and K' points, we recover a cone structure similar to the Dirac cones in the electronic structure. However, the phonon density of states does not vanish at these points because of the presence of the in-plane modes.



First Brillouin zone and out-of-plane phonon modes. The vertical axis is the phonon frequency, while the horizontal axes are momentum space on the graphene lattice. The gray surface corresponds to the OTO (optical) mode, whereas the pink surface shows the TA (acoustic) mode.

CL "Thermoelectric materials" chapter

22

Materials Physics and Technology for Nanoelectronics Carbon Materials

KU LEUVEN

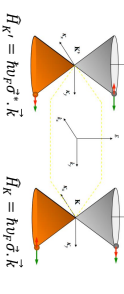
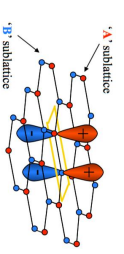
Chirality and pseudospin in graphene

Transport in graphene exhibits a novel chirality. Each graphene sublattice can be regarded as being responsible for one branch of the dispersion. These dispersion branches interact very weakly with one another.

This chiral effect indicates the existence of a **pseudospin quantum number** that is analogous to spin carriers. This quantum number is independent of the real spin, but is completely *independent* of the real spin.

pseudospin quantum number for a charge carriers. This quantum number is analogous to spin but is completely *independent* of the real spin.

The pseudospin lets us differentiate between contributions from each of the sublattices. This independence is called **chirality** because of the inability to transform one type of dispersion into another. A typical example of chirality is that you cannot transform a right hand into a left hand with only translations, scaling's, and rotations.

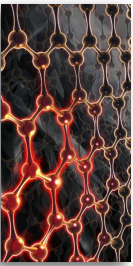


First Brillouin zone and in-plane phonon modes. The gray surface corresponds to the iTA and LA modes in pink as a function of the in-plane reciprocal vector k . The longitudinal modes are on top of the transverse modes.

KU LEUVEN

Graphene thermal conductivity

While the electronic properties have attracted the lion's share of the interest in graphene, the vibrational properties are of great importance too. They are responsible for properties such as the record thermal conductivities.



From the kinetic theory of gases, the thermal conductivity due to phonons is given by:

$$\kappa \sim c_{ph} C_v(T) \lambda$$

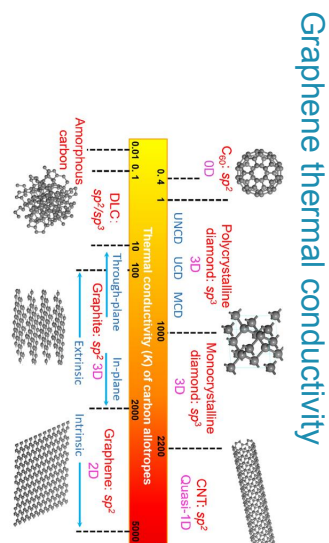
where $C_v(T)$ is the specific heat per unit volume where c_{ph} is the phonon mean free path. This implies that since c_{ph} is very large in graphene, one can expect to have high thermal conductivity.

Since graphene is composed of a light atom, where the in-plane bonding is very strong, graphene exhibits a very high value of the in-plane sound velocity, close to $c_{ph} \approx 20$ km/s.

Indeed, experiments at near room temperature obtain $\kappa \approx 3000-5150$ W/mK and a phonon mean free path of $\lambda \approx 775$ nm for a set of graphene flakes.

Materials Physics and Technology for Nanoelectronics
Carbon Materials

KU LEUVEN



Thermal conductivities of carbon allotropes (unit: $W/m \cdot K^{-1}$)

Materials Physics and Technology for Nanoelectronics
Carbon Materials

KU LEUVEN

Mechanical properties of graphene

Mechanical properties of graphene

Being only a single atom thick, and possessing an intrinsically perfect lattice, graphene is very strong and can withstand elastic deformations up to 20%.



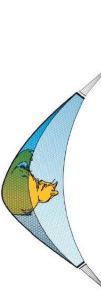
- 40 N/m breaking strength ($100\times$ steel)
- Young's modulus ~ 1 TPa
- density: 0.77 mg/m^2
- The ripples appear just like for a macroscopic material

Lee et al., Science 321, 385 (2008)

27

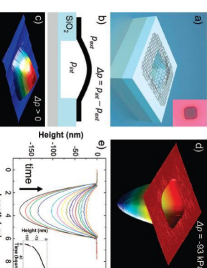
CI "Thermoelectric materials" chapter

- A hypothetical 1 m^2 hammock would weigh only 0.77 mg (less than a cat's whisker) but:
- It would bear the weight of a car without breaking (up to 4 kg)
- It would be invisible!



A hypothetical 1 m^2 hammock would weigh only 0.77 mg (less than a cat's whisker) but:

- A graphene membrane is impermeable to most gases (including Helium)
- It has a high mechanical stability
- "strongest material known"
- Low mass
- Flexible



28

Materials Physics and Technology for Nanoelectronics
Carbon Materials

KU LEUVEN

Optical properties of graphene

Graphene is very transparent for light over a wide range of wavelengths. The transmittance T can be expressed as:

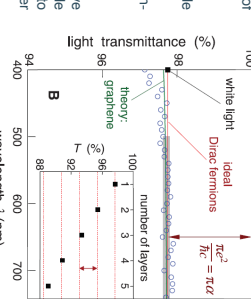
$$T = (1 + 0.5\pi\alpha)^{-2} \sim 1 - \pi\alpha \quad (\text{for } 10 \text{ layers})$$

Graphene reflects $< 0.1\%$ of the incident light in the visible region ($\sim 2\%$ for 10 layers).

Few-layer graphene can be considered made up of non-interacting layers, each absorbing $1 - T = 100 - 97.7 = 2.3\%$

→ optical absorption linearly proportional to thickness!

The practical application of graphene as transparent conductive electrode is hampered by the relatively high resistivity of single graphene layers. Multiple graphene layers are needed to achieve resistivity low enough to be truly competitive to other materials such as ITO (Indium Tin Oxide).



Materials Physics and Technology for Nanoelectronics
Carbon Materials

KU LEUVEN



Graphene NEMS

- Young's modulus: $\sim 1.10 \text{ TPa}$ (Si: $\sim 130 \text{ GPa}$)
- Elastically stretchable by 20%
- High mechanical stability
- "strongest material known"



29

KU LEUVEN

Graphene optical properties

The optical absorption of graphene arises from two distinct types of contributions, those from **intra-band** and those from **inter-band** optical transitions.

The relative importance of the two contributions depends largely on the spectral range of interest:

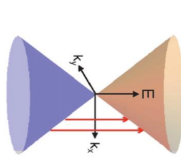
- In the **far-infrared region**, the optical response is dominated by the free-carrier (or intra-band) response. By fabricating sub-wavelength structures in graphene, one can create a tunable far-infrared response that is dominated by **plasmonic excitations** associated with these free carriers.
- In the **mid- to near-infrared region**, the optical absorbance is attributable primarily to inter-band transitions. This response is nearly frequency independent and is equal to a universal value determined by the **fine-structure constant** e^2/hc in pristine graphene. However, this optical absorption in graphene can be controlled through **electrostatic gating**, which shifts the Fermi energy and induces Pauli blocking of the optical transitions.
- In the **ultraviolet spectral range** (with the transitions approaching the saddle-point singularity), the inter-band optical absorption increases well beyond the universal value and exhibits signatures of **excitonic effects**.

Interband optical absorption in graphene

Universal optical conductivity

- Interband absorption arises from direct optical transitions between the valence and conduction bands. At frequencies above the **far-infrared region**, these interband transitions typically define the optical response of graphene. Within the tight-binding model, the optical sheet conductivity from interband transitions can be readily calculated.

For pristine graphene at zero temperature, the optical conductivity in the linear dispersion regime of graphene is found to be independent of frequency.



Schematic of interband optical transitions in graphene.

Minimally Physics and Technology in Nanoelectronics Carbon Materials

Kin Fa Mak et al., Solid State Communications 152, (2012)



31

Interband optical absorption in graphene

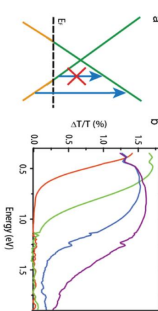
Tunable interband optical transition

- Because of the single-atom thickness of graphene and its linear dispersion with a high Fermi velocity, the Fermi energy in graphene can be shifted by hundreds of meV through electrostatic gating.

Such doping leads to a strong change in the interband absorption through Pauli blocking.

The interband transitions for photon energies below $2|E_F|$ are suppressed, while those at energies above $2|E_F|$ are unaffected. The optical response in graphene thus becomes highly tunable.

Kin Fa Mak et al., Solid State Communications 152, (2012)



(a) an illustration of interband transitions in hole-doped graphene. (b) the gate-induced change of transmission T as a function of gate voltage V_g . The values of the gate voltage referenced to that for charge neutrality, $V_0 - VC(V_g)$, for the curves - 0.75, - 1.75, - 2.75 and - 3.5 V, from left to right.

32

Minimally Physics and Technology in Nanoelectronics Carbon Materials

Kin Fa Mak et al., Solid State Communications 152, (2012)

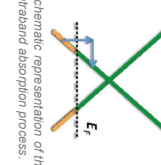


32

Intraband optical absorption in graphene

Since the speed of light c is much higher than the Fermi velocity c_{l_F} of graphene ($c/c_{l_F} \sim 300$), direct absorption of a photon by an intraband optical transition does not satisfy momentum conservation. To conserve momentum, **extra scattering with phonons or defects** is required.

Plasmons are quanta of collective oscillation of charge carriers. Direct light absorption by propagating plasmons in graphene film is not allowed due to the large momentum mismatch between photons and plasmons. However, plasmon absorption can be enabled with grating coupling, which provides an effective momentum due to the periodic grating structure.



Schematic representation of the intraband absorption process.

33

Minimally Physics and Technology in Nanoelectronics Carbon Materials



33

Graphene Synthesis

Micromechanical cleavage of bulk graphite

Fabrication of graphene

1st Isolation of graphene monolayers: K.S. Novoselov et al., Science 306, 666 (2004)

SEM of a relatively large graphene crystal (approximately 6 layers). Optical photo. Lateral size of the image 100 microns.

SEM of a fallen mass of graphite. This is the way graphene molecules were extracted from bulk graphite. To be reasonably visible in SEM, we shot a 10 nm carbon flake (30 layer thick).

34

Minimally Physics and Technology in Nanoelectronics Carbon Materials

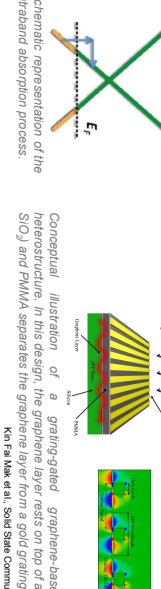
Kin Fa Mak et al., Solid State Communications 152, (2012)



34



Large graphene flake (approximately 6 layers). Optical photo. Lateral size of the image 100 microns.



Conceptual illustration of a grafting-grated graphene-based plasmonic heterostructure. In this design, the graphene layer rests on top of a dielectric (e.g. SiO_2) and PMMA separates the graphene layer from a gold grating structure.

35

Minimally Physics and Technology in Nanoelectronics Carbon Materials



35

Minimally Physics and Technology in Nanoelectronics Carbon Materials

Kin Fa Mak et al., Solid State Communications 152, (2012)



36

Minimally Physics and Technology in Nanoelectronics Carbon Materials

Kin Fa Mak et al., Solid State Communications 152, (2012)



36

Graphene fabrication: exfoliation

The most common technique to fabricate graphene is by exfoliation from HOPG (Highly Ordered Pyrolytic Graphite) by using adhesive tape.

Novoselov et al., *Science* 306, 666 (2004)

- flake size: 5 – 100 nm
- random location
- simple process for proof-of-concept
- no industrial relevance

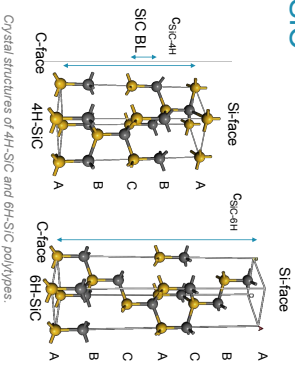


Materials Physics and Technology for Nanoelectronics
Carbon Materials

KU LEUVEN



SiC occurs in cubic form as well as several hexagonal polytypes. For graphene growth purposes, mostly hexagonal 4H and 6H SiC crystals have been used. An n-H-SiC cell is made of n SiC bilayers (BL), each containing 1 Carbon and 1 Silicon plane. SiC has 2 polar faces perpendicular to the c axis: Si-terminated SiC(0001) and C-terminated SiC(0001). Each face has 1 dangling bond per Si or C atom.



40

Hess et al., *J. Phys. Cond. Mat.* 20, 323202 (2008)

Materials Physics and Technology for Nanoelectronics
Carbon Materials

KU LEUVEN

Graphene formation by exfoliation of HOPG

1. Peel a HOPG (Highly ordered Pyrolytic Graphite) layer with razor blade
2. Thin the HOPG piece
3. Repeatedly press and release in the prepared tape
4. Find the monolayer graphite with an optical microscope

Materials Physics and Technology for Nanoelectronics
Carbon Materials

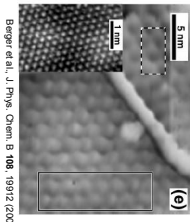
KU LEUVEN

Epitaxial graphene on c-SiC

Graphene can also be produced from silicon carbide (SiC) wafers. This is an old technique known since 1975. The number of layers depends on temperature

- Si-face SiC: few layers, decoupled
- Si-face SiC: mostly single layer

All quantum effects observed for exfoliated graphene have been observed in epitaxial graphene as well



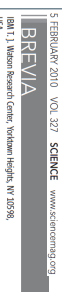
(e)

Berger et al., *J. Phys. Chem. B* 108, 19912 (2004)

Epitaxial graphene on c-SiC

First demonstration of 'wafer-scale' (2 inch) integration of graphene.

- Graphene growth carried out on a 2" SiC wafer
- Pre-cleaning @ 810 °C in 1:1 Si₂H₆:He
- Growth on the Si-face (1450 °C, 10⁻⁴ torr, 2)



BREVA

IBM T.J. Watson Research Center, Yorktown Heights, NY 10598, USA

100-GHz Transistors from Wafer-Scale Epitaxial Graphene

Y.-M. Lin, C. Dimitrakopulos, K. A. Jenkins, S. B. Farmer, H.-Y. Ong, A. Grill, P. Avouris

Materials Physics and Technology for Nanoelectronics
Carbon Materials

KU LEUVEN

SiC surface preparation

Pre-treatment in H₂
(~1000 °C)

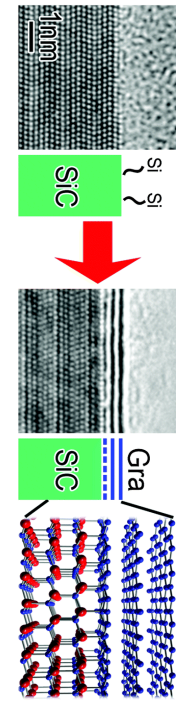
Graphene Synthesis by Si desorption (~1250–1450 °C)

5 FEBRUARY 2010 VOL 327 SCIENCE www.sciencemag.org

Materials Physics and Technology for Nanoelectronics
Carbon Materials

KU LEUVEN

Lin et al., *Science* 327, 652 (2010)



38

39

Graphene CVD

Chemical Vapor Deposition (CVD) is the most mature, cost-efficient graphene growth process that is scalable.



Requirements for the optimal (metallic) template for deposition (Pt, Cu, Ir, Pd, ...):

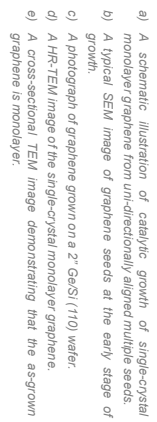
- Atomically flat and monocrystalline
- Stable thin film at high temperature
- Low carbon solubility
- Reusable (cheap)
- Capable to initiate oriented graphene growth
- Minimize graphene grain boundaries

Graphene transfer is needed after the growth process.



Materials Physics and Technology for Nanoelectronics
Carbon Materials
KU LEUVEN

Single-crystal monolayer graphene grown on hydrogen-terminated Ge(110) surface.
 $\text{SiO}_2 + \text{Ge}(110) \rightarrow \text{graphene}_{(s)} + 2\text{H}_2(g)$

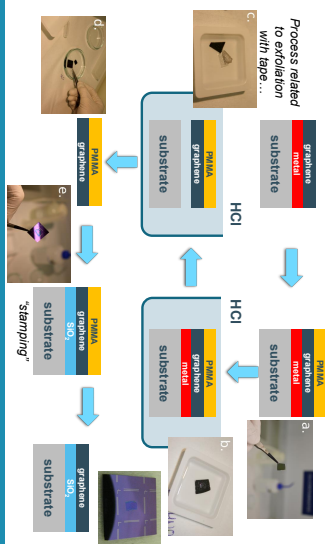


J.H. Lee et al., Science 344 (2014)



Materials Physics and Technology for Nanoelectronics
Carbon Materials
KU LEUVEN

Graphene transfer step-by-step

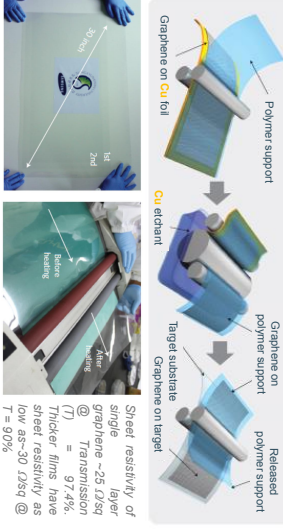


Materials Physics and Technology for Nanoelectronics
Carbon Materials
KU LEUVEN

Large sheet graphene CVD

Fabrication of large area graphene sheets by CVD on Cu foils was demonstrated.

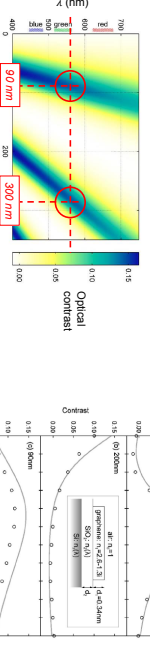
Rollable, continuous films transferred grown on Cu foils and transferred onto a flexible display after nitric acid treatment.



Bao et al., Nat. Nanotechnol. 5, 574 (2010)

Graphene visibility on dielectrics

Due to optical interference, a graphene layer becomes visible on an SiO₂ layer with the correct thickness (90 nm, 300 nm, ...)



$$\mathcal{C} = \frac{I(n_0 = 1) - I(n_1)}{I(n_0 = 1)} = \begin{cases} \cdot \text{air}, n_0 = 1 & \cdot \text{SiO}_2, n_2 = n_1(\lambda) \\ \left[\cdot \text{air}, n_0 = 1 \right] - 2.6 - 1.3t \quad (\text{bulk graphite}) & \cdot \text{SiO}_2, n_2 = n_1(\lambda) \end{cases}$$

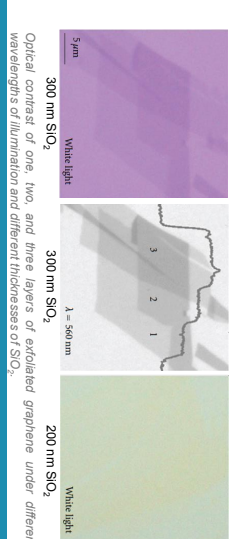
$$t = 97.4\%$$

(7)

Thicker films have a lower optical contrast as 30 nm SiO₂ @ $t = 90\%$

Optical detection of graphene

Even a monolayer of graphene can become visible on SiO₂ using an optical microscope. The contrast depends on the thickness of SiO₂, the wavelength of light used, and the angle of illumination. This feature of graphene is useful for the quick identification of few- to single-layer graphene sheets and is very important for mechanical exfoliation.

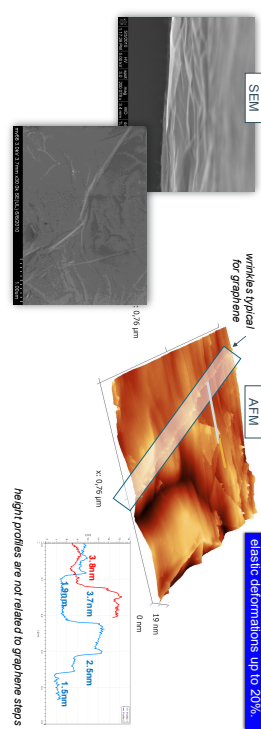


Materials Physics and Technology for Nanoelectronics
Carbon Materials
KU LEUVEN

High quality graphene on Ge(110) surfaces

Graphene morphology

When supported by a substrate graphene takes the shape of the substrate, but wrinkles can occur.



P. Huang et al. Nature 469 (2011)

Materials Physics and Technology for Nanoelectronics
Carbon Materials

KU LEUVEN

Graphene "atomic" morphology

When supported by a substrate graphene takes the shape of the substrate, as shown by the STM image. Despite the surface roughness, the honeycomb structure of the graphene is preserved.



For epitaxial graphene, extremely smooth surfaces can be achieved.

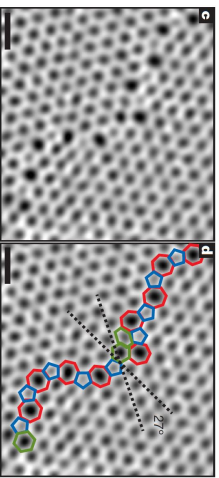
STM allows atomic characterization of the crystalline structure revealing nicely the carbon hexagonal ring.

Graphene/Fe (2001)

KU LEUVEN

Graphene defects

Defects in graphene can be observed by TEM.



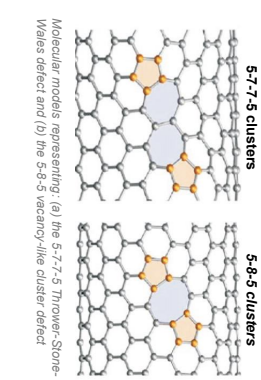
Atomic-resolution ADF-STEM image of Graphene crystal with two grains. Left: Two grains intersect with a 27° relative rotation. An aperiodic line of defects stitches the two grains together. The left image with the pentagons (blue), heptagons (red) and distorted hexagons (green) of the grain boundary outlined (scale bars: 5Å)

P. Huang et al. Nature 469 (2011)

Graphene typically accommodates two common types of carbon cluster defects with sp²-hybridized carbon. The most common cluster defect is the 5-7-5 defect, but also frequently occurring are 5-8-5 defects, both of which maintain an average of the six carbon planar rings of Graphene.

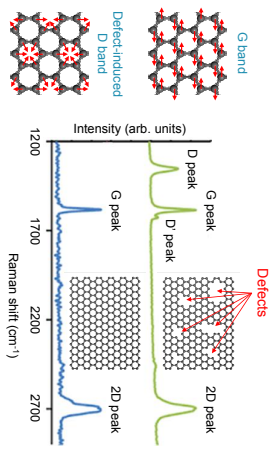
Therefore, graphene can be annealed at sufficiently high temperatures to lower its defect concentration.

Since the 5-7-5 and 5-8-5 defects are symmetry-breaking, they can be observed spectroscopically in the Raman D-band.



P. Kramp et al. Materials Today 15(3), March 2012

Raman spectrometry is a perfectly suitable characterization technique for the presence of defects in graphene layer. Pristine graphene layer exhibits strong G and 2D peaks, while defective graphene will show additional D and D' peaks in the spectrum.

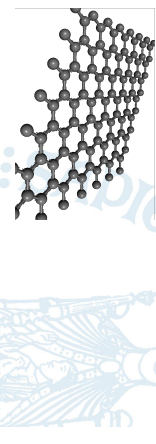


53

KU LEUVEN

Graphene

Devices & applications



Graphene defects

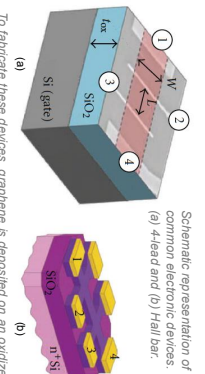
Electronic transport in graphene

Transport properties are typically measured with a graphene device similar to those shown on the adjacent figure. With this graphene device, one can tune the charge carrier density between holes and electrons by applying a gate voltage (V_g) between the (doped) silicon substrate and the graphene flake. The gate voltage induces a surface charge density n_{ss} :

$$n_{ss} = \frac{\epsilon_0 \epsilon_r V_g}{t q}$$

where ϵ_0 is the SiO_2 permittivity, q is the electron charge, and t is the thickness of the SiO_2 layer.

This charge density change shifts accordingly the Fermi level position (E_F) in the band structure,



Schematic representation of common electronic devices.
(a) 4-terminal Hall bar and (b) Hall bar.

To fabricate these devices, graphene is deposited on an oxidized silicon wafer. Electrical contacts, usually made of gold, are defined using a lithographic process or a stencil mask to avoid photoresist contamination. Electrodes are generally patterned in a 4-terminal or Hall bar configuration. Lastly, the device can be cleaned by annealing at ultrahigh vacuum or in H_2/Ar gas, or by applying a large current density ($\sim 10^8 \text{ A}/\text{cm}^2$) through it to remove adsorbed contamination.

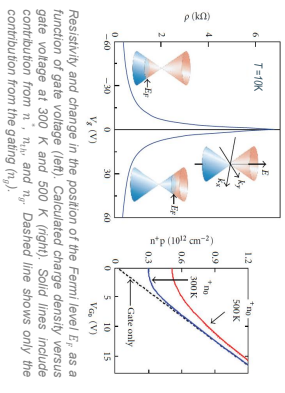
Materials Physics and Technology for Nanoelectronics
Carbon Materials

KU LEUVEN

Electronic transport in graphene

Due to the special shape of the band diagram, an **anomalous** electric field effect (i.e. both electron and hole conduction) is observed in graphene.

The peak in the **resistivity** versus gate voltage curve occurs when the Fermi level is aligned with the Dirac point (i.e. where the two cones touch each other) as the density-of-states (DOS) disappears at that point. Typically, charge density can be tuned from 10^{11} to 10^{13} cm^{-2} by applying a gate voltage that moves E_F from 10 to 400 meV away from the Dirac-point.

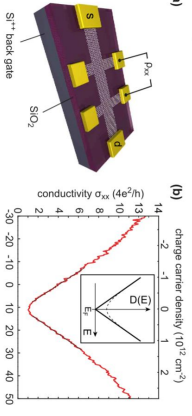


Materials Physics and Technology for Nanoelectronics
Carbon Materials

KU LEUVEN

Electronic transport in graphene

At the Dirac point, the carrier density n should theoretically vanish, but thermally generated carriers (n_{th}) and electrostatic spatial inhomogeneity (n_r) limit the minimum charge density.



(a) Schematic of a contacted graphene Hall-bar device. (b) Conductivity as a function of back-gate voltage V_B at $T = 2\text{K}$. By varying the carrier density via the back-gate charge transport is tuned from hole- to electron-like conductivity. The charge neutrality point is offset from $V_B = 0$ V due to residual doping of the graphene. In the inset the smearing of the density of states around the charge-neutrality point due to electron-hole-pair creation is sketched.

Materials Physics and Technology for Nanoelectronics
Carbon Materials

KU LEUVEN

Mobility in suspended graphene

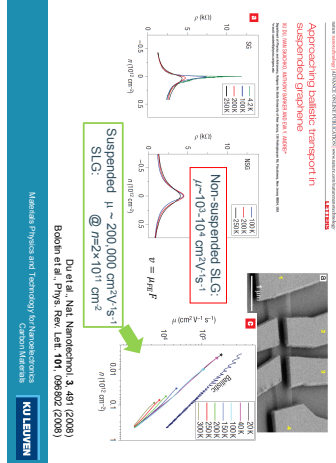
Concerning electronic applications, graphene has attracted considerable attention due to its high carrier mobility.

The high mobility in suspended graphene has been experimentally demonstrated.

The resistance of graphene depends strongly on the carrier density and the temperature.

The mobility in graphene is limited by various scattering mechanisms.

Approaching realistic transport in suspended graphene



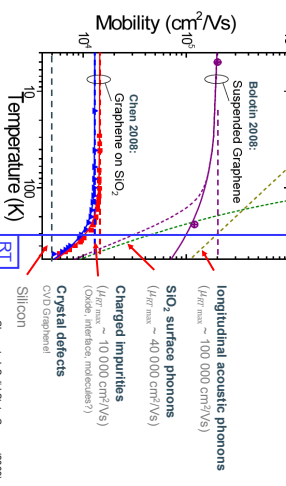
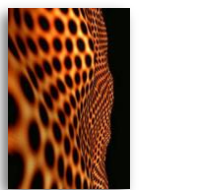
Bolotin et al., Nat. Nanotechnol. 3, 492 (2008)

Das et al., Nat. Nanotechnol. 3, 492 (2008)

KU LEUVEN

Graphene transistor: fundamental limits

The mobility in graphene is limited by various scattering mechanisms.



Cai et al., Solid State Comm. (2009)

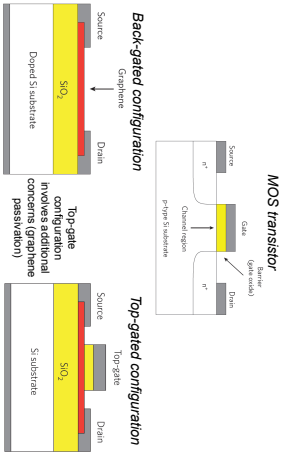
KU LEUVEN

Si-based FET vs graphene-based FET

Graphene generated a lot of interest for FET devices due to its high carrier mobility and because an atomically thick channel would allow for extreme scaling.

What else do we need?

- Low I_{off} (low static power dissipation)
- n - and p -doping (CMOS)
- Gate oxide: top-gated configuration preferred over back-gate.



Materials Physics and Technology for Nanoelectronics
Carbon Materials

KU LEUVEN

57

KU LEUVEN

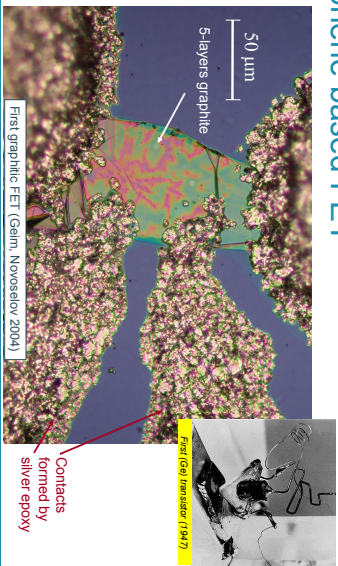
62

KU LEUVEN

62

KU LEUVEN

Graphene based FET



63

63

63

Materials Physics and Technology for Nanoelectronics
Carbon Materials

KU LEUVEN

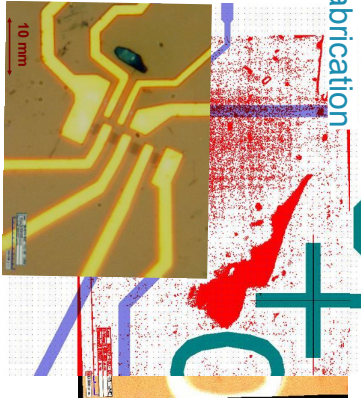
Graphene device fabrication

Design:

- Flake identification
- Image processing
- Import in layout design software
- Designing device shape
- Design for contacts

Fabrication:

- E-beam process for shape definition, followed by O₂ plasma etching
- E-beam step followed by metalization and lift-off



64

64

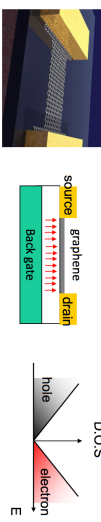
64

Materials Physics and Technology for Nanoelectronics
Carbon Materials

KU LEUVEN

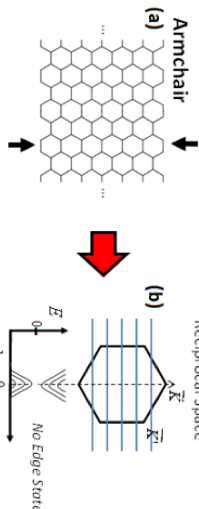
Graphene Field-Effect Transistor (FET)

The poor I_{on}/I_{off} ratio of graphene FETs due to bandgap makes them unsuitable for logic applications.

Poor I_{on}/I_{off} ratio...
Bad for digital switches!

GNR electronic structure

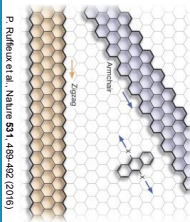
Due to its quasi 1D nature, electron states are **quantized** in the directions perpendicular to the GNR axis (k_{\perp}), while the states in the direction along the GNR axis (k_{\parallel}) are continuous. This leads to the formation of **1D sub-bands** for electrons in the k_{\parallel} direction.



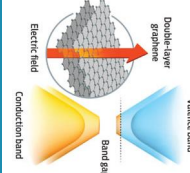
Bandgap in graphene ?

Pristine single-layer (SLG) and bilayer (BLG) graphene are semi-metallic. In order to be useful for field-effect devices, a bandgap must be created. A bandgap can be *engineered* by symmetry-breaking or quantum confinement.

symmetry-breaking



quantum confinement

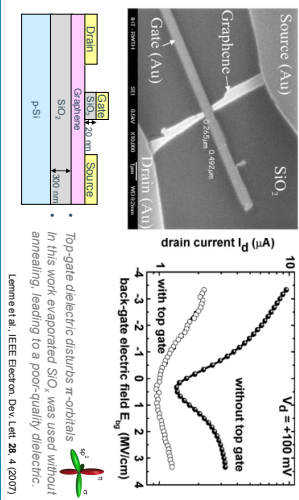


65

KU LEUVEN

Demonstration of a ‘classical’ field-effect devices using a top gate structure.
Notice the reduction in the drive current when a gate insulator is used. Furthermore, the device has a very low I_{on}/I_{off} ratio, limiting its applicability.

In this work evaporated SO₂ was used without annealing, leading to a poor-quality dielectric.



66

KU LEUVEN

Materials Physics and Technology for Nanoelectronics
Carbon Materials

KU LEUVEN

Graphene field-effect devices

65

Materials Physics and Technology for Nanoelectronics
Carbon Materials

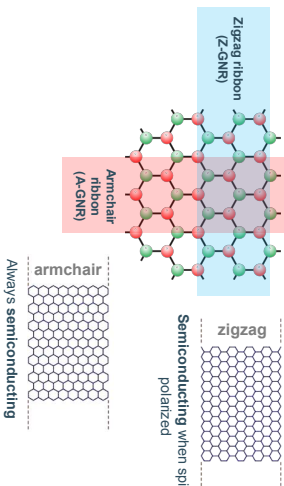
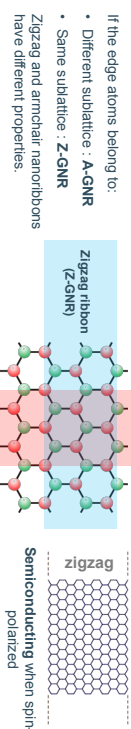
KU LEUVEN

66

Materials Physics and Technology for Nanoelectronics
Carbon Materials

KU LEUVEN

Graphene nanoribbons



66

Materials Physics and Technology for Nanoelectronics / Carbon Materials

KU LEUVEN

Graphene nanoribbons

Some approaches have shown potential for large-scale fabrication of GNRs with controlled alignment:

- Bottom-up**
 - organic synthesis method in solution
 - Templated growth of on SiC or on other substrates
 - Direct-growth on nickel nanostructures
 - Direct growth from a DNA template
 - Growth from catalyst composite nanofbers
- Top-down**
 - Nanowire lithography
 - Narrowing of GNRs from edges
 - Block-copolymer lithography
 - Unzipping carbon nanotubes

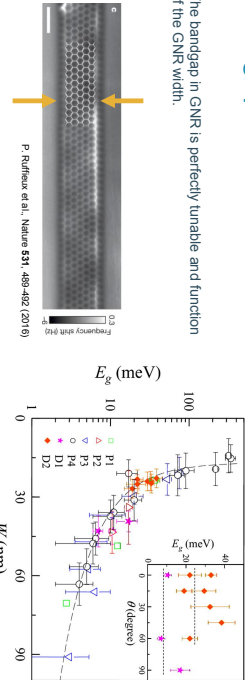
Challenges: scalable GNR, with smooth edges and controlled width

Materials Physics and Technology for Nanoelectronics / Carbon Materials

KU LEUVEN

Bandgap in GNR

The bandgap in GNR is perfectly tunable and function of the GNR width.



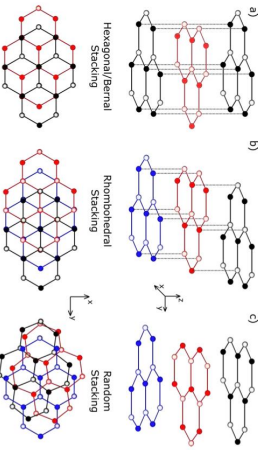
P. Ruffieux et al., Nature 531, 489-492 (2016)

Energy gap versus width of the graphene nanoribbon. The inset shows the bandgap versus angle of the nanoribbon.

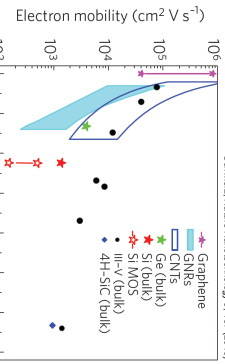
Dashed lines in the inset show the value of E_g as predicted by the empirical scaling of E_g versus width (W).

Multilayer graphene

Bi-layer graphene (BLG) consists of two single layer graphene layers stacked on top of each other.



Side and top view of different graphene layer stacks: a) hexagonal / Bernal, b) rhombohedral and c) random stacking.

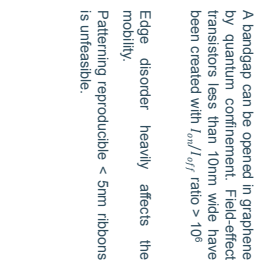


Schwarz, Nature Nanotechnology 5, 487 (2010)

KU LEUVEN

Benchmarking of graphene nanoribbons

Graphene nanoribbons show substantial suppression of performance. When a bandgap is opened the electron mobility drops considerably. As a result it is difficult for graphene to beat performance of more standard technologies.

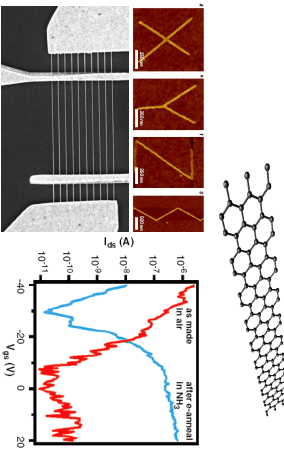


Wang et al., Nature Chem. 2010, SCIENCE 2010

KU LEUVEN

Bandgap opening in graphene: nanoribbon

A bandgap can be opened in graphene by quantum confinement. Field-effect transistors less than 10nm wide have been created with I_{on}/I_{off} ratio > 10^6 . Edge disorder heavily affects the mobility. Patterning reproducible < 5nm ribbons is unfeasible.



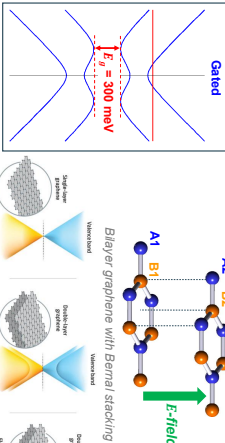
Wang et al., Nature Chem. 2010, SCIENCE 2010

KU LEUVEN

Bandgap opening in graphene bi-layers

In bilayer graphene without gating, the lowest CB and highest VB in BLG touch each other at K and no bandgap is present.

In bilayer graphene with **Bernal stacking**, a bandgap occurs when an electric field is applied due to symmetry breaking

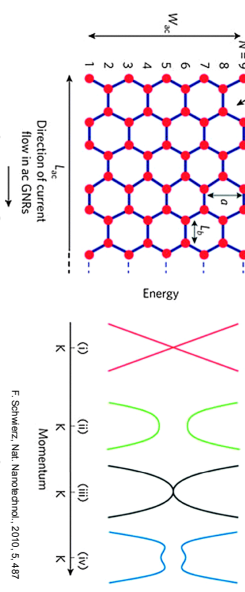


Opening of a bandgap in graphene bilayers due to a perpendicular E field.

Materials Physics and Technology for Nanoelectronics
Carbon Materials

KU LEUVEN

Bandgap in graphene bi-layers



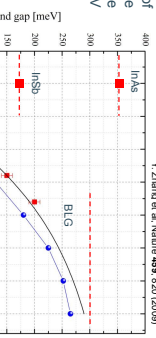
(a) Schematic demonstration of an armchair GNR. (b) Band structure near the K point of (i) bulk graphene, (ii) graphene nanoribbons, (iii) bilayer graphene, and (iv) bilayer graphene in an applied perpendicular electric field.

F. Schweiß. Nat. Nanotechnol. 2010, 5, 487

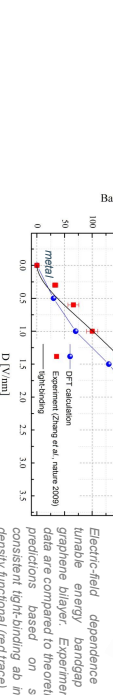
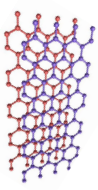
76

Bandgap in graphene bi-layers

Stacking two bilayer of graphene gives the possibility of tuning the energy gap up to 300 meV by a vertical electric field.



Y. Zhang et al. Nature 459, 820 (2009)

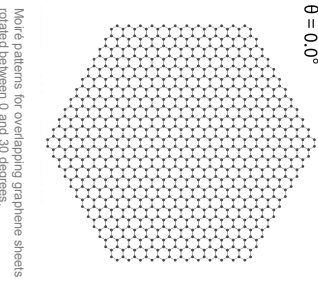


77

Twistronics

When a graphene bilayer is twisted so that the top sheet is rotated out of alignment with the lower sheet, the unit cell (the smallest repeating unit of the material's 2D lattice) becomes enlarged. The variation of the 'twist' angle between layers of graphene (or other 2D materials) affects their electronic, optical and mechanical properties.

A **moiré pattern** is produced in which the local stacking arrangement varies periodically. This emerging field of research is called 'twistronics' which offers new approach to device engineering.



Moiré patterns for overlapping graphene sheets rotated between 0 and 30 degrees.

Materials Physics and Technology for Nanoelectronics
Carbon Materials

KU LEUVEN

Moiré patterns in Graphene

- For 8.8° rotation, the moiré pattern that emerges has a central superlattice hexagon surrounded by six others of the same size. Each of these moiré hexagons occupies about a quarter to a third of the entire hexagonal field in each direction.
- At 4.4° rotation, the central superlattice hexagon expands to about twice its previous size, covering about one-half to two-thirds of the entire field.
- At 2.2° rotation, the central superlattice hexagon covers the $\theta = 2.2^\circ$ entire original bounding hexagon.
- For 1.1° rotation, the angle that produces the interesting effects in graphene, the superlattice seems to have disappeared completely and the pattern looks almost like a single sheet without any more.

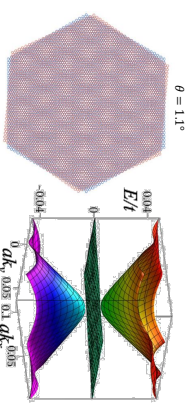
F. Schweiß. Nat. Nanotechnol. 2010, 5, 487

78

Effects of rotation in twisted bilayer graphene

For rotation angles of $\sim 1.1^\circ$ (**the magic angle**), regions in which the atoms are directly above each other (the lighter regions in the pattern) form narrow electron energy bands, in which electron correlation effects are enhanced. This results in the generation of a non-conducting state (a Mott insulator), which can be converted into a **superconducting state** if charge carriers are added to the graphene system by applying a small electrical field.

This Mott insulator is a material that should be a metal but which, because of strong repulsion between electrons, does not conduct.



79

Materials Physics and Technology for Nanoelectronics
Carbon Materials

KU LEUVEN

Metal contacts to graphene

Cf. "Semiconductors" chapter.

When a metal and a semiconductor come into contact, charges are transferred from higher energy states to lower energy states until the energy levels are balanced in an equilibrium state. Due to the small density of states in a semiconductor, there is no band bending along the vertical direction known as the depletion. In a similar manner, graphene can also be modeled as a semiconductor with a zero bandgap, and band gap is necessary if graphene has a finite thickness. Graphene has no band gap, instead of an energy band, the "Dirac energy level" ($E_{D\sigma}$) would be a proper term for graphene. Dirac energy level bending in graphene along the lateral direction does not occur, but there is a work function shift in graphene.

It was first theoretically estimated that graphene on various crystalline metals can be doped due to the presence of an interface dipole layer induced by the charge transfer. In addition to the shift of the work function or graphene underneath metal, there is a gradual bending of the Dirac energy level along the horizontal direction near the contact edge due to the work function difference between the exposed graphene and the graphene underneath the metal. This region is known as the charge transfer region.

81

Materials Physics and Technology for Nanoelectronics
Carbon Materials



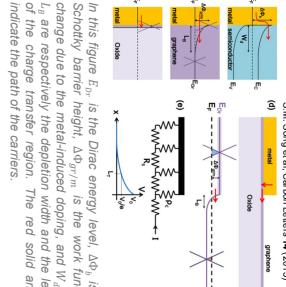
Metal contacts to graphene

The facial contact between a metal and graphene typically results in large contact resistance dominated by the contact length rather than the contact area.

Graphene underneath metal is doped in holes and the channel graphene is negatively doped by the back-gate voltage. The thicker E_D underneath the metal represents the broadening of the density of states near the Dirac energy level.

The model of the graphene-metal contact includes the contact resistivity (ρ_c) and sheet resistance (R_s). Transfer length (L_T) is the effective contact length which is defined with the distance where the potential drops to 1/e times from the edge.

The model of the graphene-metal contact includes the contact resistivity (ρ_c) and sheet resistance (R_s). Transfer length (L_T) is the effective contact length which is defined with the distance where the potential drops to 1/e times from the edge.



In this figure E_D is the Dirac energy level, $\Delta\Phi$ is the Schottky barrier height, $\Delta\Phi_{Dop}$ is the work-function change due to the metal-induced doping, and V_g and L_T are respectively the depletion width and the length of the charge transfer region. The red solid arrows indicate the path of the carriers.

Materials Physics and Technology for Nanoelectronics
Carbon Materials



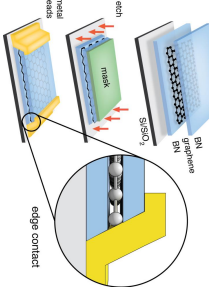
Cf. "Semiconductors" chapter.

Metal contacts to graphene

An alternative approach to overcome the facial contact is to use the edge contact structure which is formed by a covalent bond between the metal atoms and the graphene.

This contact is expected to show significantly lower contact resistance compared to the facial contact.

Theoretical reports estimated that the contact resistivity could be as low as 10 to 10³ times the facial contact based on a quantum tunneling process.



Schematic illustration of an edge contact to a graphene layer sandwiched between two hexagonal Boron Nitride (h-BN) layers.

82

Materials Physics and Technology for Nanoelectronics
Carbon Materials

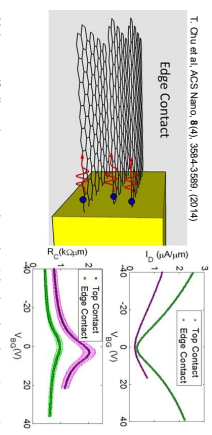


Metal contacts to graphene

Contact modules with edge contact were developed and demonstrated.

An about 2 times lower contact resistance is observed in edge-contacted few layer graphene (FLG) devices compared to those with conventional top contacts.

Using a self-aligned process, graphene is etched and carbon atoms at the cut edges are directly contacted by a subsequently deposited metal layer. The covalent/bond formed between metal and carbon atoms allow for a lower contact resistivity compared to the weak van der Waals bonds under conventional top contacts. These edge contacts bypass the tunneling resistances between layers and allow direct current injection into individual graphene layers.



83

Materials Physics and Technology for Nanoelectronics
Carbon Materials



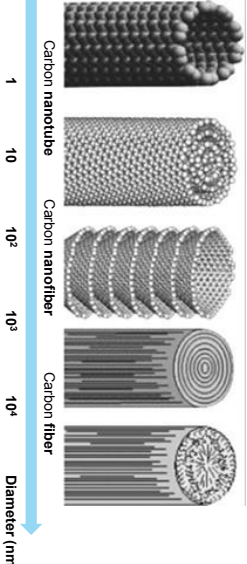
Carbon filaments in different flavors

SWCNT

MWCNT

CNF

CF

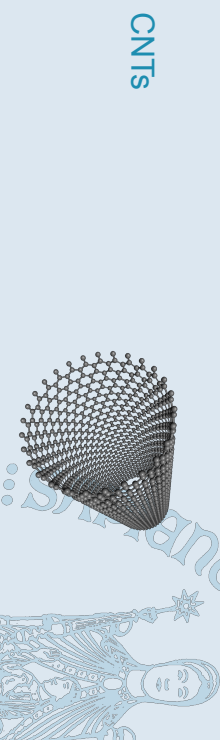


84

Materials Physics and Technology for Nanoelectronics
Carbon Materials

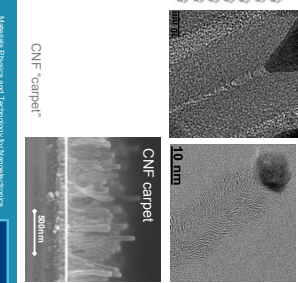
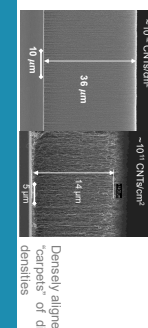
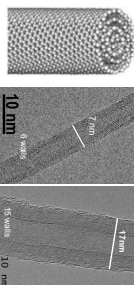


CNTs

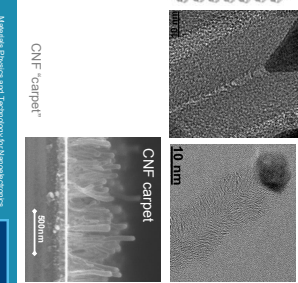
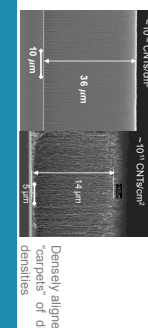


Carbon filaments in different flavors

Multi-Walled CNT (MWCNT)



Carbon nanofibers (CNF)



Electronic properties of CNTs

The electronic properties of CNTs can be understood by looking to the electronic properties of graphene. The sp^2 bonded structure from a graphene plane provides some remarkable properties of the graphene band structure.

The carbon atoms in graphene form a hexagonal lattice on a two-dimensional plane. Each carbon atom is about $a_{C-C} = 1.42 \text{ \AA}$ from its three neighbors, with each of which it shares one σ -bond. The fourth bond is a π - sp^2 hybridisation bond, which is oriented in the z -direction (out-of-plane).

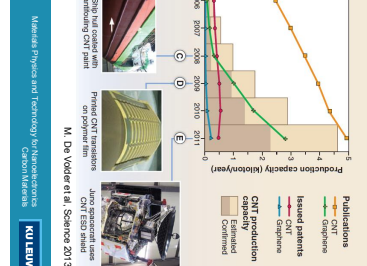
- * single $2p_z$ orbital forming the σ bonds in the xy plane
- * remaining $2p_z$ orbital (π orbit) exists perpendicular to the xy plane

92

Trends in CNT research and applications

Carbon nanotubes have found their way in many applications,

(A) Journal publications and issued worldwide patents per year, along with estimated annual production capacity (B to E) Selected CNT related products: composite bicycle frame, anisotropic coatings, printed electronics and electrostatic discharge shielding.



Materials Physics and Technology for Nanoelectronics
Carbon Materials

KU LEUVEN

93

Carbon nanotubes

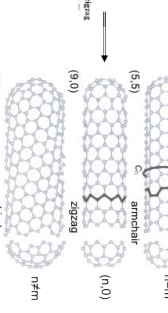
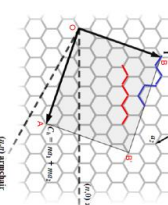
Single Walled Nano Tubes (SWNTs) are obtained by wrapping a graphene sheet along chiral directions.

The 2D unit cell: This rectangle is rolled-up in the chiral vector direction, i.e. the segment OB is put together with segment AB'.

The pair of (n,m) indices thus

$c_0 = m\hat{a}_1 + n\hat{a}_2$; chiral vector, with (n,m) the indices of the tube CNT.

T , translation vector perpendicular to c_0 .



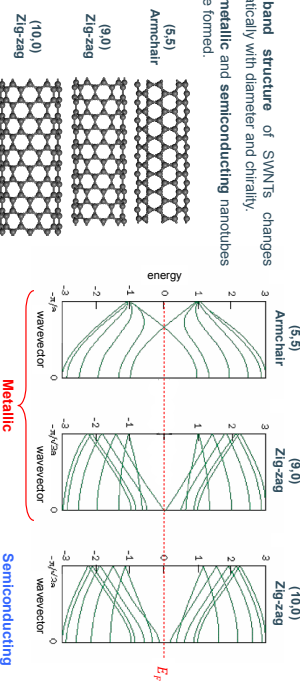
Materials Physics and Technology for Nanoelectronics
Carbon Materials

KU LEUVEN

94

Band structure of SWNTs

The band structure of SWNTs changes dramatically with diameter and chirality. Both metallic and semiconducting nanotubes can be formed.



95

CNTs

Fundamentals & properties

Materials Physics and Technology for Nanoelectronics
Carbon Materials

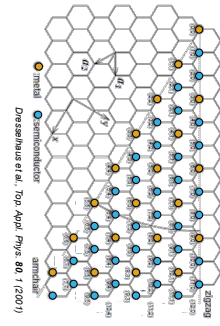
KU LEUVEN

96

Carbon nanotubes

Statistically, in a random SWNTs mixture, 1/3 are metallic and 2/3 semiconducting.

- (n, n) armchair SWNTs \Rightarrow always **metallic**
- $(n, 0)$ zigzag SWNTs \Rightarrow metallic if n is multiple of 3
- $n - m = 3k \pm 1$, k integer \Rightarrow **metallic** SWNTs
- $n - m = 3k \pm 1$, k integer \Rightarrow **semiconducting** SWNTs



Dresselhaus et al., *Top Appl Phys* 90, 1 (2011)

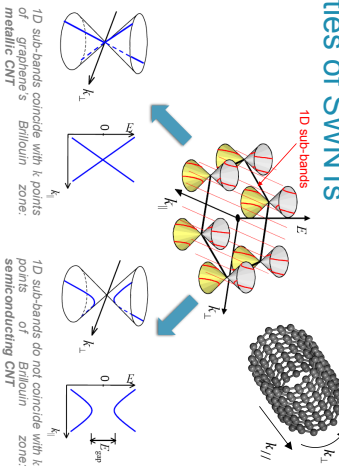
Materials Physics and Technology for Nanoelectronics
Carbon Materials

KU LEUVEN

Electronic properties of SWNTs

This rule is related to the symmetry of the CNT.

Due to its quasi 1D nature, electron states are quantized in the directions perpendicular to the CNT axis (k_{\perp}), while the states in the direction along the CNT axis (k_{\parallel}) are continuous. This leads to the formation of **1D sub-bands** for electrons in the k_{\parallel} direction



Materials Physics and Technology for Nanoelectronics
Carbon Materials

KU LEUVEN

Electronic properties of SWNTs

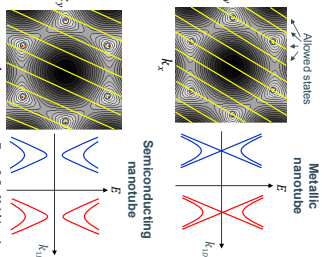
The band structure of SWNTs can (approximately) be determined from that of graphene.

In graphene the wave-vectors k_x and k_y can assume arbitrary (continuous) values in the reciprocal space (infinite 2D sheet).

In a SWCNT the wave-vector along the circumference is fixed and the wave-vectors k_x and k_y are therefore linearly related (lines). The band structure is determined by m and n values.

\rightarrow Electron confinement \rightarrow quantization of the wave vector along circumference.

\rightarrow Each band is a "slice" through the dispersion curve of graphene

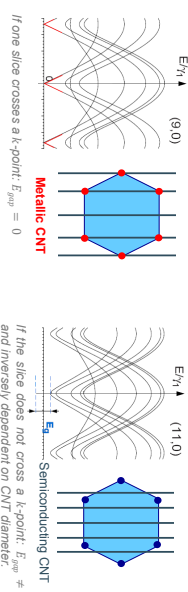


Materials Physics and Technology for Nanoelectronics
Carbon Materials

KU LEUVEN

Electronic properties of SWNTs

The SWNT band structure obtained by "slicing" the $E - k$ dispersion of graphene along planes defined by the quantized k_{\perp} vector, depends on the chirality of the CNT. This leads to metallic and semiconducting nanotubes.



Semiconducting CNT

If the slice does not cross a k -point: $E_{gap} \neq 0$

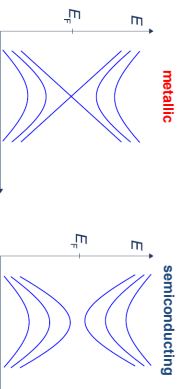
98

Materials Physics and Technology for Nanoelectronics
Carbon Materials

KU LEUVEN

Conduction in CNTs

The electronic band structure of a carbon nanotube is **quasi one-dimensional**: it consists of a set of one-dimensional subbands, shown schematically in the figure below. The larger the diameter of the CNT, the smaller the energy separation between the different subbands. Each subband can conduct **two** electrons with opposite spin.



Schematic representation of the band diagram of (a) a metallic SWCNT and (b) a semiconducting SWCNT. The symbols E , E_F and k_{\parallel} represent respectively the Fermi energy and the k -vector in the direction parallel to the CNT axis.

99

Materials Physics and Technology for Nanoelectronics
Carbon Materials

KU LEUVEN

The resistance of a single walled CNT

CNTs have an intrinsic resistance. With each subband, one unit of quantum resistance is associated. The unit of **quantum resistance** is:

$$R_{Quantum,unit} = \frac{1}{h} = 12.9 \text{ k}\Omega$$

$R_{Quantum,unit} = \frac{1}{h} = 12.9 \text{ k}\Omega$

It includes conduction by two electrons with opposite spin. When multiple subbands carry current, the total quantum resistance is the quantum unit resistance divided by the number of available subbands.

The quantum resistance of a single walled semiconducting CNT is:

$$R_{Quantum,SWCNT} = \frac{1}{2} R_{Quantum,unit} = 6.5 \text{ k}\Omega$$

with $R_{Quantum}$ the quantum resistance associated with each sub-band i and T_i the corresponding transmission coefficient.

$$R_{Contact} = \frac{1}{\sum T_i} \cdot R_{Quantum,i}$$

Metal

100

Materials Physics and Technology for Nanoelectronics
Carbon Materials

KU LEUVEN

The resistance of a single walled CNT

The inter-subband scattering depends on the diameter of the CNT. The energy separation between the Fermi level and higher order subbands for a metallic SWCNT is roughly proportional to $1/d$, with d the diameter of the CNT.

This gives rise to two counteracting effects:

- 1) the value of the quantum resistance is expected to decrease (more channels contribute)

2) the scattering is expected to increase due to coupling between the subbands.

Additional sources of scattering are imperfections, adsorbed molecules, effect of the surrounding material and carrier excitation into higher order subbands.

Both elastic (no energy loss) and inelastic scattering (with energy loss) generate an extra component in the resistance of CNTs.

Elastic scattering is suppressed near the Fermi level due to symmetry reasons because the electronic wavefunction is smeared out over the whole nanotube circumference. Inelastic scattering can come from acoustic phonons, optical phonons and zone boundary phonons.

Metamaterials Physics and Technology for Nanoelectronics
Carbon Materials

101

KU LEUVEN

The resistance of a single walled CNT

Acoustic phonon scattering is always present, even at low voltages.

- Typical values for the mean free path $l_{\text{mfp,phon}}$ in case of acoustic scattering are $l_{\text{mfp,phon}} = 1 - 2 \mu\text{m}$. Converting this to resistance per unit length according to the formula $\rho = \frac{h}{4e^2 l_{\text{mfp,phon}}} = \frac{1}{l_{\text{mfp,phon}}}$ results in a typical value of about: $\rho_{\text{ac,phon}} = 4 - 7 \text{k}\Omega/\mu\text{m}$.

Optical phonon/zone boundary phonons scattering can occur when the applied voltages are sufficiently large.

- The threshold voltage for these scattering mechanisms is typically $V_{\text{th, opt/phon}} = 200 \text{ mV}$ (optical phonon) and $V_{\text{th, zp/phon}} = 160 \text{ mV}$ (zone boundary phonon).
- The mean free path is typically about $l_{\text{mfp, opt/phon}} = 200 \text{ nm}$ for optical phonon scattering and $l_{\text{mfp, zp/phon}} = 10 - 40 \text{ nm}$ for zone boundary phonon scattering. However the total scattering length is also determined by the applied voltage V :

$$R_{\text{opt/phon}} = \frac{h}{4e^2 l_{\text{scattering, total}}} = 6.5 \text{ k}\Omega \frac{l}{l_{\text{mfp, opt/phon}} + l_{\text{mfp, opt/phon}}}$$

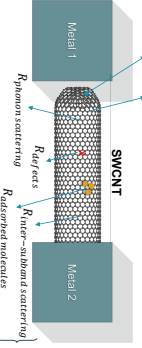
with V the applied voltage, and provided that $V > V_{\text{th}}$.

- For a scattering length of 30nm (dominant zone boundary scattering) the resistance per unit length is about $\rho_{\text{opt/phon}} = 200 \text{ k}\Omega/\mu\text{m}$.

102

Metamaterials Physics and Technology for Nanoelectronics
Carbon Materials

KU LEUVEN



As an overall result the externally measured resistance of a single walled CNT shows an important contribution from the contact resistance and the quantum resistance that are independent on the length of the CNT.

The scattering contribution related to phonon interactions is dependent on the CNT length and the applied voltage. When the contact resistance is neglected the overall resistance of a high-quality single walled CNT can be approximated by:

$$R_{\text{S,CNT}} = R_{\text{quantum,metalless}} + \rho_{\text{phonon}} l + \rho_{\text{opt,phon}} l$$

Inductance of a CNT

The inductance consists of magnetic and kinetic inductance:

- I_{mag} corresponds to the inertia towards changes in **magnetic energy** of the carriers upon current flow.

- The value of the magnetic inductance per unit length is of the order of $L_{\text{mag}} \sim 1 \text{nH}/\mu\text{m}$.

- I_{kin} corresponds to the inertia towards changes in the **kinetic energy** of the carriers upon current flow.

- It is calculated from equating the kinetic energy per unit length in a 1D wire with the $\frac{1}{2}I^2L$ energy of the kinetic inductance.

- The total kinetic inductance for a metallic SWCNT is typically in the order of $L_{\text{kin}} \sim 16 \text{nH}/\mu\text{m}$.

In CNTs the kinetic inductance will usually dominate the magnetic inductance. This is an important characteristic. In macroscopic circuits, long thin wires are usually considered to have relatively large (magnetic) inductances. This is **not the case** in CNTs where the **kinetic inductance dominates**.

Metamaterials Physics and Technology for Nanoelectronics
Carbon Materials

103

KU LEUVEN

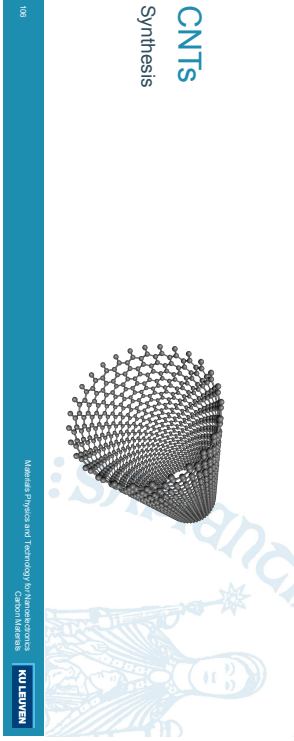
CNT growth

The CNT growth process generally consists of 3 steps:

1. The **catalyst deposition**: metal (compound) nanoparticle which catalyzes thermal decomposition of carbon-containing molecule
 - determines position & diameter of CNT on substrate
 - deposition techniques:
 - electrochemical deposition (ECD)
 - sputtering + anneal

2. The (plasma-enhanced) **pretreatment**
3. The **CNT growth**: carbon source, e.g. methane

- Growth techniques:
 - Chemical Vapor Deposition (CVD)
 - Plasma-Enhanced Chemical Vapor Deposition (PECVD)



104

Metamaterials Physics and Technology for Nanoelectronics
Carbon Materials

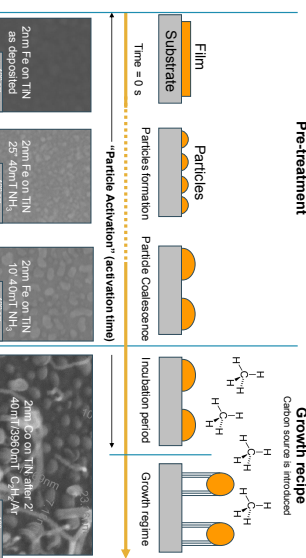
KU LEUVEN

103

Metamaterials Physics and Technology for Nanoelectronics
Carbon Materials

KU LEUVEN

CNT growth

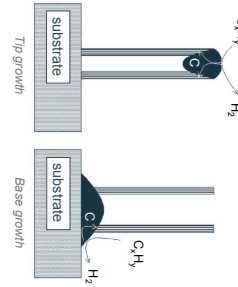


109 Materials Physics and Technology for Nanoelectronics, Carbon Materials KU LEUVEN

CNT growth

The catalyst-substrate interaction determines the **growth mode**:

- **IP-growth:**
 - Weak interaction between substrate and catalyst nanoparticle
 - Poor catalyst wetting on metal substrates (i.e. large contact angle)
 - (semi) spherical nanoparticles
- **Base-growth:**
 - Strong interaction between substrate and catalyst nanoparticle
 - Good wetting on oxide substrates (i.e. small contact angle)
 - Determined by amount of catalyst (film thickness), pre-treatment and morphology
 - Solid-state reactions between substrate and metal nanoparticle
 - e.g. $\text{Fe}_3\text{O}_4 + \text{TiO}_2 \rightarrow \text{FeTiO}_3$ ($\theta_c < 90^\circ$)
 - May be facilitated in plasma (e.g. hydrogen plasma)

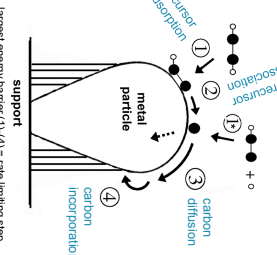


110 Materials Physics and Technology for Nanoelectronics, Carbon Materials KU LEUVEN

CNT growth

The CNT growth involves various steps. The step with the largest energy barrier limits the growth rate.

- Carbon formation (1-2)
 - Chemical decomposition at catalyst (Fe, Ni, Co) surface
 - Adsorption + dissociation
 - 'Bulk' diffusion, dissolves into the metal catalyst and diffuses towards growth site
 - Concentration gradient: from decomposition site ([C] to crystallization site [C])
 - Enhanced by local temperature difference for exothermic decomposition and endothermic crystallization
 - Surface diffusion
 - Formation of Carbide intermediates
 - Incorporation of carbon at step edge

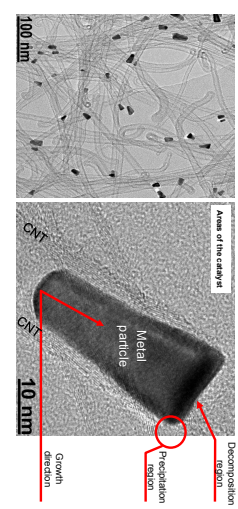


111 Materials Physics and Technology for Nanoelectronics, Carbon Materials KU LEUVEN

CNT growth mechanism

High resolution cross-sectional TEM measurements provide more insight into the details of the CNT growth.

Predominant crystal steady-state reaches the minimum of the growth, i.e. the minimum of the surface free energy and $C_{\text{adsorption}}/C_{\text{released}} = 1$, the grown carbon nanostructure is a perfect CNT.



112 Materials Physics and Technology for Nanoelectronics, Carbon Materials KU LEUVEN

CNT growth by Chemical Vapor Deposition

CNTs can be produced by various techniques. For high quality CNTs chemical vapor deposition (CVD) is the preferred method.

A substrate is prepared with a layer of metal catalyst particles (Ni, Co, ...) and then heated up to 700°C.

Two gases are blend into the reactor: a process gas and a carbon gas (e.g. CH_4).

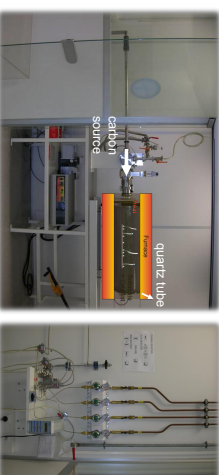
The carbon gas is broken apart at the surface of the catalyst particle and the carbon moves to the edges to form nanotubes.



113 Materials Physics and Technology for Nanoelectronics, Carbon Materials KU LEUVEN

CNT growth by Chemical Vapor Deposition

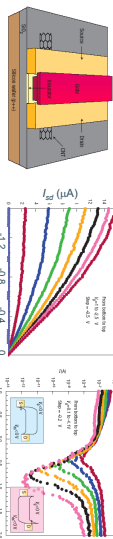
Laminar gas (CH_4) flow in tube furnace



114 Materials Physics and Technology for Nanoelectronics, Carbon Materials KU LEUVEN

Nanotube FET

- For the fabrication of FET's with CNTs, only **semiconducting** CNTs can be used with a well-defined bandgap. This requires a growth process with **perfect control** on the chirality and diameter of the CNTs. This is **not** possible at present.
- However, with **pick-and-place** methods, CNT devices have been demonstrated.



122
Bandgap: 0.5 – 1 eV
On-off ratio: $\sim 10^6$
Mobility: $\sim 100,000 \text{ cm}^2/\text{V}\cdot\text{sec}$ @ RT
Max current density: $> 10^6 \text{ A/cm}^2$

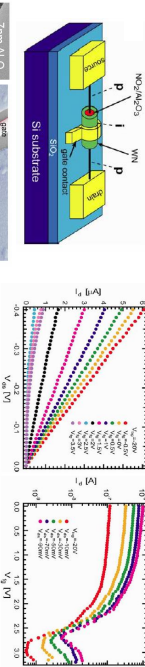
Ph. Avouris et al. Nature Nanotechnology 2, 605 (2007)

Materials Physics and Technology for Nanoelectronics
Carbon Materials

KU LEUVEN

Gate-all-around CNT FET

Gate-all-around CNT FET demonstrated using 'pick-and-place' of a CNT.

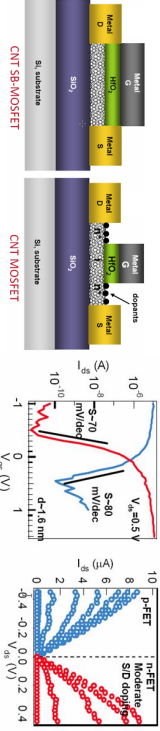


123
Metallic Physics and Technology for Nanoelectronics
Carbon Materials

Zhifeng Chen et al. APL 2008
KU LEUVEN

CNT FET structures

Both Schottky-barrier FETs and regular MOSFETs with 'doped' source/drain regions have been demonstrated.



SB-MOSFET: Gate modulates the carrier injection at the S/D Schottky (metal) contacts
CNT-MOSFET: Gate modulates the charge density of the nanotube channel

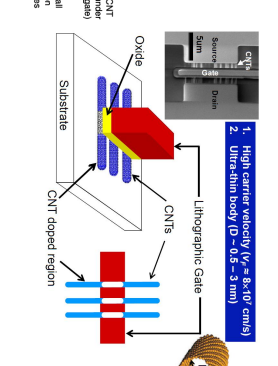
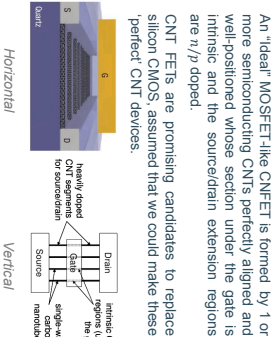


A. Javey et al. Nano Letters, 2004, 2005

Carbon nanotube FET

There are some imperfections inherent to CNT synthesis and CNFET manufacturing process that may eclipse the expectations.

- CNT growth process**
 - NO control of chirality
 - Percentage of metallic CNTs
 - SD doping variations
 - Mispositioned and misaligned CNTs
- CNFET manufacturing process**
 - Intrinsic CNT (under the gate)
 - Heavily doped for source/drain nanotubes
 - Vertical
 - Horizontal

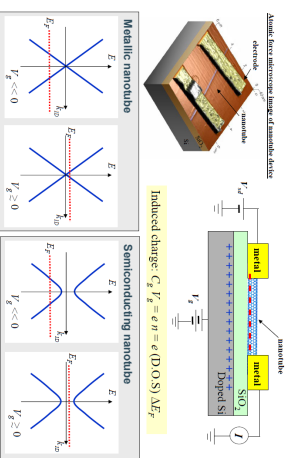


125
Metallic Physics and Technology for Nanoelectronics
Carbon Materials

KU LEUVEN

CNT FET

In a CNT FET (Field Effect Transistor) the carrier density is tuned by the field effect. This is illustrated aside for a back-gated device where the Si substrate is used as control gate.



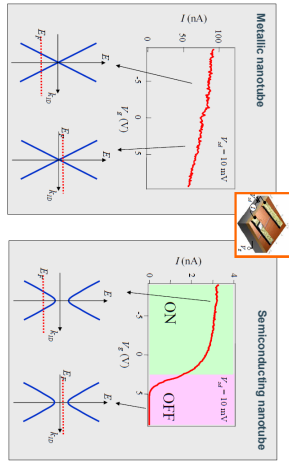
A. Javey et al. Nano Letters, 2004, 2005

KU LEUVEN

Electrical transport in nanotube devices

Only in semiconducting nanotubes the current can be sufficiently modulated to obtain an acceptable ON/OFF ratio of the transistor. Metallic transistors must be avoided in transistor applications.

Currently there is no method available that allows to directly produce semiconducting CNTs only in a controlled way on a substrate, necessary to fabricate CNT circuits.



Materials Physics and Technology for Nanoelectronics
Carbon Materials

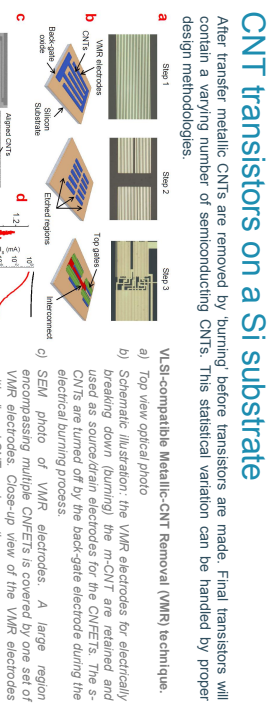


CNT transistors on a Si substrate

CNT transistors and circuits have been fabricated from mixed semiconducting and metallic nanotubes transferred as a 'tapestry' onto a Si wafer.

A CNT transfer technique was developed which transfers CNT from as-grown on a crystalline quartz substrate (where the CNTs grown horizontally) to a target substrate. In this way a complete Si wafer can be densely covered with aligned CNTs.

After transfer metallic CNTs are removed by 'burning' before transistors are made. Final transistors will contain a varying number of semiconducting CNTs. This statistical variation can be handled by proper design methodologies.



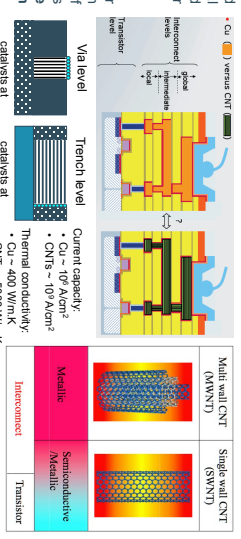
P. Wong et al., Stanford, IEDM 2011
Materials Physics and Technology for Nanoelectronics
Carbon Materials



CNT interconnects

CNTs exhibit enhanced electrical and thermal properties over Cu and could probably be used for interconnects.

To replace Cu by CNT for interconnects, a high nucleation density of MWCNT or SWCNT is required to overcome the contact and quantum resistance issues.



Materials Physics and Technology for Nanoelectronics
Carbon Materials



CNT interconnects

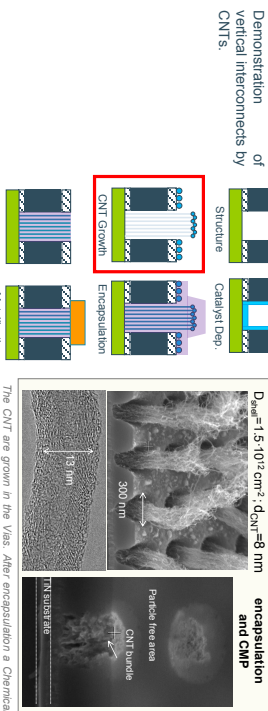
Demonstration of vertical interconnects by CNTs.

CNT growth and encapsulation



CNT growth
 $D_{\text{CNT}} = 1.5 \cdot 10^{12} \text{ cm}^{-2}$, $d_{\text{CNT}} = 8 \text{ nm}$

After encapsulation and CMP



N. Chodziewicz et al., J. Electrochem Soc. 157(10) 2010

132

CNT interconnect

Demonstration of CNT growth and electrical conductivity in vias.

a) SEM view of CNTs in via



b) SEM view of CNTs in via



vias

oxide

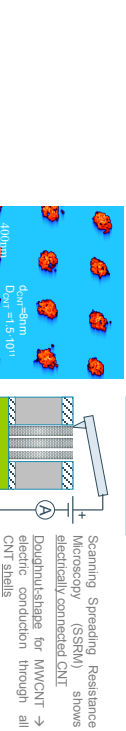
MWCNT

Scanning Spreading Resistance Microscopy (SSRM)

Electrically connected CNT

Doughnut shape for MWCNT \rightarrow

electric conduction through all CNT shells



W. De Geyter et al., KU Leuven, IEDM 2011
Materials Physics and Technology for Nanoelectronics
Carbon Materials

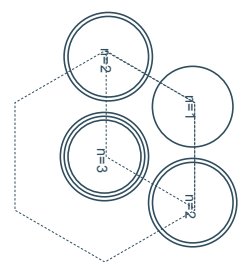


Resistance of a CNT bundle

In a CNT bundle, the shell density determines R , and not the number of CNTs.

The resistance of a single CNT shell, R_{scNT} , is only a weak function of the CNT diameter (\sim SWCNT).

The lower resistance in a CNT bundle is obtained for a higher CNT shell density.



Resistance of CNT bundle:

$$R_{\text{CNT,bundle}} = \frac{R_{\text{scNT}}}{\frac{8}{\pi} n_{\text{scNT}}}$$

number of CNT: $N = 4$
total number of CNT shells: $\sum_0^N n_{\text{scNT}} = 8$

P. Vereeken, IMEC
Materials Physics and Technology for Nanoelectronics
Carbon Materials

Optimum packing density for low resistance

Bundle of CNT (SW)

One MW-CNT

A higher stacking density can be obtained with SWCNTs than with MWCNTs.
Maximum CNT density:
$$\left(\sum_0^N n_{\text{scNT}} \right)_{\text{max}} = 2 \times 10^{14} \text{ cm}^{-2}$$

with:

- hexagonal stacking
- smallest SWCNT with diameter of 0.4nm
- inter-tube distance of 0.34nm

$$\left(\sum_0^N n_{\text{scNT}} \right) = 13$$

$$\left(\sum_0^N n_{\text{scNT}} \right) = 4$$

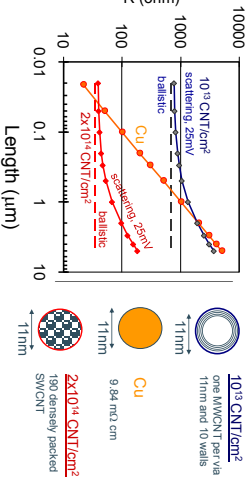
Realistic target:
 5×10^{13} shells cm^{-2}

P. Vereeken, IMEC

Materials Physics and Technology for Nanoelectronics
Carbon Materials

KU LEUVEN

When plotting the resistivity as a function of the interconnect length for various densities of CNT shells and for Cu, it is found that $R_{\text{scNT}} < R_{\text{Cu}}$ only at longer interconnect length (dependent on CNT density and dependent on voltage). For short interconnect lengths the quantum resistance dominates the resistance.



P. Vereeken, IMEC

136

Materials Physics and Technology for Nanoelectronics

KU LEUVEN Clement Mardling
imec Eric & Lucile Van der Auweraer
KU Leuven Koenraad De Smedt
KU Leuven Francesco Molina Lopez
KU Leuven Koenraad De Smedt
KU Leuven Eric & Lucile Van der Auweraer

KU LEUVEN

134